# Evidences for significant electron-phonon coupling in high Tc cuprates: Fermi blockade of the coupling with doping: results and Stochastic Method of Analytic Continuation


**Andrey S. Mishchenko**

RIKEN
Center for Emergent Matter Science
(CEMS)

# Evidences for significant electron-phonon coupling in high Tc cuprates: Fermi blockade of the coupling with doping: results and Stochastic Method of Analytic Continuation


**Andrey S. Mishchenko**

RIKEN
Center for Emergent Matter Science
(CEMS)

**Physical results**
**(by Diagrammatic Monte Carlo and numeric analytic continuation)**

**Stochastic Optimization Consistent Constrains method (SOCC)**

# Not serious: OPTIMISTIC INTEREST DIAGRAMM.

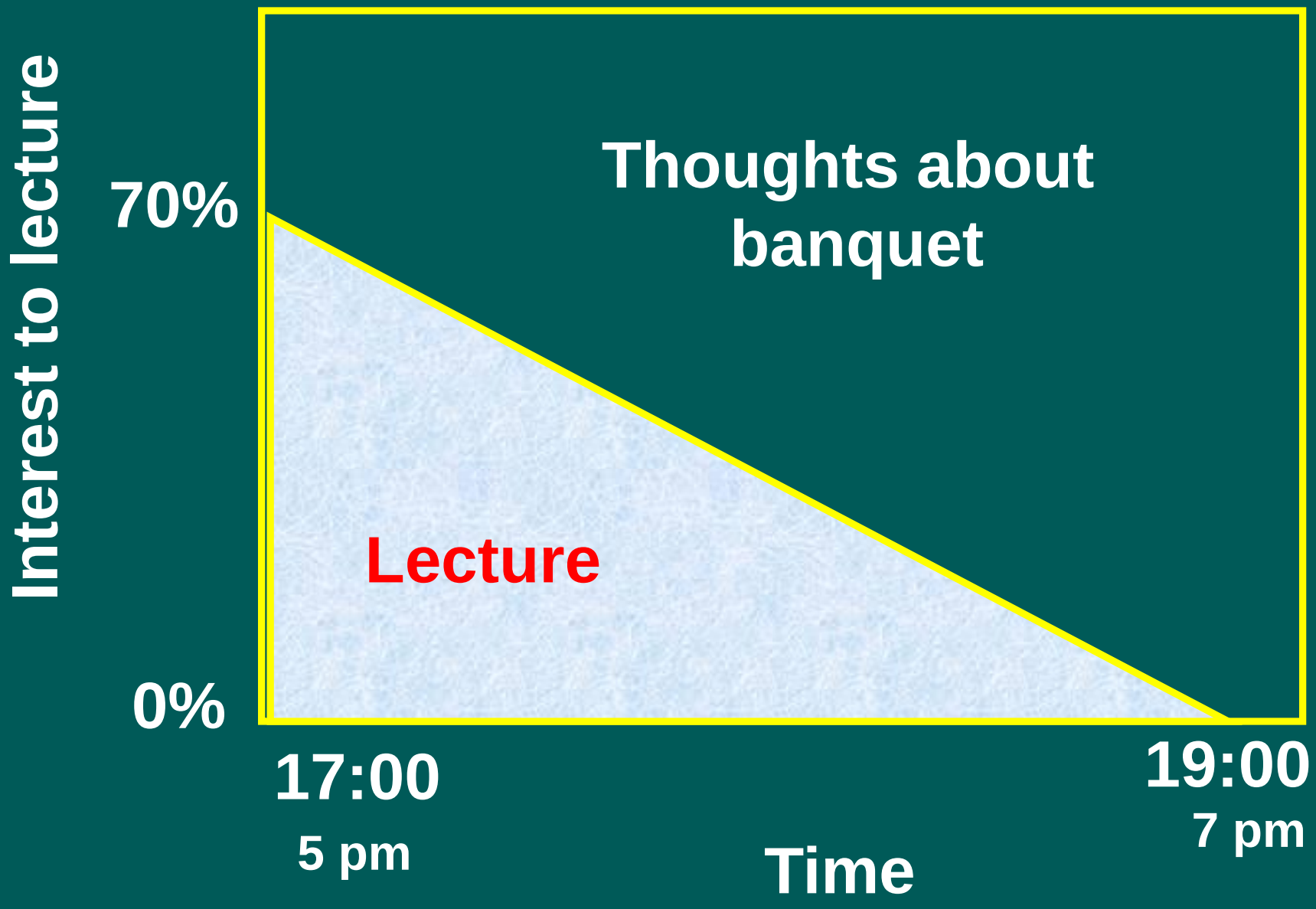

理化学研究所

# RIKEN, CEMS

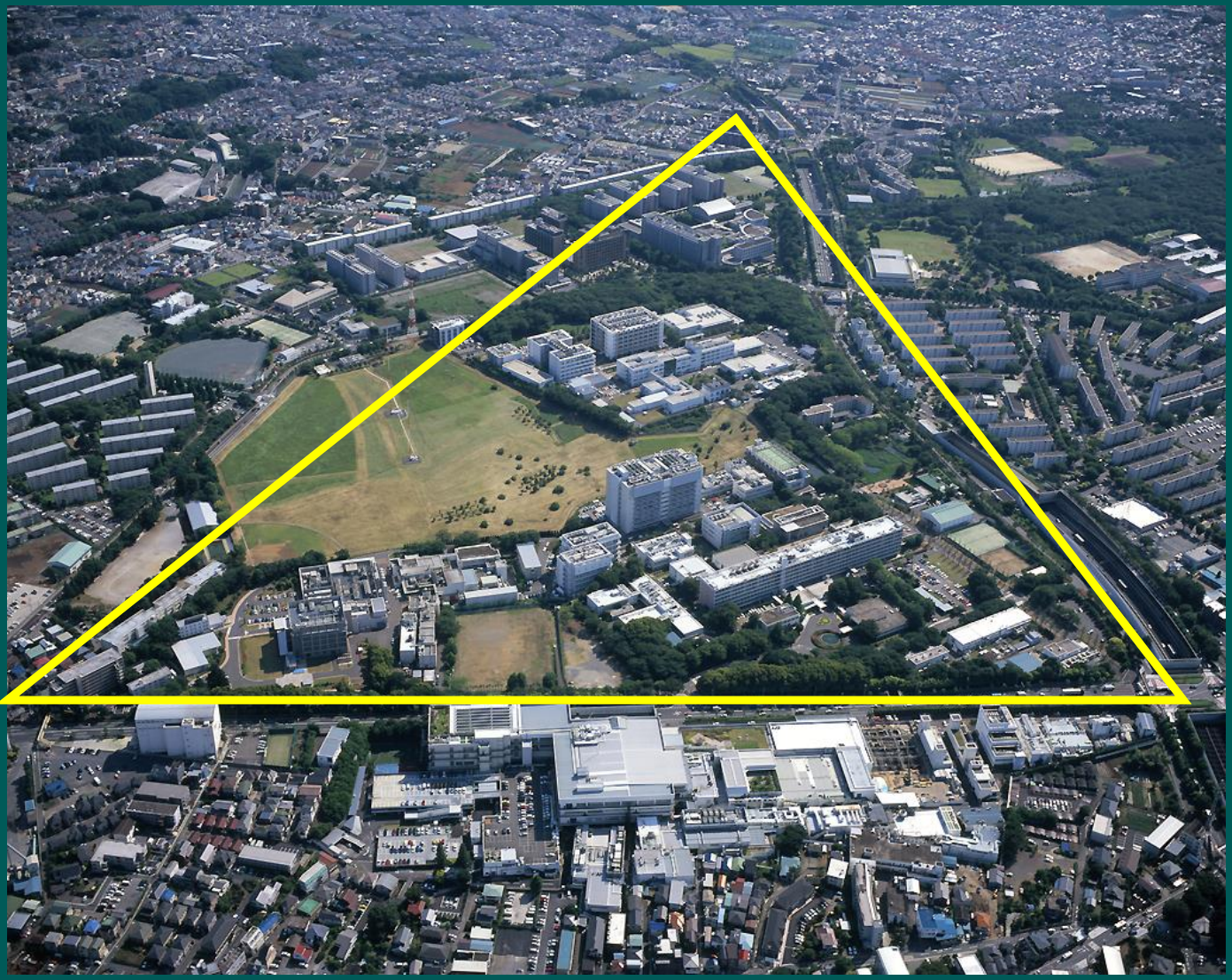

# A. S. Mishchenko

## RIKEN (Institute of Physical and Chemical Research), Japan

# A. S. Mishchenko

**RIKEN** (Institute of Physical and Chemical Research), **Japan**

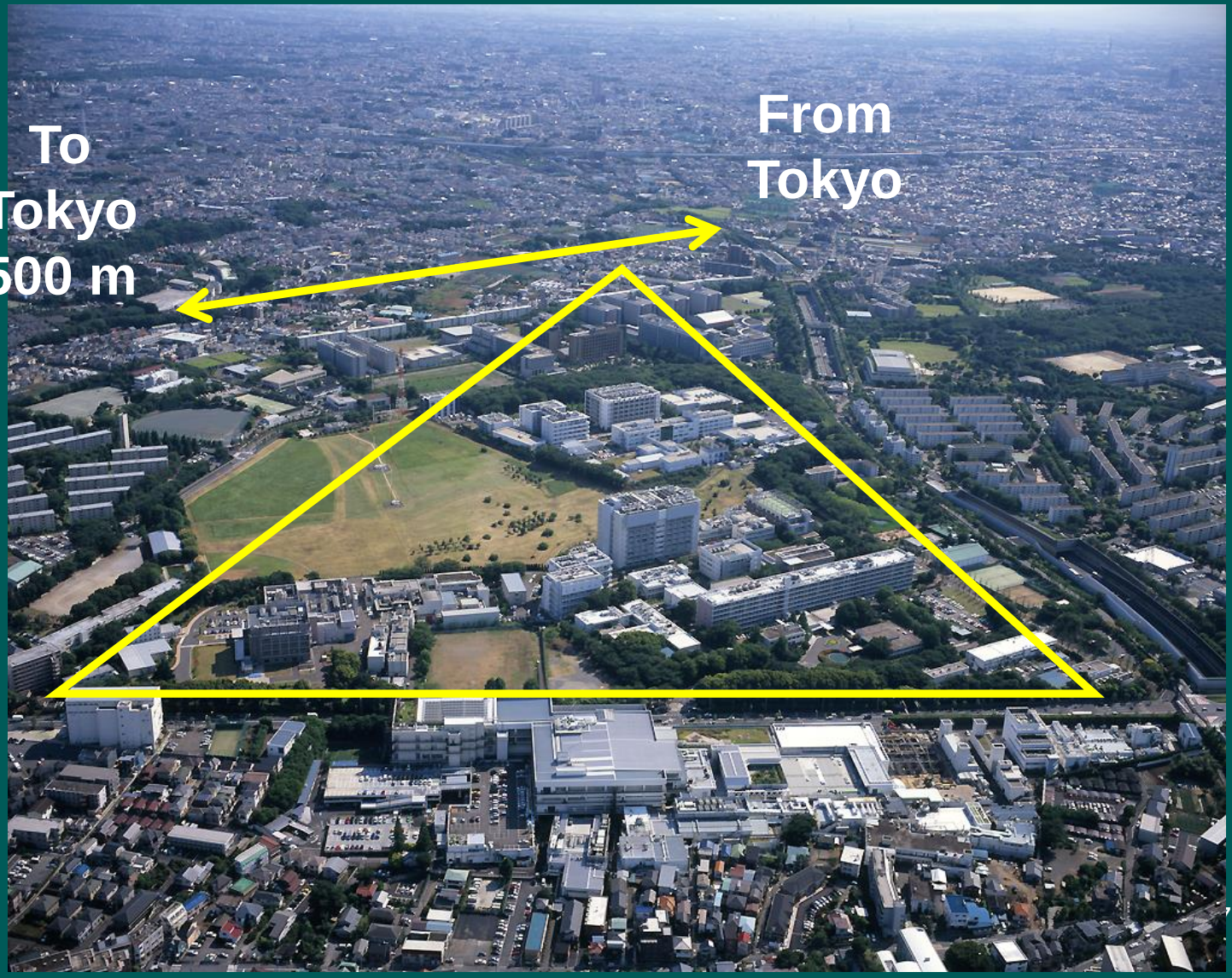

# 1994-1999: Kondo, Spin Liquid


**Trieste, 70th anniversary © Darya Zelentsova**

# 1986-1987: Polaron, Lang-Firsov

## Don Quixote and Sancho Panza

Trieste,
70th anniversary
© Darya Zelentsova

# 1986-1987: Polaron, Lang-Firsov

One can treat polaron either in weak or srong coupling limit only!

1. DMC
2. Analytic continuation

ARPES, OC, etc.

# Evidences for significant electron-phonon coupling in high Tc cuprates: Fermi blockade of the coupling with doping: results and Stochastic Method of Analytic Continuation


**Andrey S. Mishchenko**

RIKEN
Center for Emergent Matter Science
(CEMS)

# Electron-phonon coupling in underdoped cuprates


## A S Mishchenko

George Sawatzky, Vancouver

Naoto Nagaosa, Tokyo

Giulio de Filippis and Vittorio Cataudella Napoli

Z.-X. Shen, Stanford

Jan Zaanen, Leiden

Christian Bernhard, Kyungwan Kim Freiburg

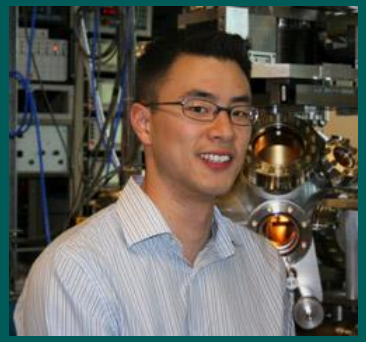

Kyle Shen, Cornell University

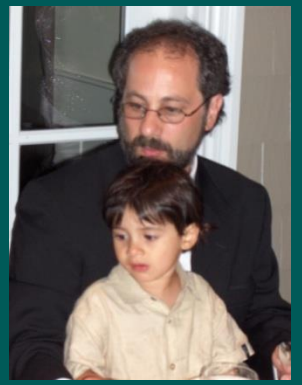

Tom Devereaux, Stanford


RIKEN

Are **Hubbard-related models**

enough to describe the physics

of **high $T_c$ materials** or one needs

an additional coupling to some

**extra bosonic field** which is

not included into Hubbard model?

# Hubbard-related models

## Introduction to Hubbard Model-1

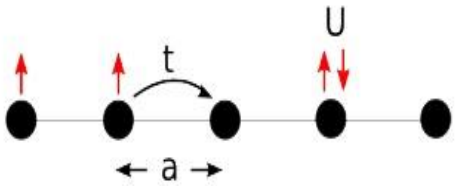


**t** → hopping matrix element
**U** → on-site Coulomb repulsion

$$\mathcal{H} = \epsilon \sum_{i,\sigma} \hat{n}_{i\sigma} - t \sum_{\langle i,j\rangle,\sigma} \left( \hat{c}^{\dagger}_{i\sigma} \hat{c}_{j\sigma} + \text{h.c.} \right) + U \sum_{i} \hat{n}_{i\uparrow} \hat{n}_{i\downarrow}$$

$\mathcal{H}_{\text{band}}$ $\mathcal{H}_{\text{Coulomb}}$

*J.Hubbard, Proc. Roy. Soc. Lond. (1963-1967)*

$\hat{n}_{i\sigma} = \hat{c}^{\dagger}_{i\sigma} \hat{c}_{i\sigma}$ $\hat{c}^{\dagger}_{i\sigma}$, $\hat{c}_{i\sigma}$ creation/annihilation operators

Band term is easy to solve; introduce → $\hat{c}_{j\sigma} = \frac{1}{\sqrt{N}} \sum_{k} e^{i \frac{2\pi k}{N} j} \hat{b}_{k\sigma}$

**N**: number of atoms

7

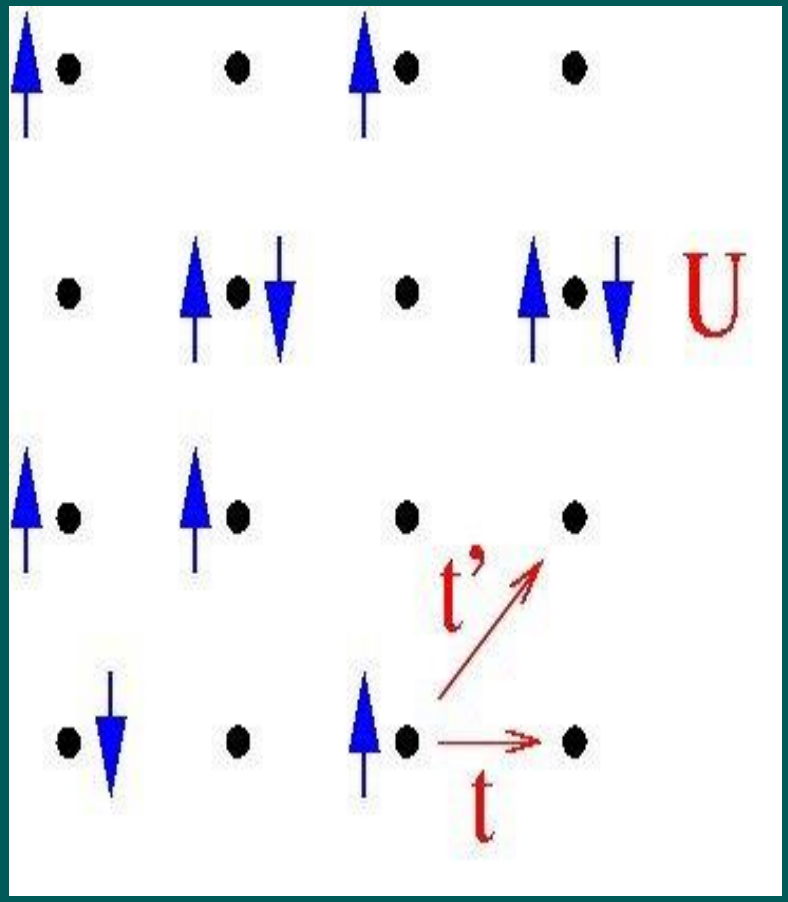


**Large U>>t → t-J model**

# additional coupling to some extra bosonic field

## Motivation and model

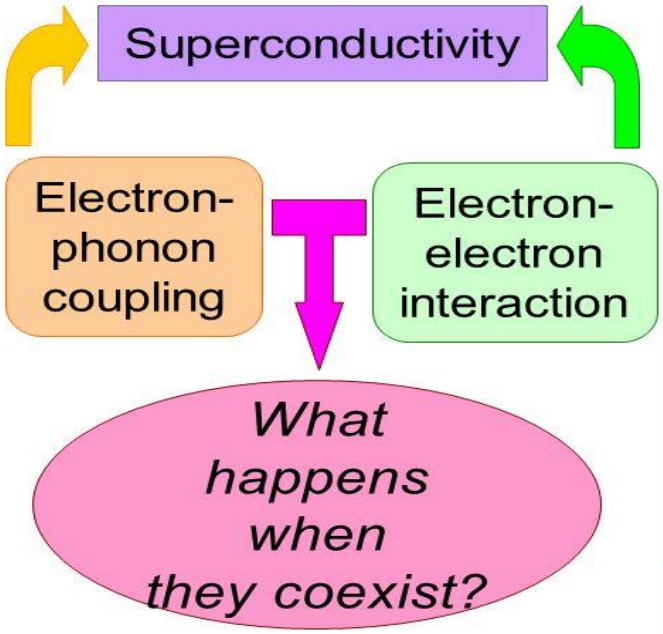


Holstein-Hubbard model

$$H = -t\sum_{i,\sigma}(c^{\dagger}_{i+1,\sigma}c_{i,\sigma} + \text{H.c.}) + U\sum_{i} n_{i\uparrow}n_{i\downarrow} + g\sum_{i,\sigma} n_{i\sigma}(b_i + b_i^{\dagger}) + \omega\sum b_i^{\dagger}b_i$$

Electron-electron repulsion

Electron-phonon coupling

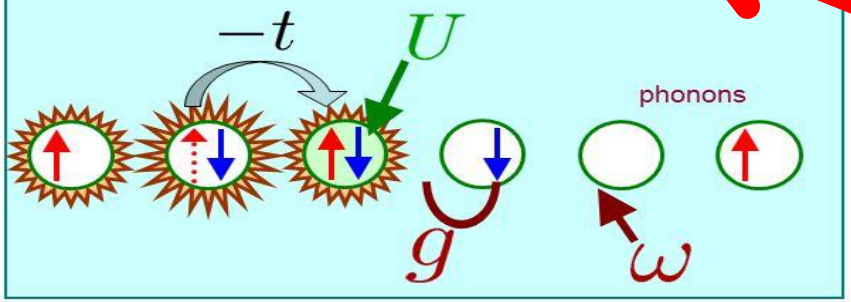

1. Explanation of
   (a) ARPES;
   (b) optical conductivity;
   (c) T-dependence of the spectral properties;
   (d) pump-probe evolution of the optical conductivity
   (e) Raman

   **in underdoped cuprates**

   requires strong electron-boson coupling

2. Naively, experimental data indicate that increase of doping decreases manifestations of the electron-boson coupling

3. We solve famous sign-problem in Mote Carlo for many-particle Fermi-polarons system and explain what happens with electron-boson coupling when doping of high $T_c$ cuprates increases.

1. Explanation of

(a) ARPES; (b) optical conductivity;

(d) pump-probe evolution of the optical conductivity

in underdoped cuprates requires strong electron-boson coupling

ARPES

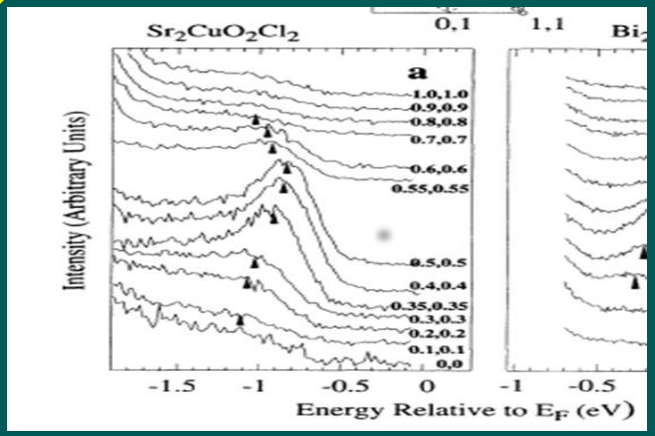


Optical conductivity

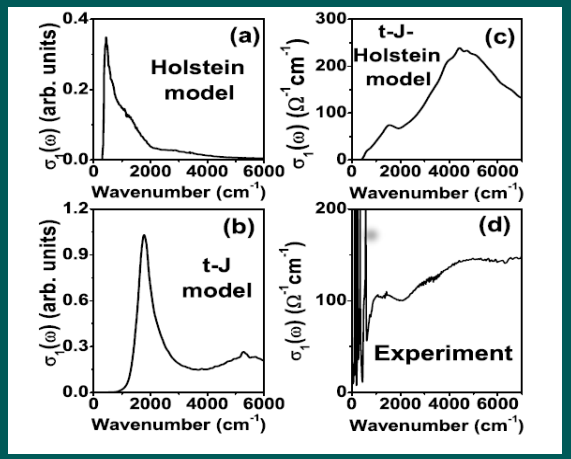


Pump-probe in optical conductivity

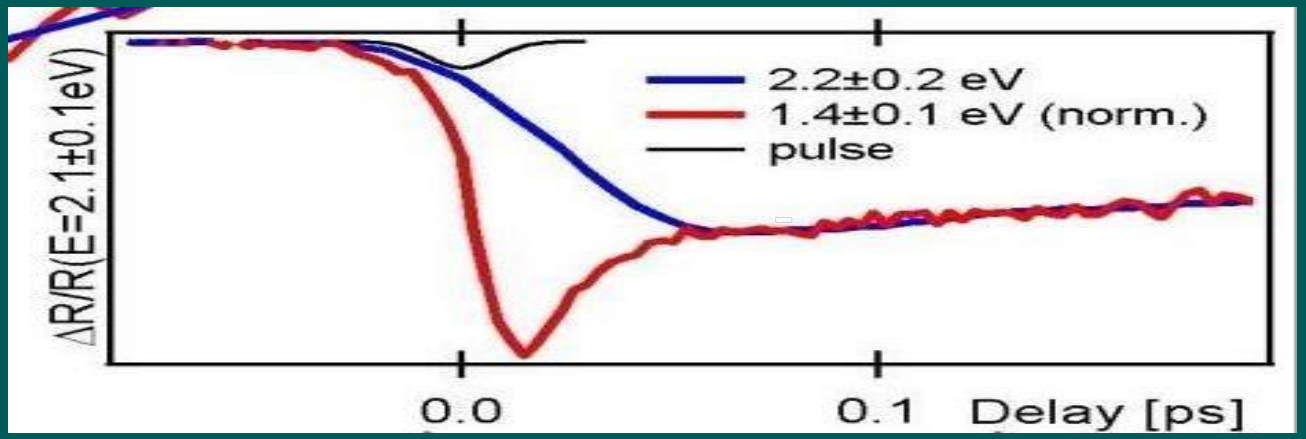

**There is no considerable manifestation of electron-boson coupling in spectroscopy of doped compounds.**

## 2. Naively, experimental data indicate that increase of doping decreases manifestations of the electron-boson coupling

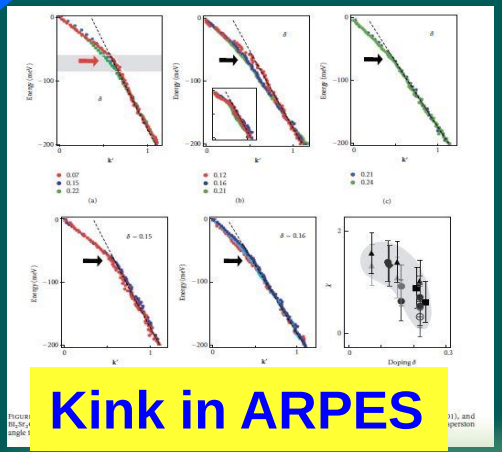

Kink in ARPES

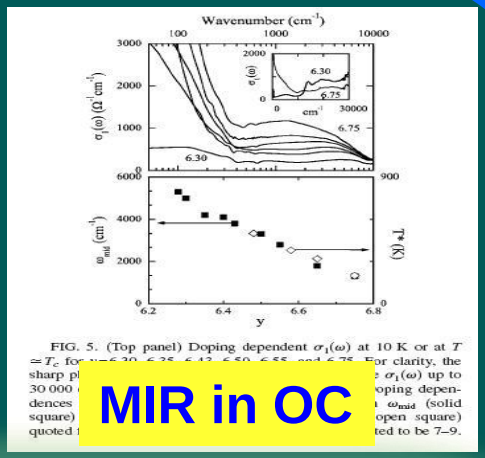


FIG. 5. (Top panel) Doping dependent $\sigma_1(\omega)$ at 10 K or at $T \simeq T_c$ for

MIR in OC

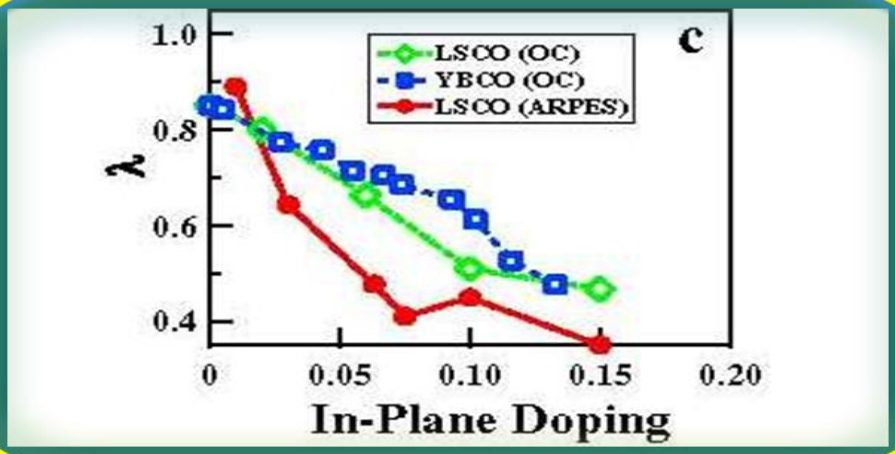


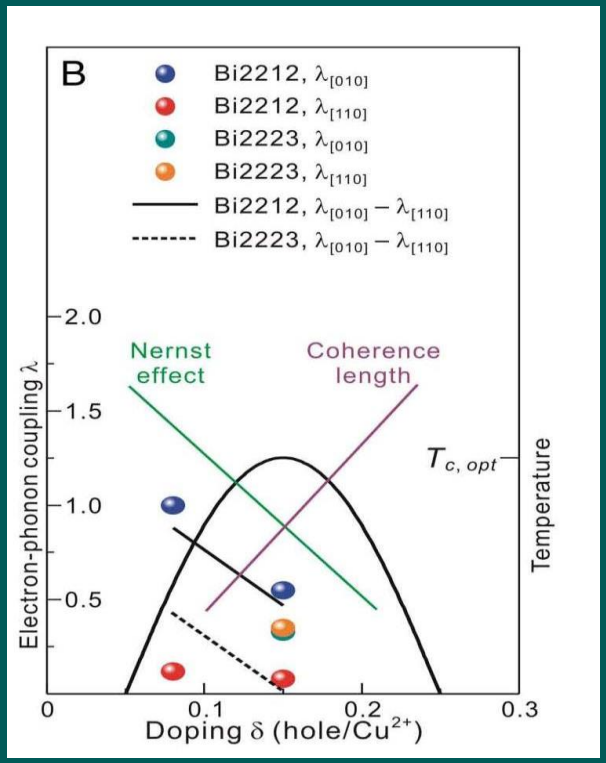


Other properties

# Fermi screening in finite density Fermi system?

# Famous
# sign-problem in
# Diagrammatic Monte Carlo
# (unbiased method)
# for many-particle
# Fermi system

**Naoto Nagaosa**
**RIKEN, U. Tokyo**

**Nikolay Prokof’ev**
**UMASS**

# Funeral of

# electron-phonon interaction in doped cuprates

# Funeral of the manifestations of electron-phonon interaction in doped cuprates in spectroscopy

**Why we need additional electron-boson interaction on top of Hubbard model to explain**

# ARPES

# (in undedoped)

# ARPES



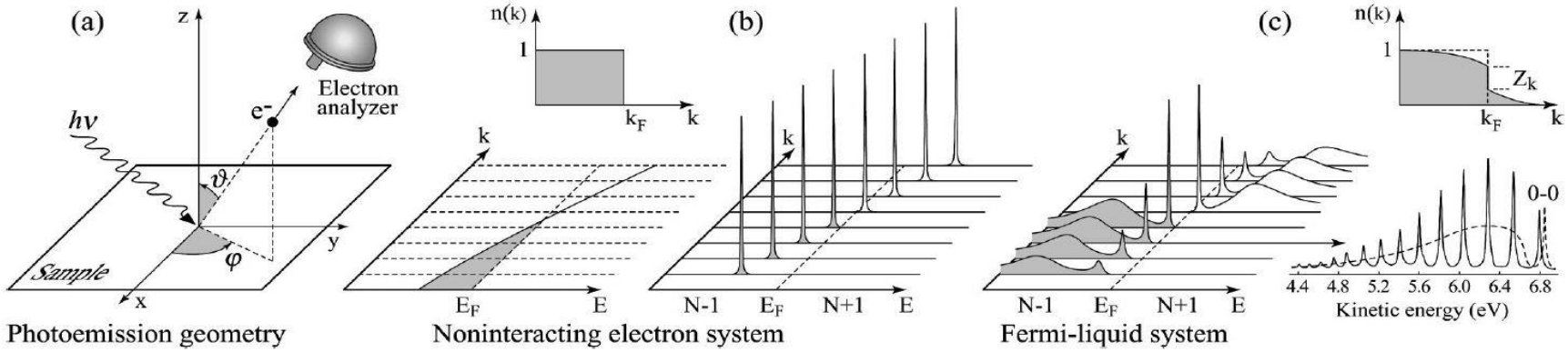


FIG. 3. Angle-resolved photoemission spetroscopy: (a) geometry of an ARPES experiment in which the emission direction of the photoelectron is specified by the polar ($\vartheta$) and azimuthal ($\varphi$) angles; (b) momentum-resolved one-electron removal and addition spectra for a noninteracting electron system with a single energy band dispersing across $E_F$; (c) the same spectra for an interacting Fermi-liquid system (Sawatzky, 1989; Meinders, 1994). For both noninteracting and interacting systems the corresponding ground-state ($T=0$ K) momentum distribution function $n(\mathbf{k})$ is also shown. (c) Lower right, photoelectron spectrum of gaseous hydrogen and the ARPES spectrum of solid hydrogen developed from the gaseous one (Sawatzky, 1989).

ARPES experiments), one can relate the kinetic energy and momentum of the photoelectron to the binding energy $E_B$ and crystal momentum $\hbar\mathbf{k}$ inside the solid:

$$E_{kin} = h\nu - \phi - |E_B|, \quad (1)$$

$$\mathbf{p}_{\|} = \hbar\mathbf{k}_{\|} = \sqrt{2mE_{kin}} \cdot \sin\vartheta. \quad (2)$$

Here $\hbar\mathbf{k}_{\|}$ is the component parallel to the surface of the electron crystal momentum in the *extended* zone scheme. Upon going to larger $\vartheta$ angles, one actually

# ARPES



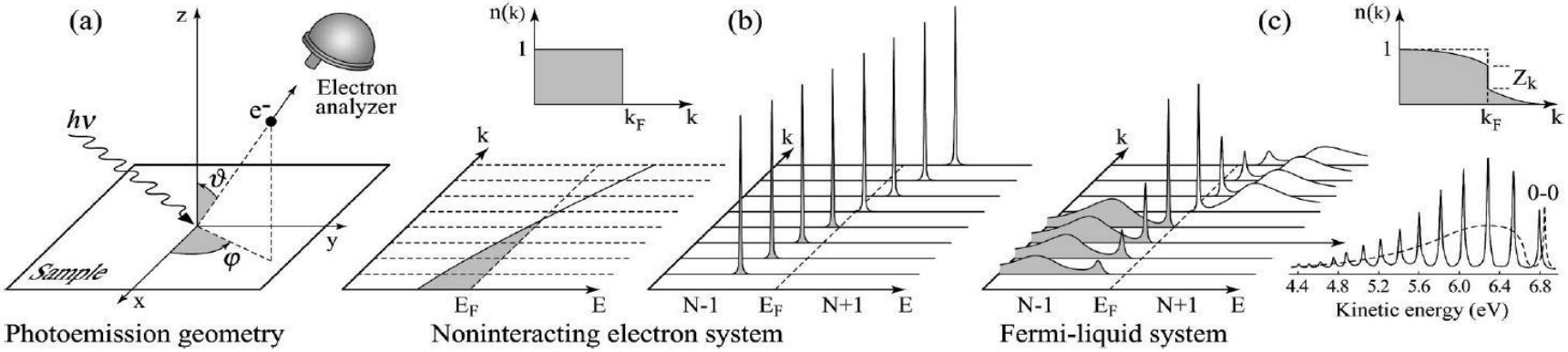


FIG. 3. Angle-resolved photoemission spetroscopy: (a) geometry of an ARPES experiment in which the emission direction of the photoelectron is specified by the polar ($\vartheta$) and azimuthal ($\varphi$) angles; (b) momentum-resolved one-electron removal and addition spectra for a noninteracting electron system with a single energy band dispersing across $E_F$; (c) the same spectra for an interacting Fermi-liquid system (Sawatzky, 1989; Meinders, 1994). For both noninteracting and interacting systems the corresponding ground-state ($T=0$ K) momentum distribution function $n(\mathbf{k})$ is also shown. (c) Lower right, photoelectron spectrum of gaseous hydrogen and the ARPES spectrum of solid hydrogen developed from the gaseous one (Sawatzky, 1989).

to obtain the *one-particle spectral function* $A(\mathbf{k},\omega) = A^+(\mathbf{k},\omega) + A^-(\mathbf{k},\omega) = -(1/\pi)\,\mathrm{Im}\,G(\mathbf{k},\omega)$, with

$$A^{\pm}(\mathbf{k},\omega) = \sum_m |\langle \Psi_m^{N\pm1} | c_{\mathbf{k}}^{\pm} | \Psi_i^N \rangle|^2 \delta(\omega - E_m^{N\pm1} + E_i^N) \tag{11}$$

and $G(\mathbf{k},\omega) = G^+(\mathbf{k},\omega) + [G^-(\mathbf{k},\omega)]^*$, which defines the *retarded Green's function*. Note that $A^-(\mathbf{k},\omega)$ and $A^+(\mathbf{k},\omega)$ define the one-electron removal and addition spectra which one can probe with direct and inverse photoemission, respectively. This can be seen, for the

# Typical ARPES of interacting system

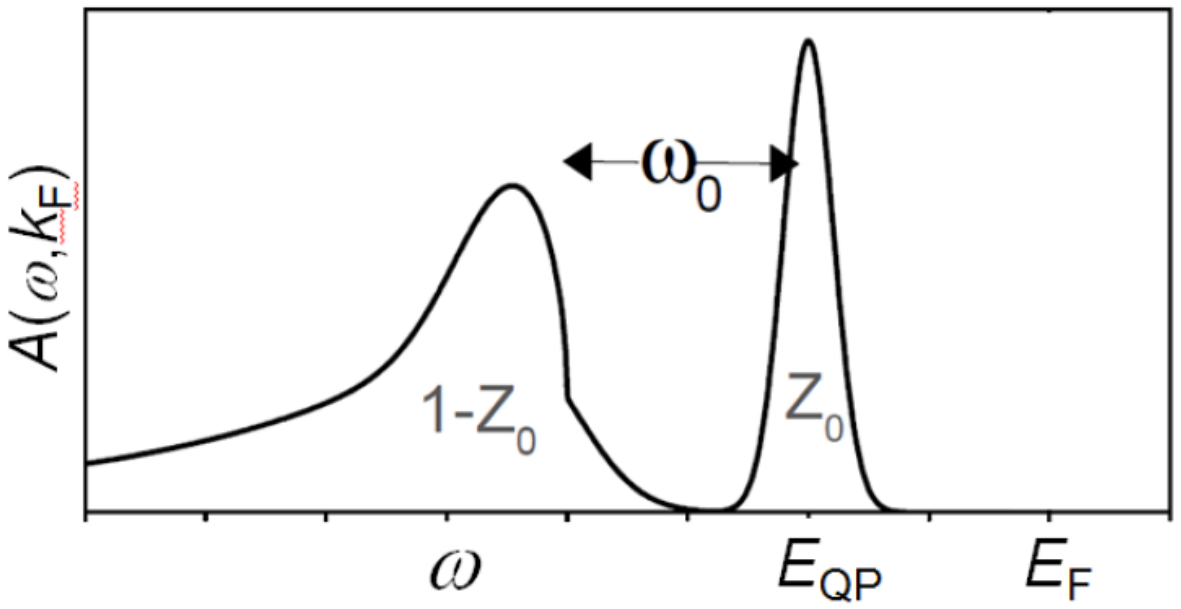


**Fig. 10.** Sketch of the polaron spectral function $A(\omega,\mathbf{k})$ at low electron excitation energy $E(\mathbf{k}) - E_F$. The characteristic peak-dip-hump (PDH) spectral shape is formed by the quasiparticle (QP) peak followed by the phonon sideband tail corresponding to a sequence of optical phonons with frequency $\omega_0$.

# Typical ARPES of interacting system

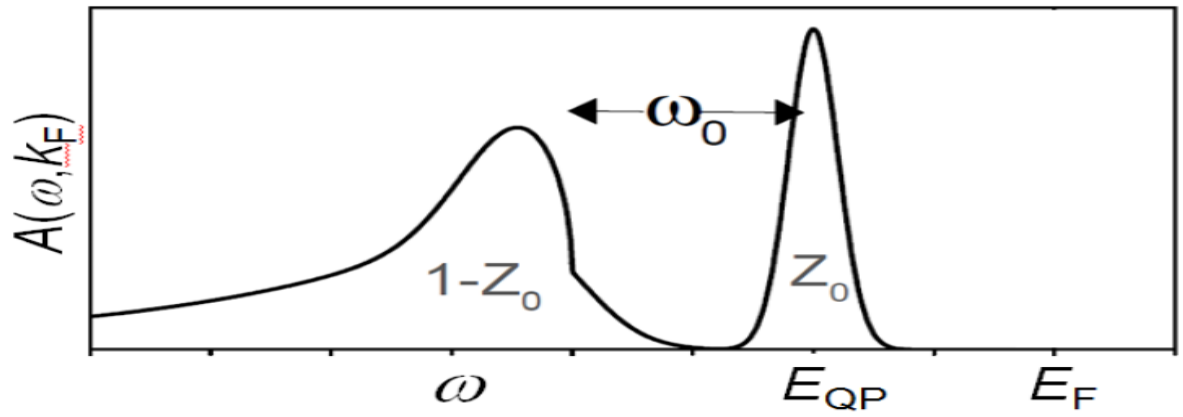


**Fig. 10.** Sketch of the polaron spectral function $A(\omega,\mathbf{k})$ at low electron excitation energy $E(\mathbf{k}) - E_F$. The characteristic peak-dip-hump (PDH) spectral shape is formed by the quasiparticle (QP) peak followed by the phonon sideband tail corresponding to a sequence of optical phonons with frequency $\omega_0$.

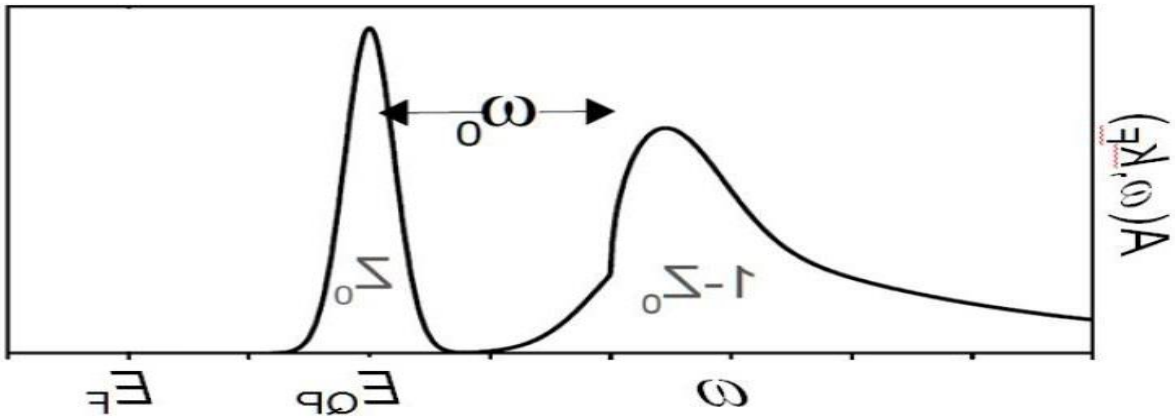

# Typical ARPES of interacting system

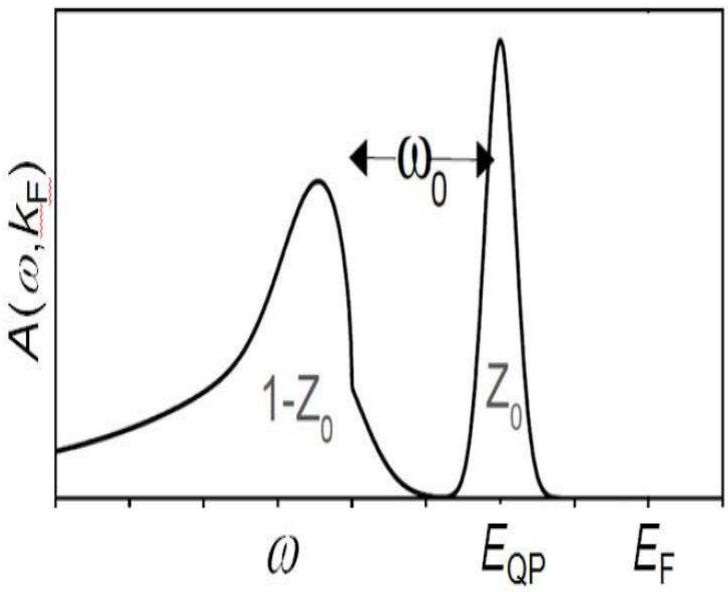


**Fig. 10.** Sketch of the polaron spectral function $A(\omega,\mathbf{k})$ at low electron excitation energy $E(\mathbf{k}) - E_F$. The characteristic peak-dip-hump (PDH) spectral shape is formed by the quasiparticle (QP) peak followed by the phonon sideband tail corresponding to a sequence of optical phonons with frequency $\omega_0$.

**Fig. 10.** Sketch of the polaron spectral function $A(\omega,\mathbf{k})$ at low electron excitation energy $E(\mathbf{k}) - E_F$. The characteristic peak-dip-hump (PDH) spectral shape is formed by the quasiparticle (QP) peak followed by the phonon sideband tail corresponding to a sequence of optical phonons with frequency $\omega_0$.

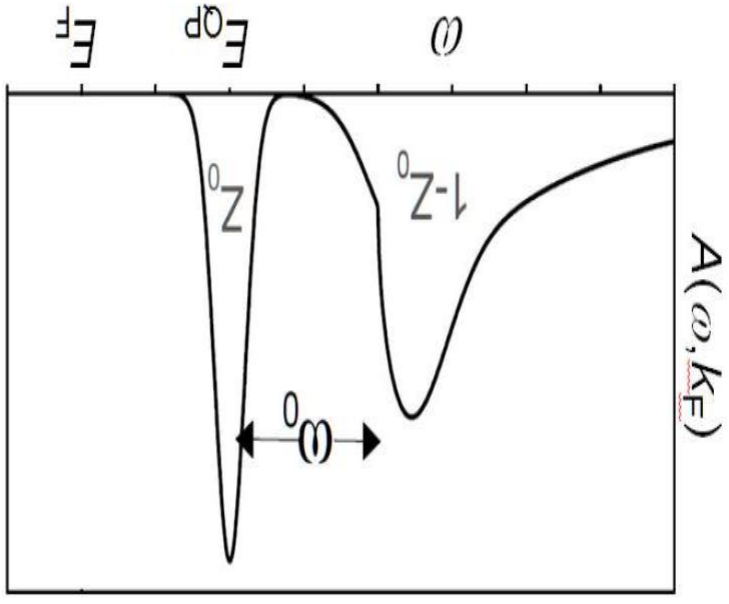

**Standard t-J model** (Hubbard large U) where hole moves in the antiferrromagnet.

Extended t-J model well describes the dispersion of the quasiparticle

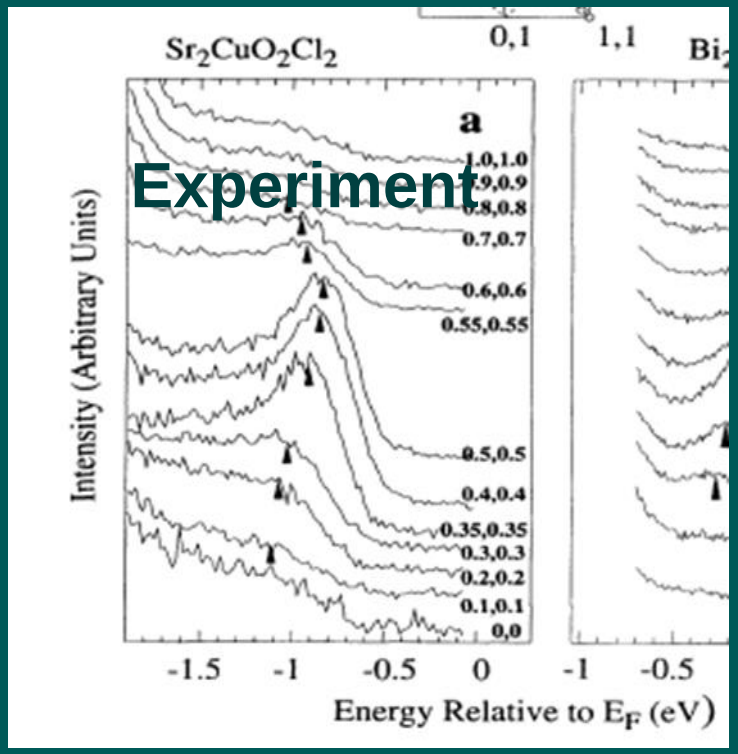


Wells et al, PRL (1995)

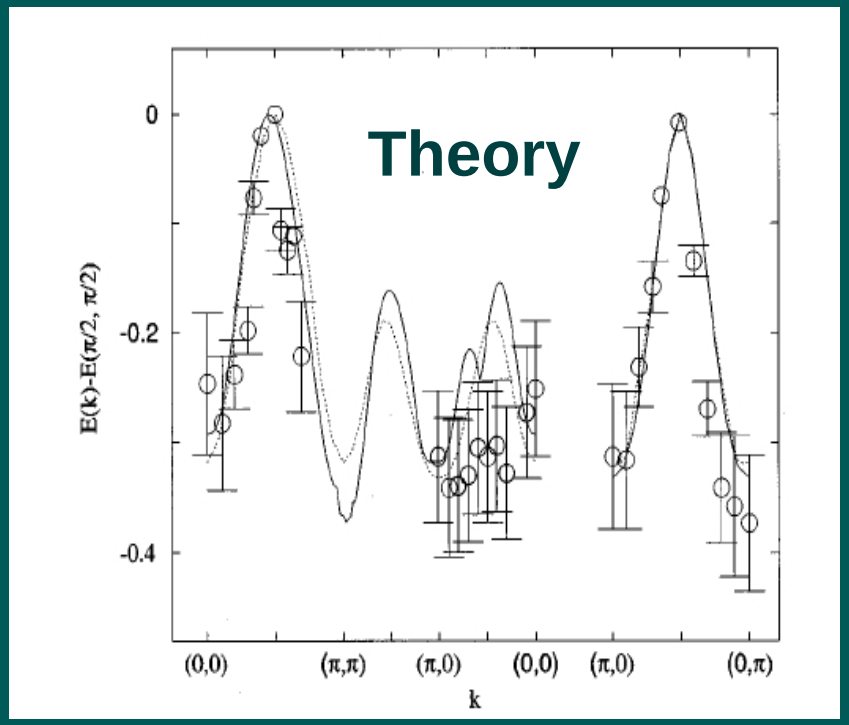


T. Xiang and J.M. Whetley, PRB, vol.54, R12653 (1996)

# Standard t-J model ……

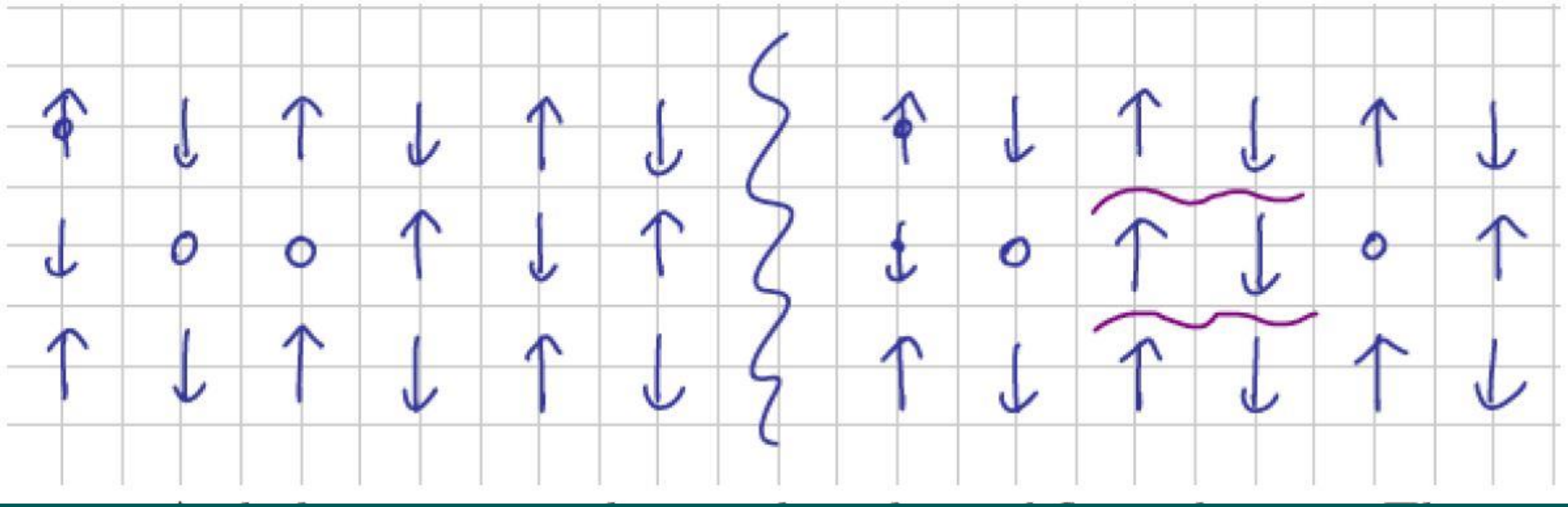

**String of the overturned pins prevent hole from free movement.**

# Theory: spectral function

Diagrammatic Monte Carlo

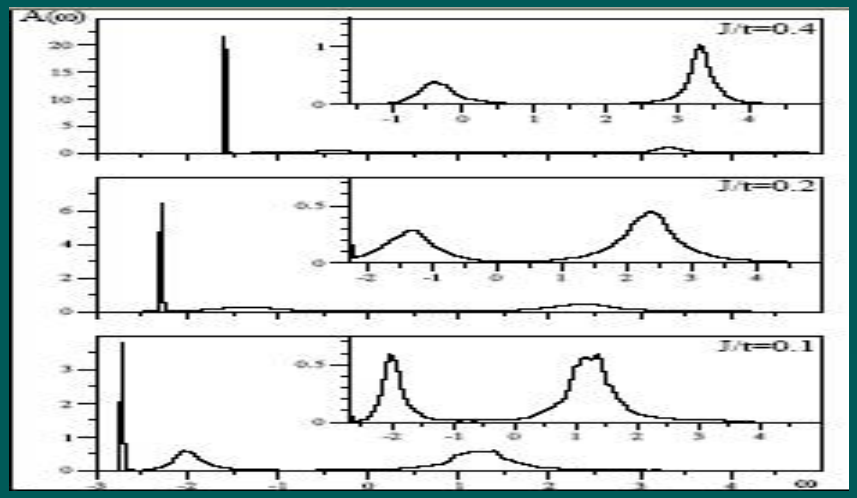


*ASM, B.V. Svistunov and N.V. Prokof'ev, PRB, vol. 64, 033101 (2001)*

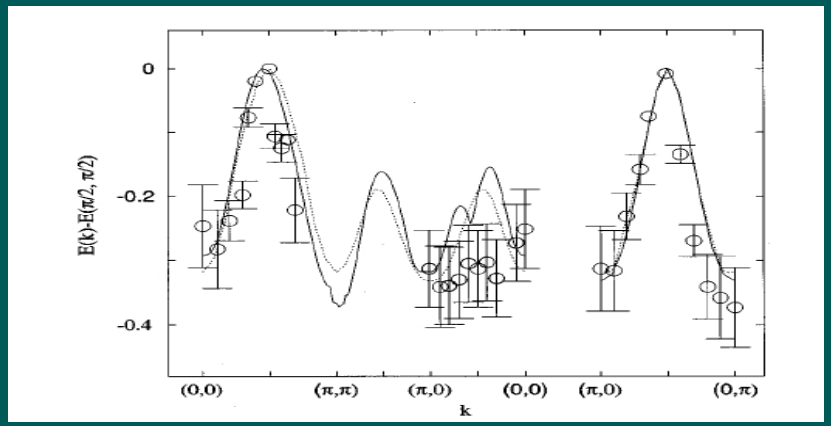


T. Xiang and J.M. Whetley, PRB, vol.54, R12653 (1996)

# Experiment: ARPES

**Extended t-J model gives wrong description of the peak width in ARPES**

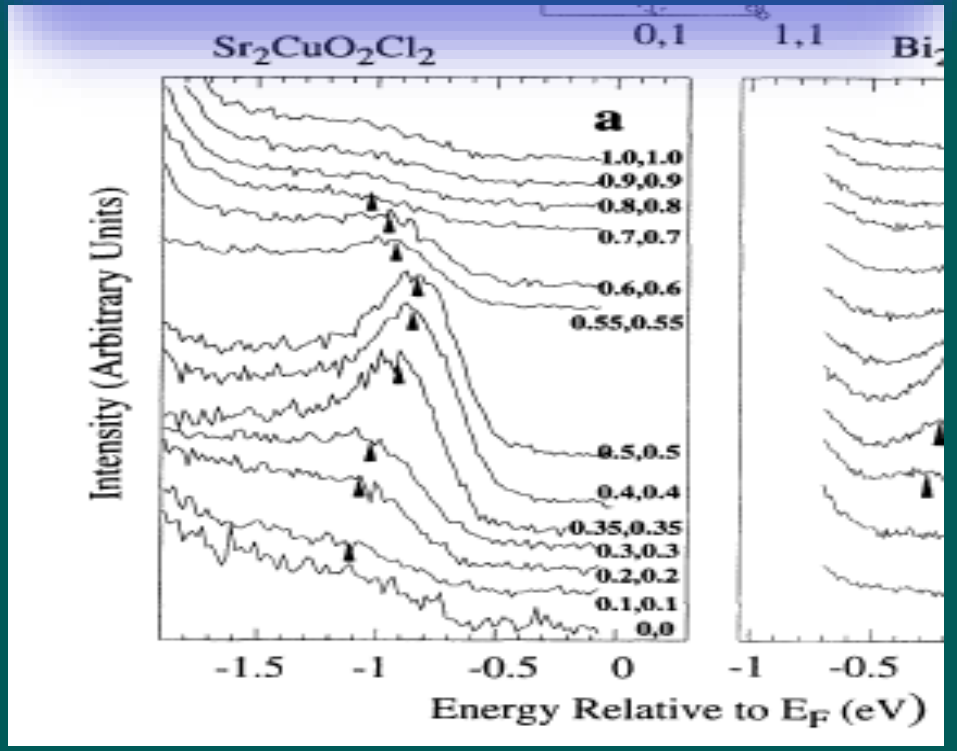


Wells et al, PRL (1995)

# Theory: spectral function

## Diagrammatic Monte Carlo

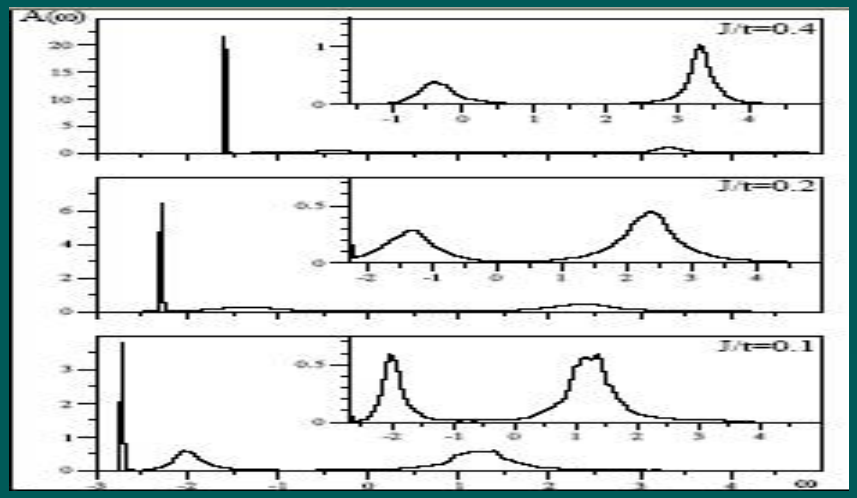


*ASM, B.V. Svistunov and N.V. Prokof'ev, PRB, vol. 64, 033101 (2001)*

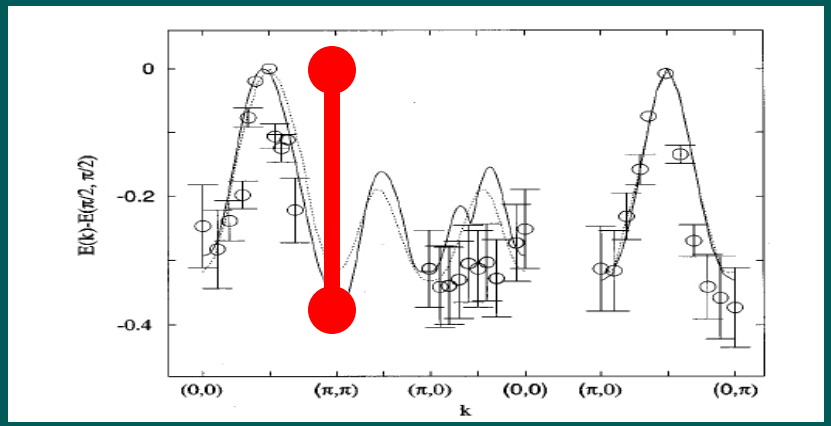


T. Xiang and J.M. Whetley, PRB, vol.54, R12653 (1996)

# Experiment: ARPES

**Extended t-J model gives wrong description of the peak width in ARPES**

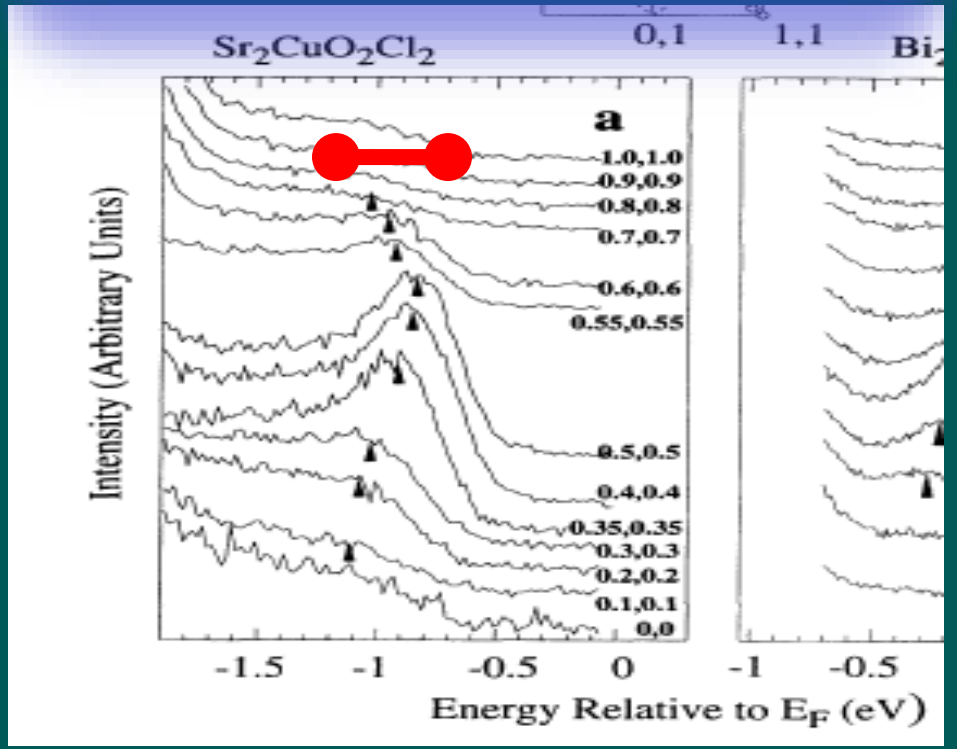


Wells et al, PRL (1995)

# Standard spin-wave approximation for a hole in the t-J model.

Hole with dispersion $\varepsilon(k)$ in the field magnons and EXTRA BOSONS

$$H^{(0)}_{tt't''-J} = \Sigma_k \varepsilon(k)\, h_k^+ h_k + \Sigma_k \upsilon(k)\, \alpha_k^+ \alpha_k + \Sigma_k \omega_{ph}\, b_k^+ b_k$$

Scattering on magnons: $H_{h\text{-}m} = N^{-1} \Sigma_{k,q} M_{k,q} [\, h_k^+ h_{k-q} \alpha_q + h.c.]$

… and on EXTRA bosons: $H_{h\text{-}ph} = N^{-1} \Sigma_{k,q} \gamma [\, h_k^+ h_{k-q} b_q + h.c.]$

***Dimensionless coupling constant : $\lambda = \gamma^2 / 4t\omega_{ph}$***

***$g = \lambda / 2$***

**Crossover to strong-coupling regime usually happens at λ=1**

# ARPES: dependence on the el-boson coupling

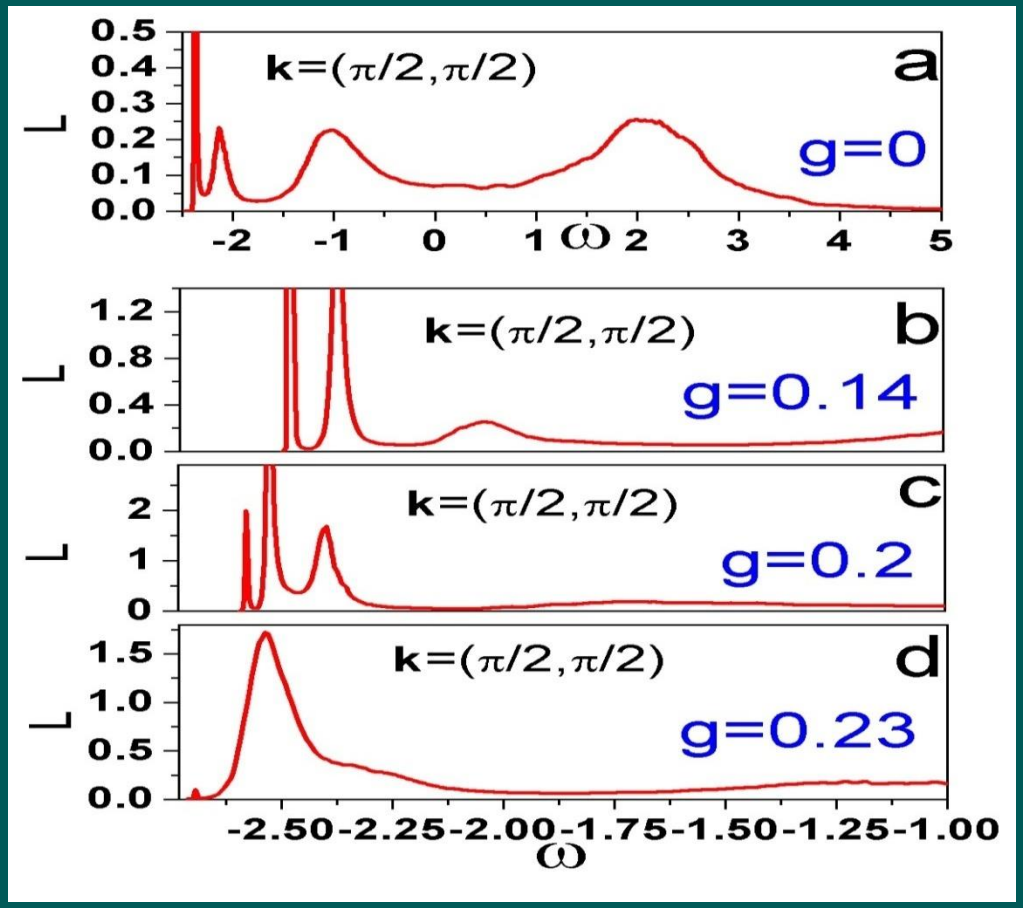


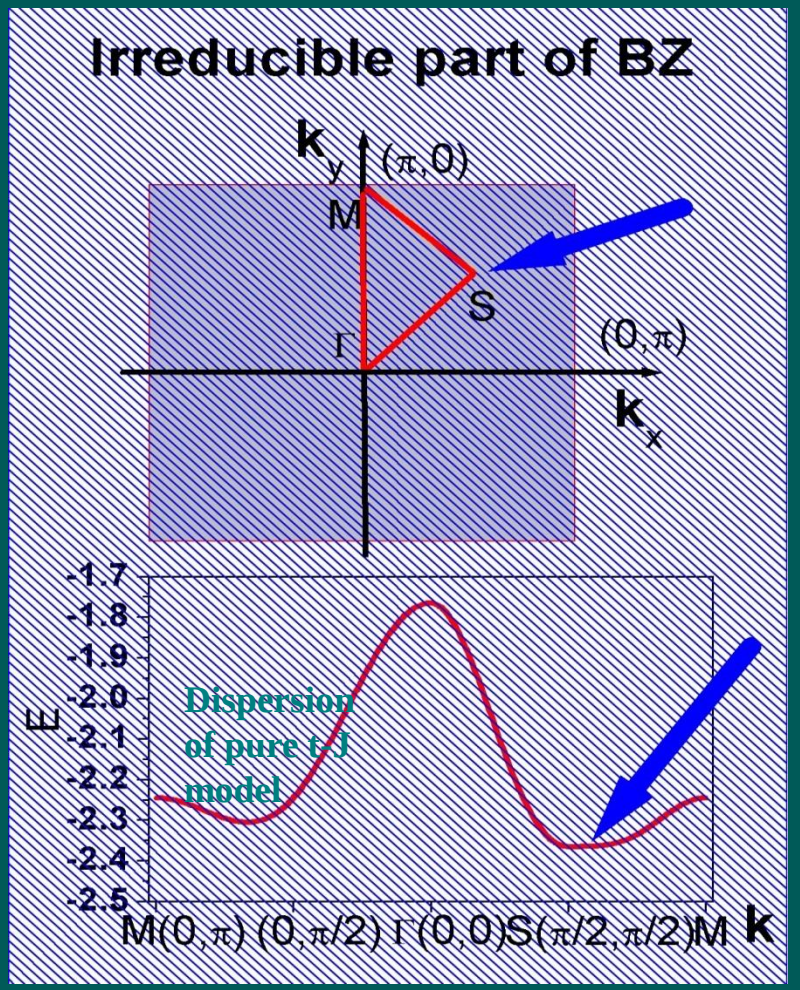


**ASM and N. Nagaosa,**
**Phys. Rev. Lett. 93, 036402 (2004)**

# Dispersion of the Franck-Condon peak

g=0.23

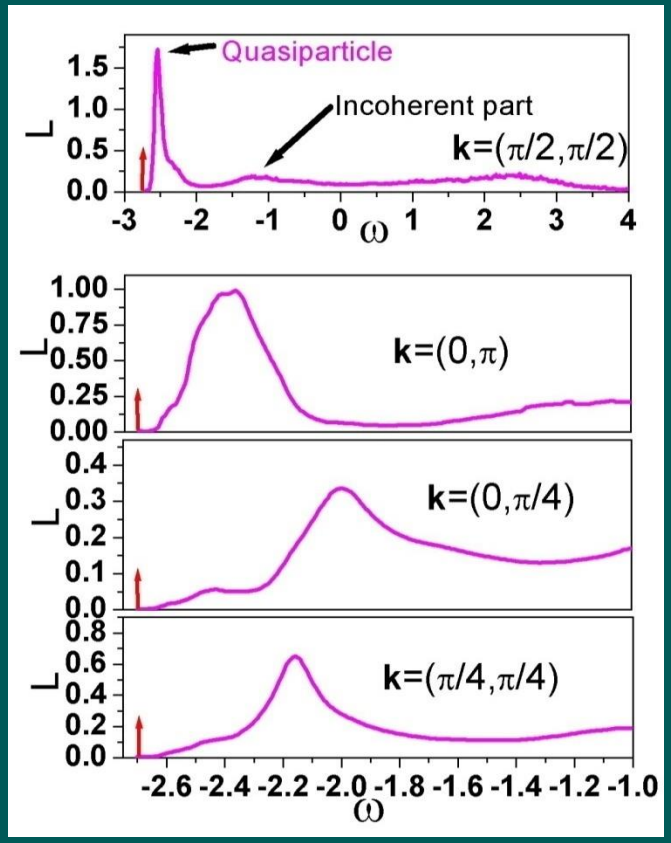


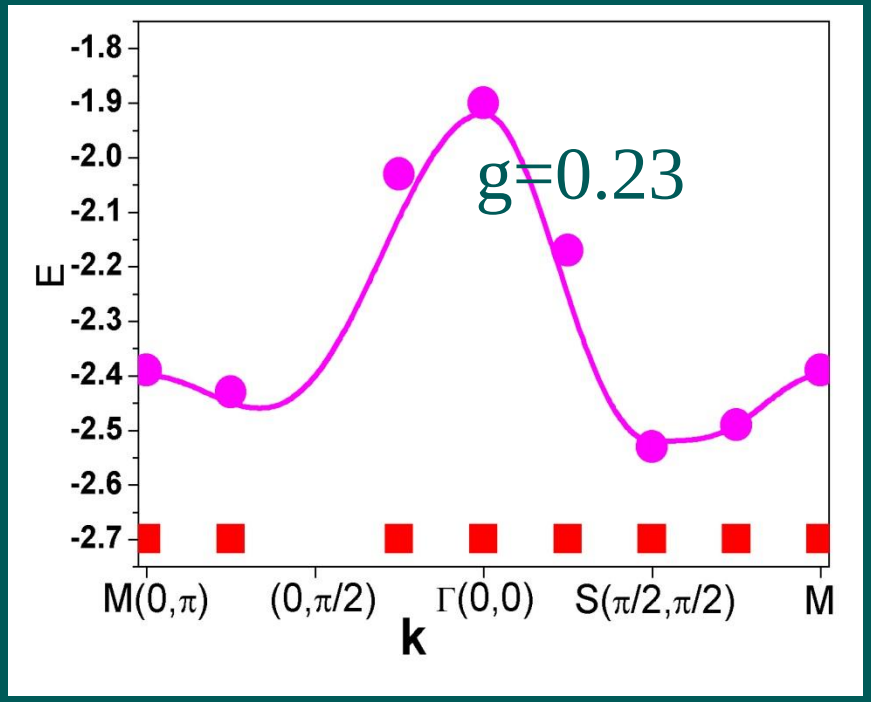


**Surprise: dispersion of wide peak *exactly* reproduces result of the t-J model.**

ASM and N. Nagaosa,
Phys. Rev. Lett. 93, 036402 (2004)

# Dispersion of the Franck-Condon peak

g=0.23

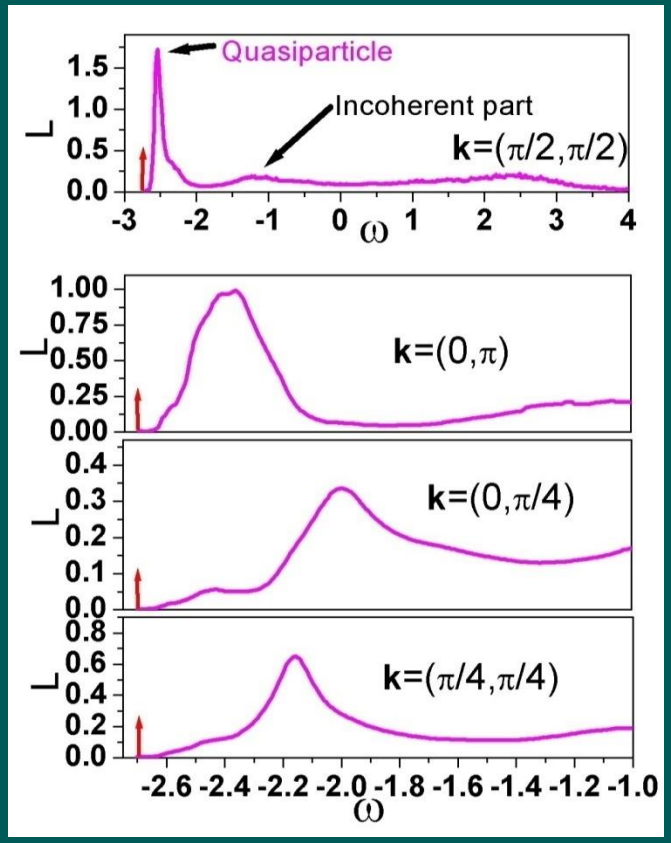


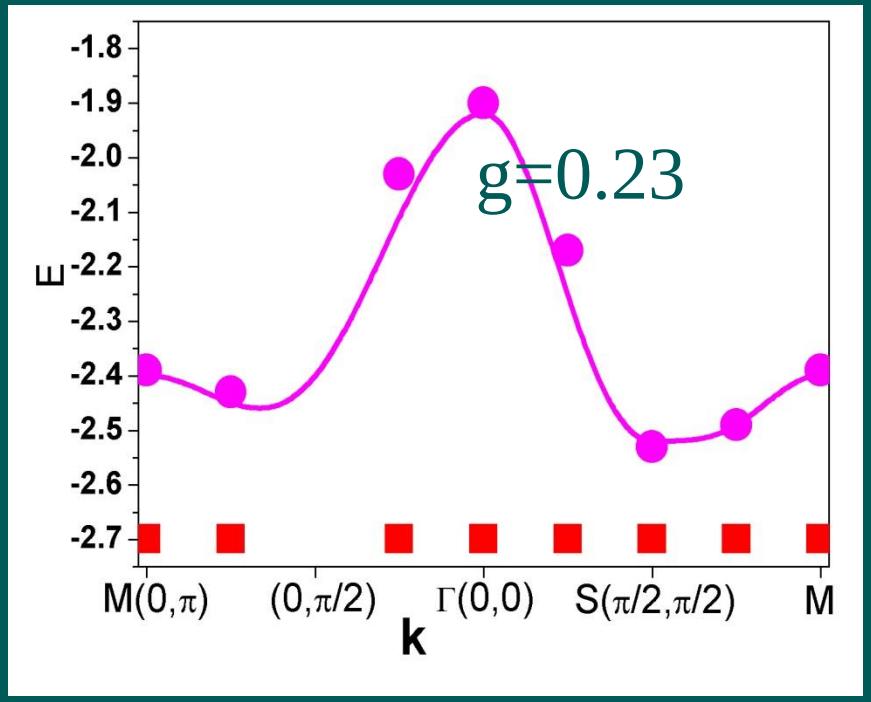


It is difficult to see real quasiparticle
because of small weight.

**ASM and N. Nagaosa,**
**Phys. Rev. Lett. 93, 036402 (2004)**

# Dispersion of the Franck-Condon peak

g=0.23

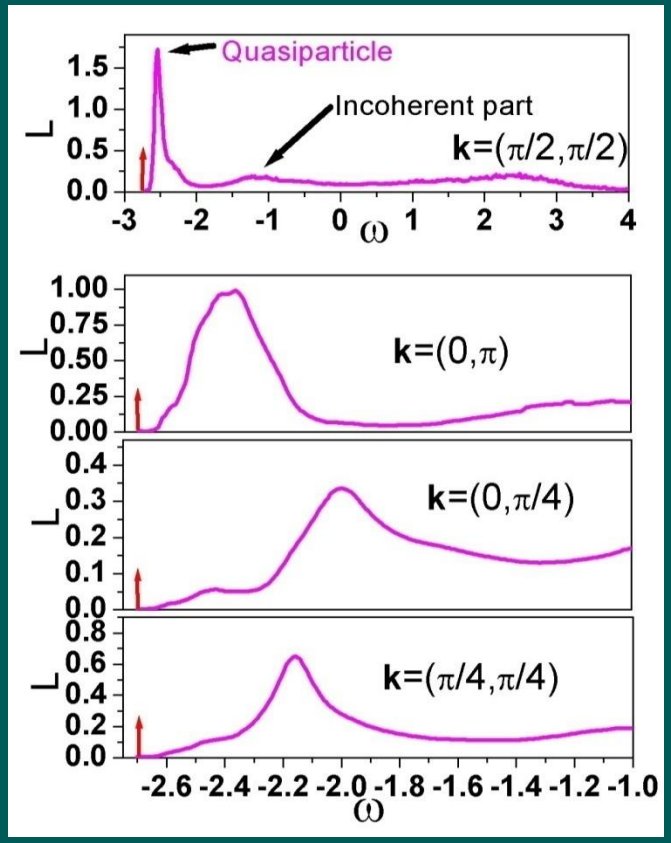


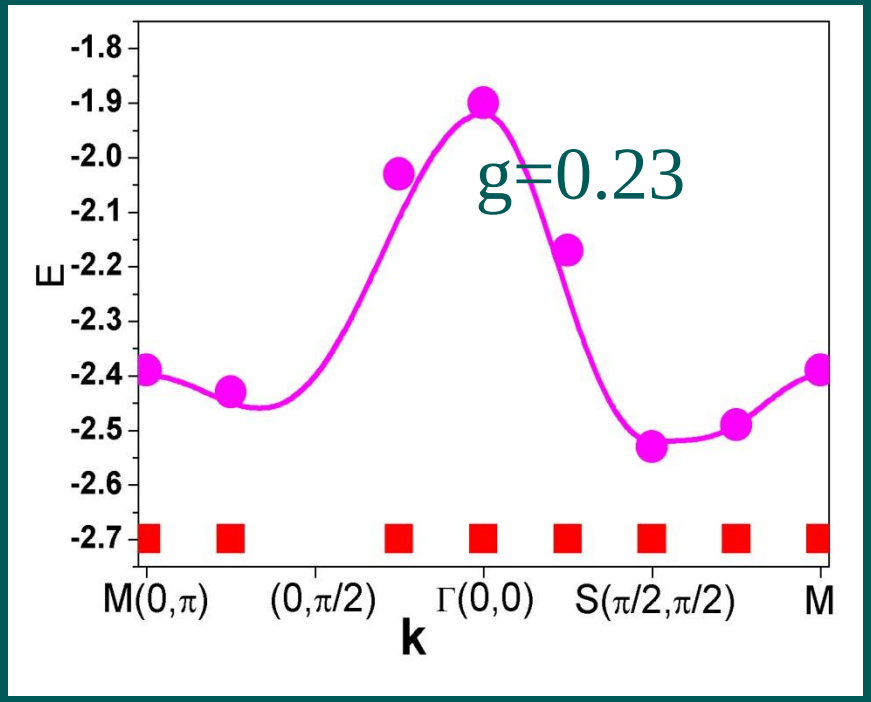


It is difficult to see real quasiparticle
because of small weight.

**ASM and N. Nagaosa,**
**Phys. Rev. Lett. 93, 036402 (2004)**

***Chemical potential !!!!!***

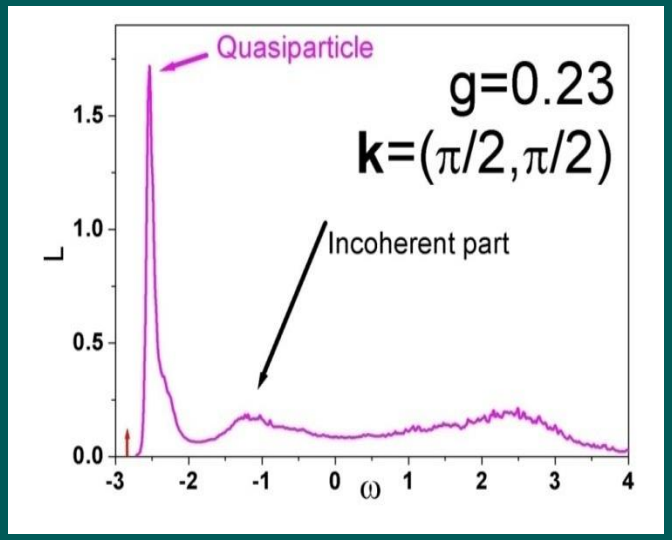


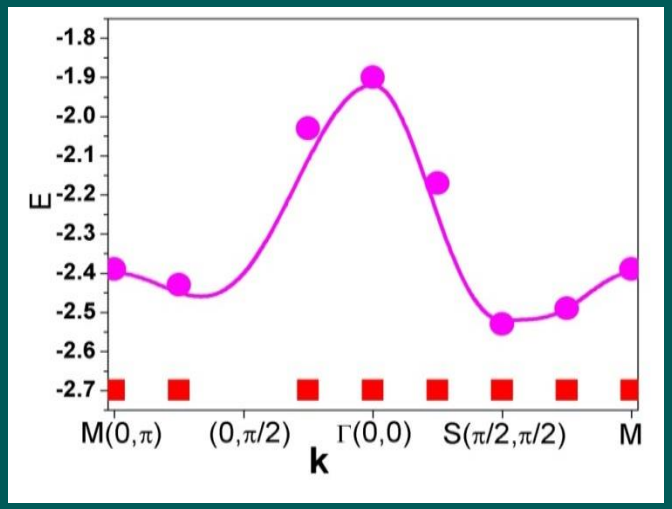


**Chemical potential must be separated from the "fake" QP**

**μ**

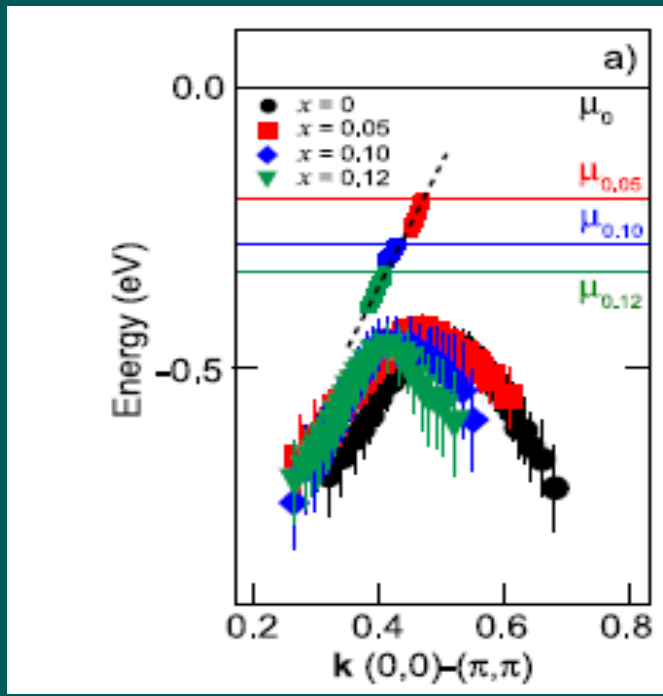


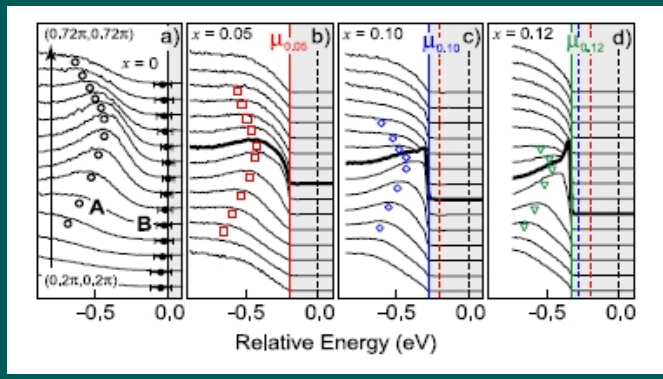


ASM and N. Nagaosa,
Phys. Rev. Lett. 93, 036402 (2004)

K. M. Shen et al
Phys. Rev. Lett. 93, 267002 (2004)

# Linewidth ratio W(x,x)/W(π/2,π/2) exactly reproduces experiment

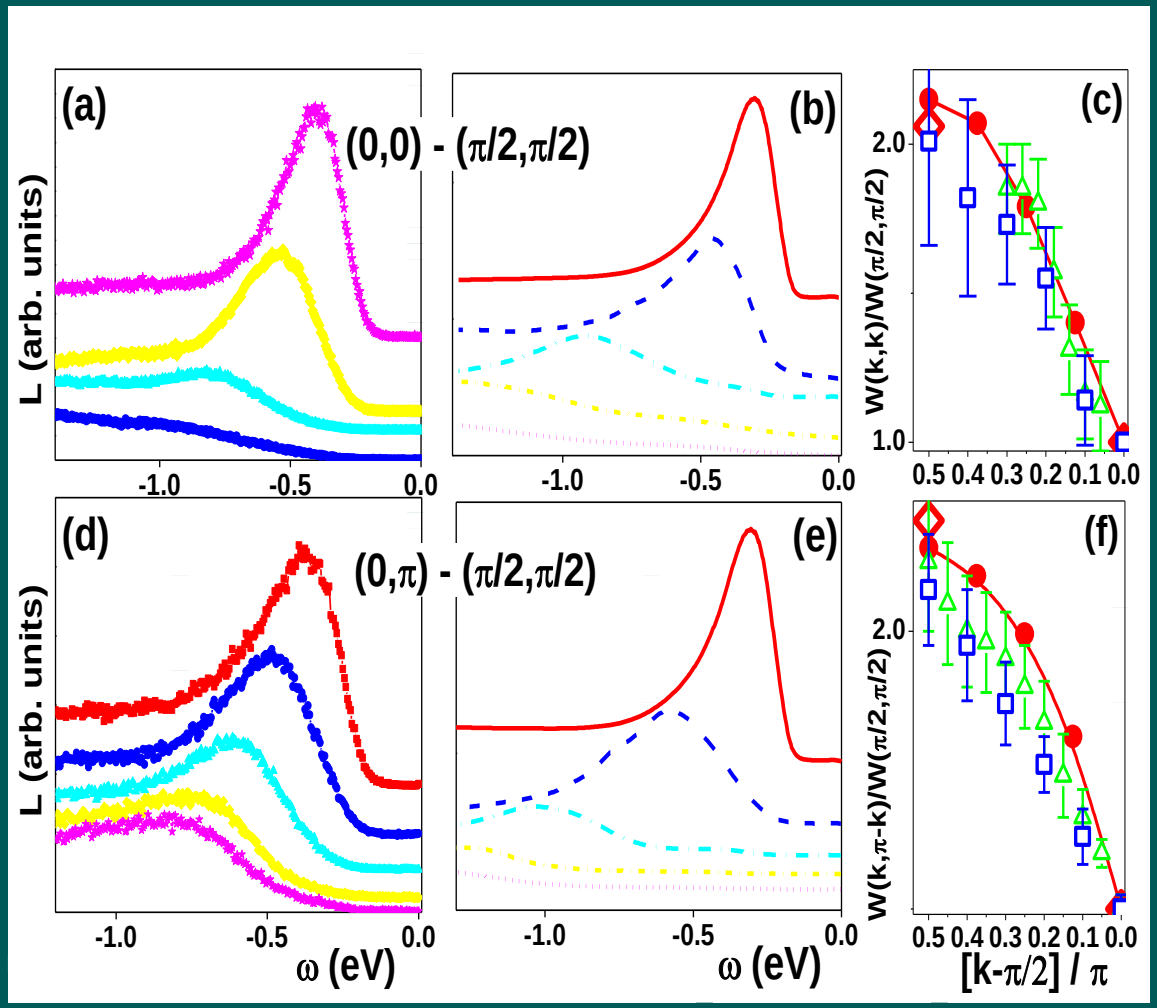


**The ratio**
**W(x,x) / W(π/2,π/2)**
**is universal**
**in theory**
**for any λ in**
**strong coupling**
**regime**
**(λ=0.7,1.0)**
**and universal**
**in experiment**
**for different**
**compounds**
**$(Sr,Ca)_2CuO_2Cl_2$**

Why we need additional electron-boson interaction on top of Hubbard model to explain

# OPTICAL CONDUCTIVITY

# (underdoped !!!)

# Optical conductivity: Are there some contributions from both magnetic (Hubbard) and EXTRA bosonic systems ?

## MIR in experiment

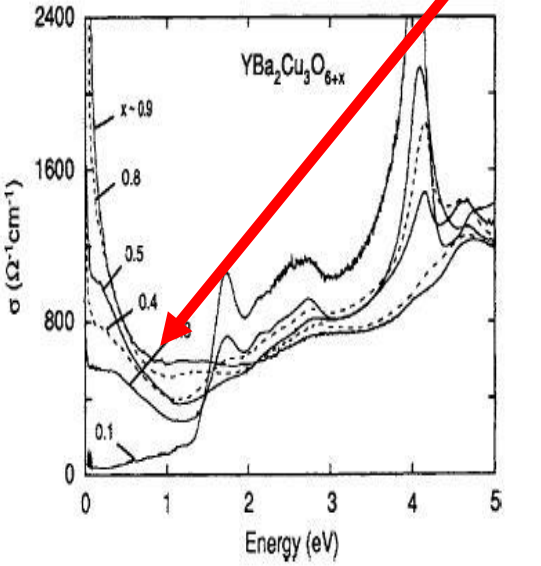


FIG. 10. In-plane ($E \perp c$) optical conductivity $\sigma(\omega)$ obtained from a Kramers-Kronig analysis of the reflectivity data for various compositions of $YBa_2Cu_3O_{6+x}$. Adapted from Cooper, Reznik, *et al.*, 1993.

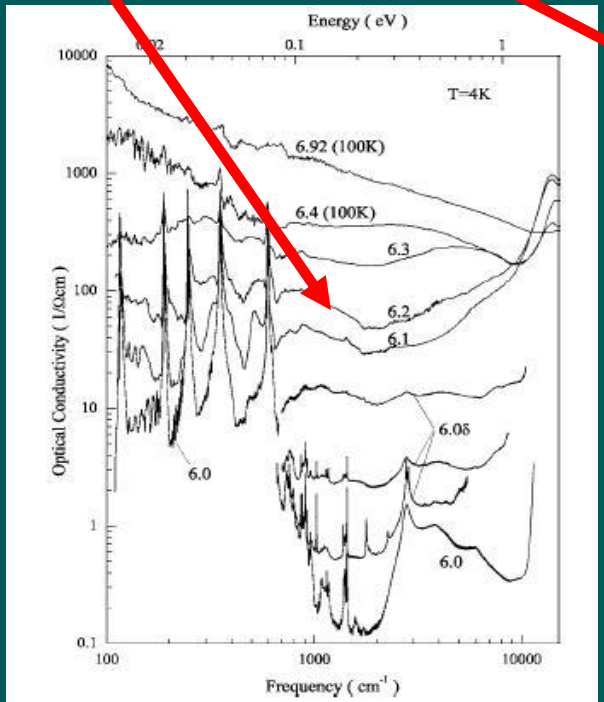


FIG. 9. Doping dependence of $YBa_2Cu_3O_x$ at 4 K (100 K for the superconducting samples with $x$=6.4 and 6.92). From Gruninger, 1999.

Basov

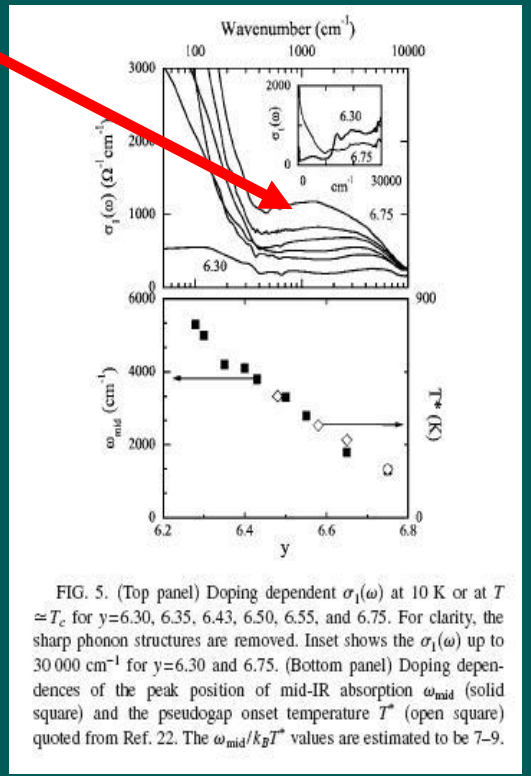


FIG. 5. (Top panel) Doping dependent $\sigma_1(\omega)$ at 10 K or at $T \simeq T_c$ for $y$=6.30, 6.35, 6.43, 6.50, 6.55, and 6.75. For clarity, the sharp phonon structures are removed. Inset shows the $\sigma_1(\omega)$ up to 30 000 cm$^{-1}$ for $y$=6.30 and 6.75. (Bottom panel) Doping dependences of the peak position of mid-IR absorption $\omega_{mid}$ (solid square) and the pseudogap onset temperature $T^*$ (open square) quoted from Ref. 22. The $\omega_{mid}/k_BT^*$ values are estimated to be 7–9.

**Cooper, Reznik et al 1993**

**Gruninger 1999**

**Lee at al 2005**

# MIR – contradiction with experiment No 1

**Pure t-J model**

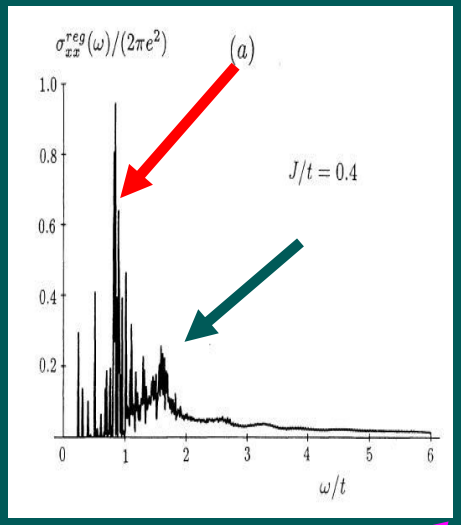


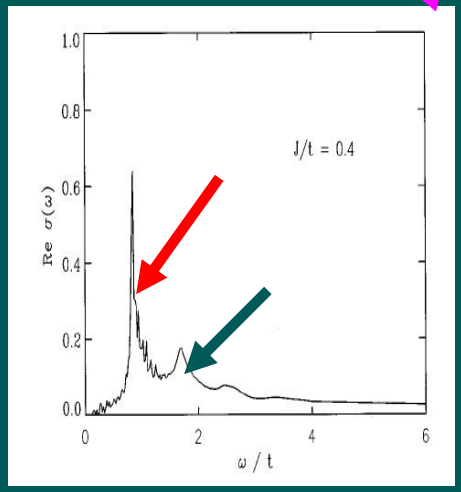


**Experiment:**
**MIR = 0.5 eV**
**at low doping**

**Theory:**
**t=0.4 eV, J=0.35t.**
**MIR = 0.28 eV**

**Experiment**

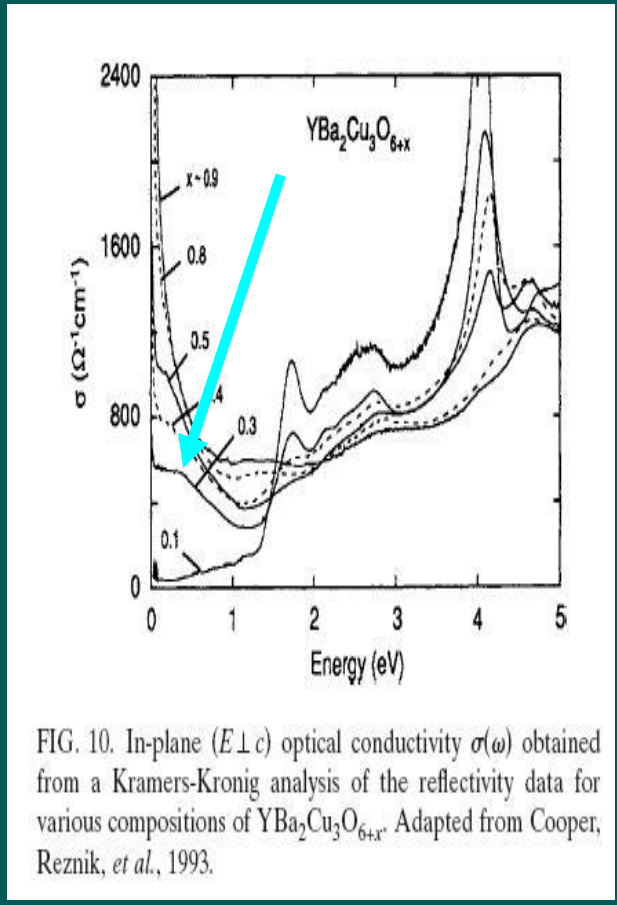


FIG. 10. In-plane ($E \perp c$) optical conductivity $\sigma(\omega)$ obtained from a Kramers-Kronig analysis of the reflectivity data for various compositions of $YBa_2Cu_3O_{6+x}$. Adapted from Cooper, Reznik, *et al.*, 1993.

# MIR – contradiction with experiment No2

**Pure t-J model**

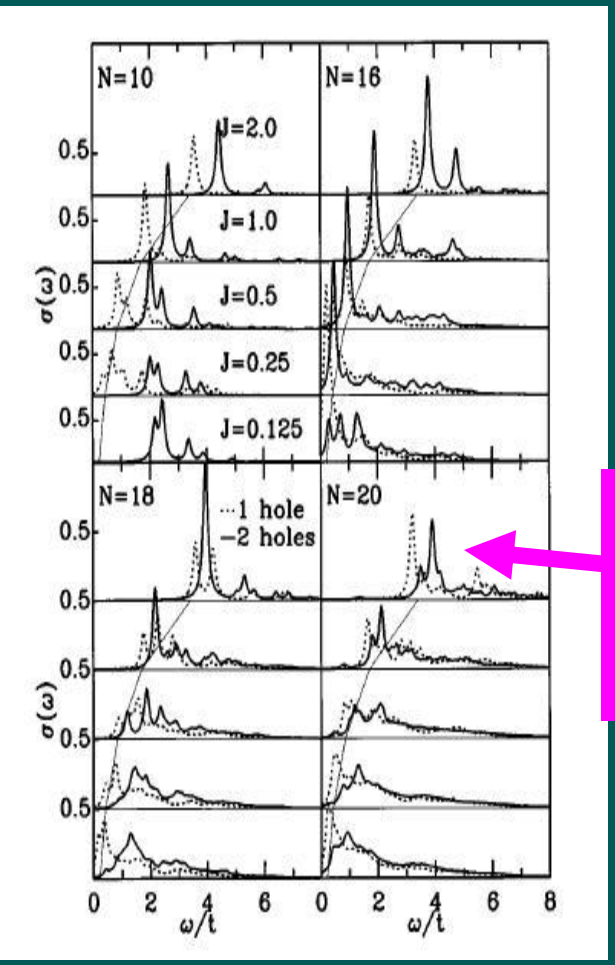


**Experiment:**
**MIR energy decreases with with doping.**

**Theory: other way around.**

**Extra bosons?**

**Experiment**

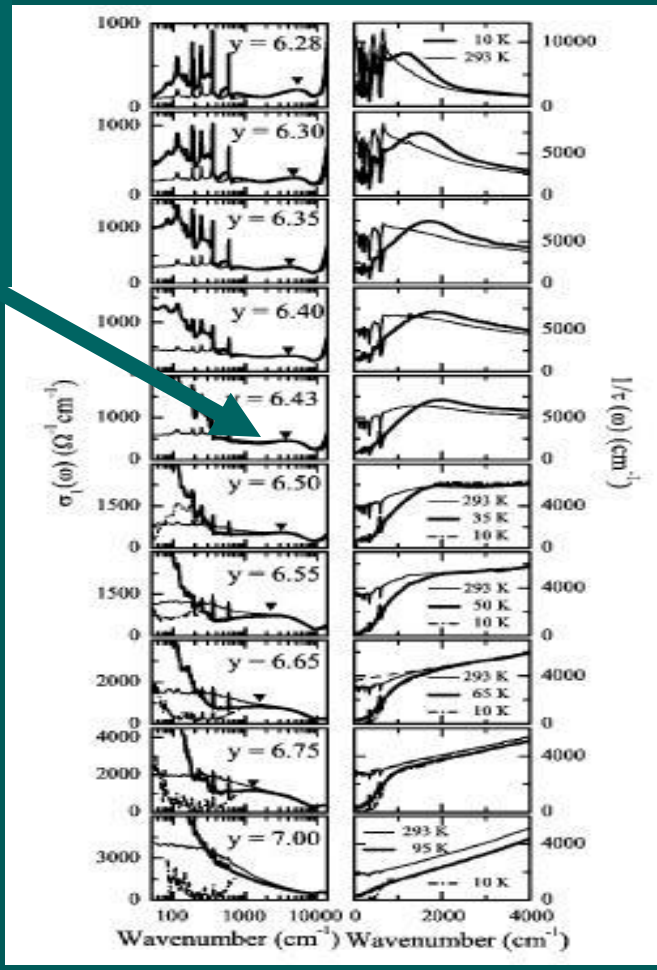

# Evolution of the OC with electron-boson coupling (Hubbard-Holstein model, i.e. electron-boson coupling on top of Hubbard model).

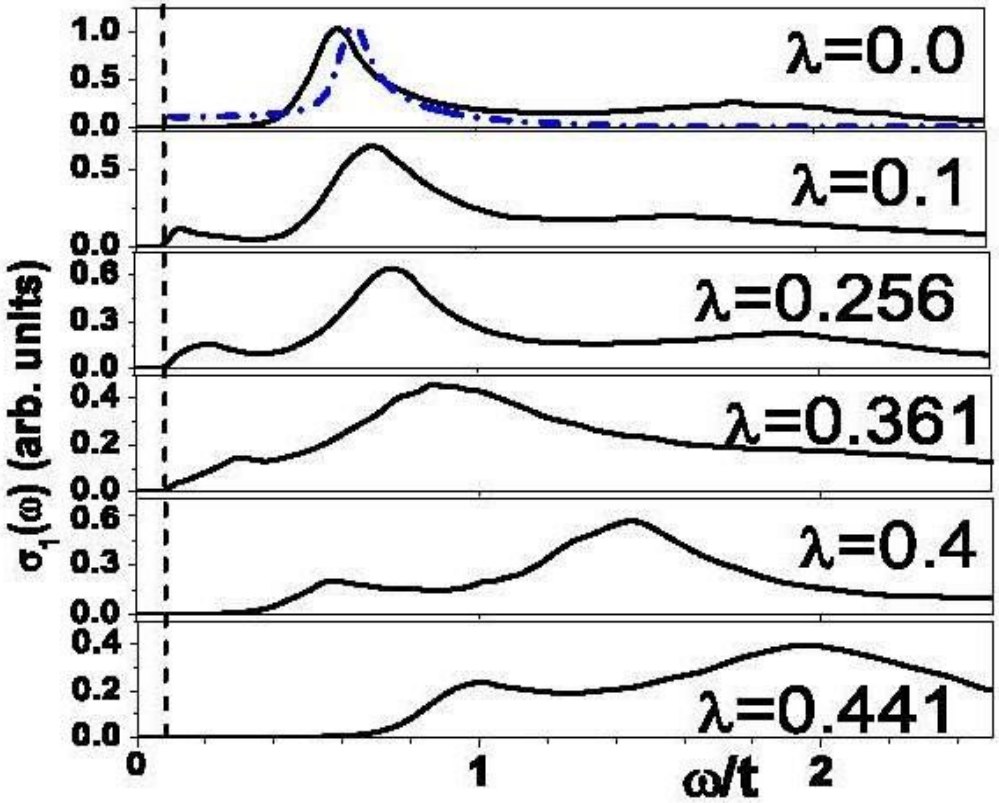


Diagrammatic Monte Carlo and SOCC

ASM, N. Nagaosa, Z.-X. Shen, G. De Filippis, V. Cataudella, T. P. Devereaux, C. Bernhard, K.W. Kim, and J. Zaanen, Phys. Rev. Lett. 100, 166401 (2008)

# Two peaks in OC

Phonon

Peak I

Peak II

OC t-J-Holstein

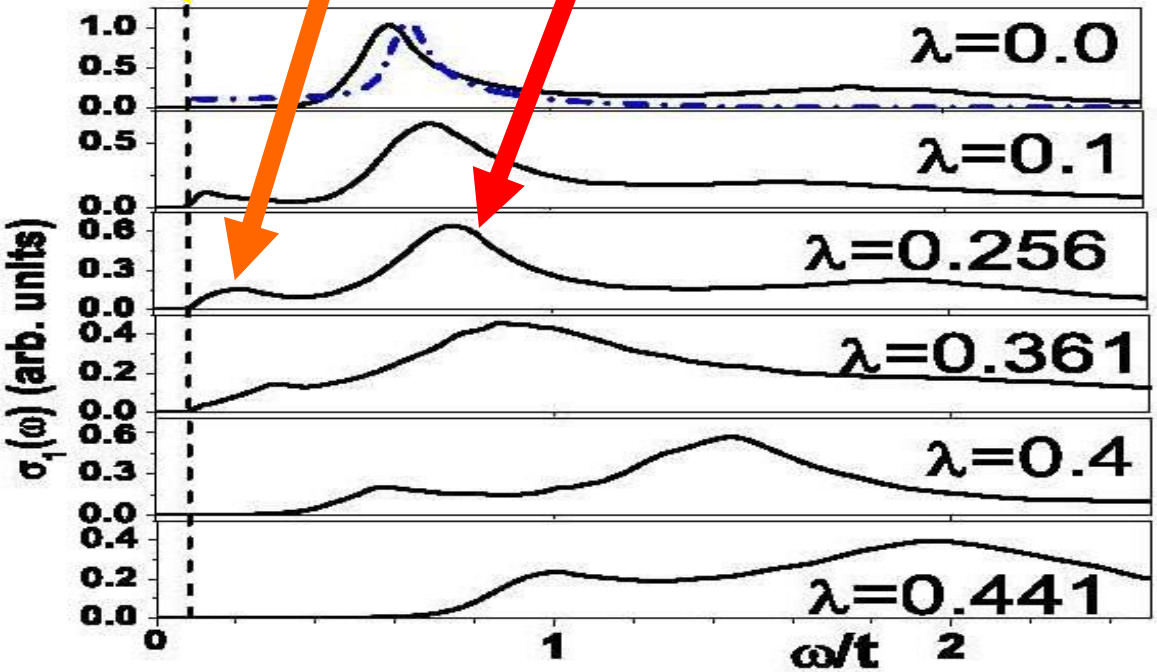


OC Holstein

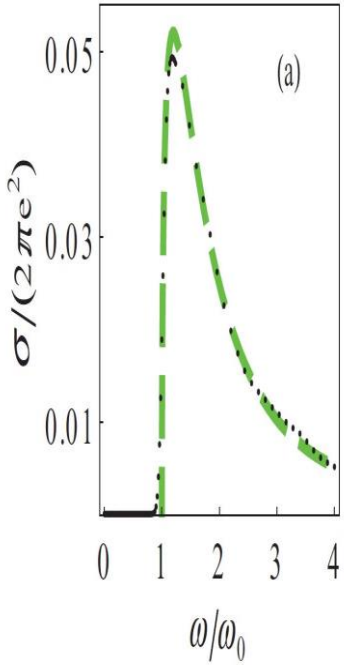


ASM, N. Nagaosa, Z.-X. Shen, G. De Filippis, V. Cataudella, T. P. Devereaux, C. Bernhard, K.W. Kim, and J. Zaanen, Phys. Rev. Lett. 100, 166401 (2008)

# Diagrammatic Monte Carlo

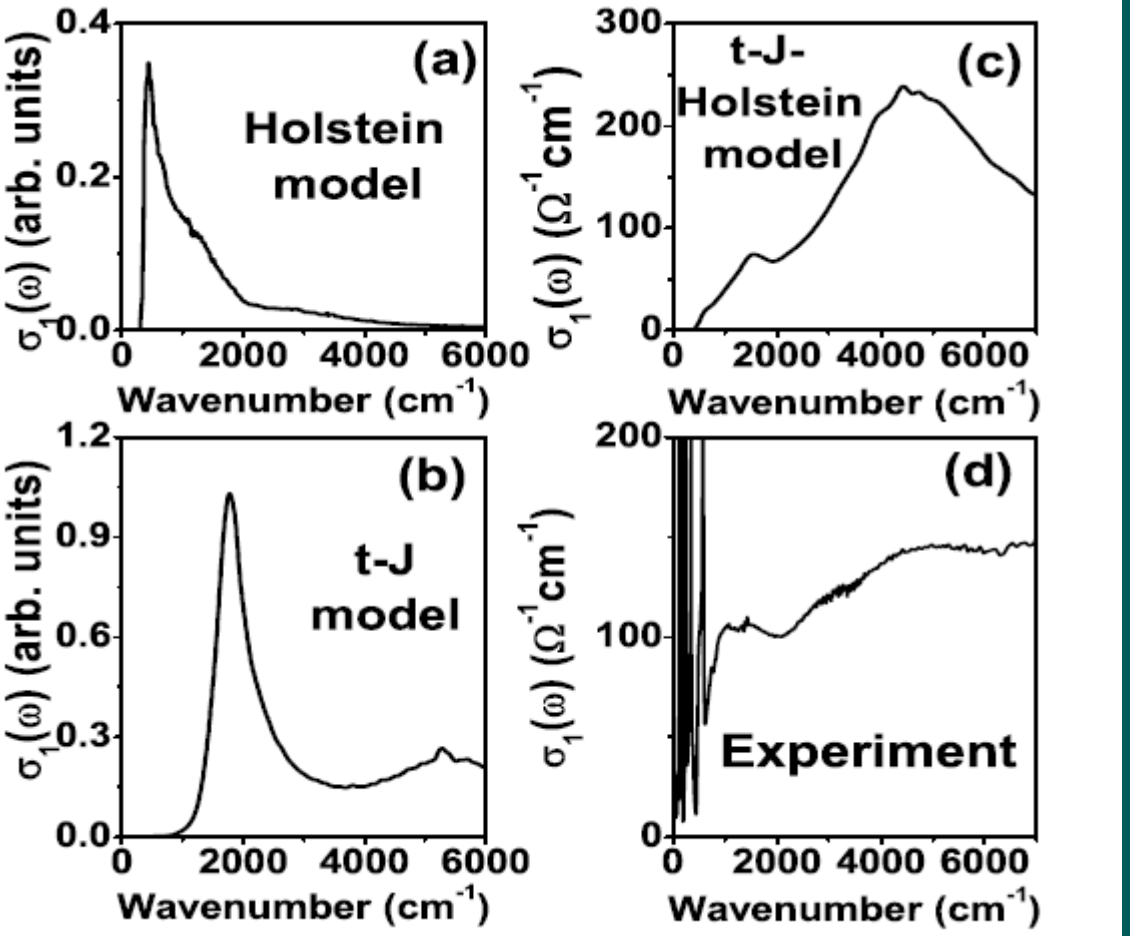


**Note: for 2-peak structure of the optical conductivity both magnetic system and a coupling to an extra magnetic mode is required.**

**Ellipsometry:**
**1.5% hole doped**
**$(Eu_{1-x}Ca_x)Ba_2Cu_3O_6$**


ASM, N. Nagaosa, Z.-X. Shen, G. De Filippis, V. Cataudella, T. P. Devereaux, C. Bernhard, K.W. Kim, and J. Zaanen, Phys. Rev. Lett. 100, 166401 (2008)

**Why we need additional electron-boson interaction on top of Hubbard model to explain**

# TEMPERATURE DEPENDENCE (underdoped !!)

# Temperature dependence of ARPES

George Sawatzky

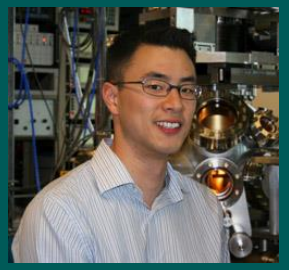

Kyle Shen and Z.-X. Shen et al

**The linewidth, seems, extrapolates to zero ……**

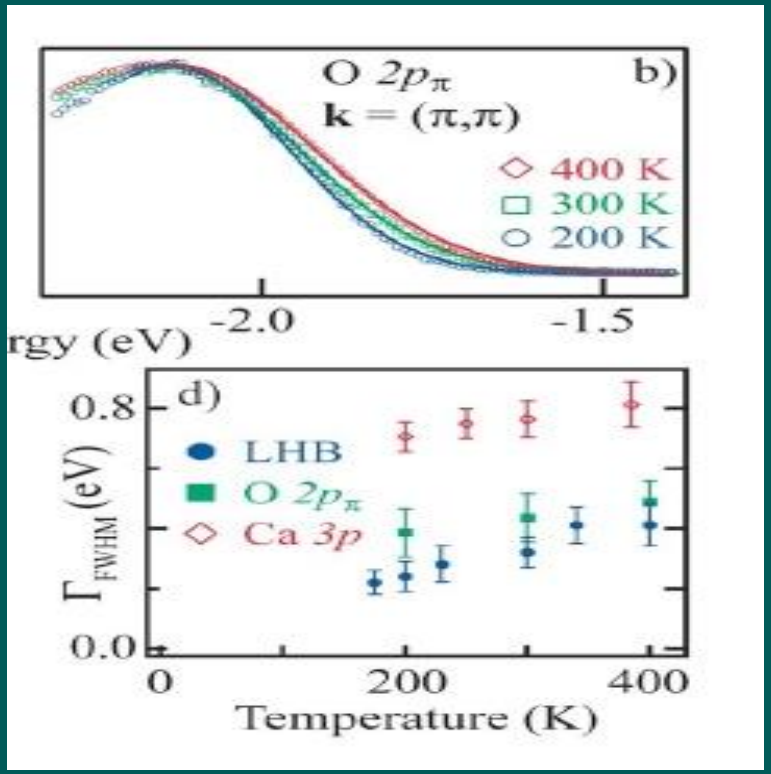


K.M. Shen, Phys. Rev. B 75, 075115 (2007)

# Temperature dependence of ARPES

Mona Berciu
Vancouver

**Momentum Average Berciu Method (MABM)**

Giulio de Filippis

and

Vittorio Cataudella

Napoli

**Self-Consistent Born Approximation (SCBA)**

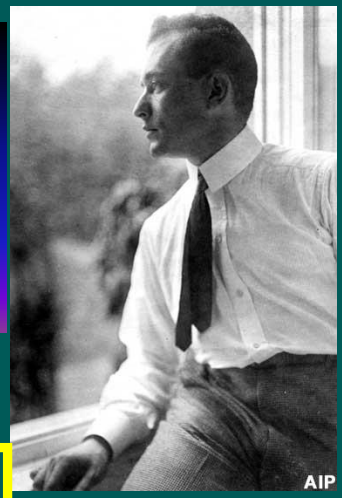


Max Born
1882-1970

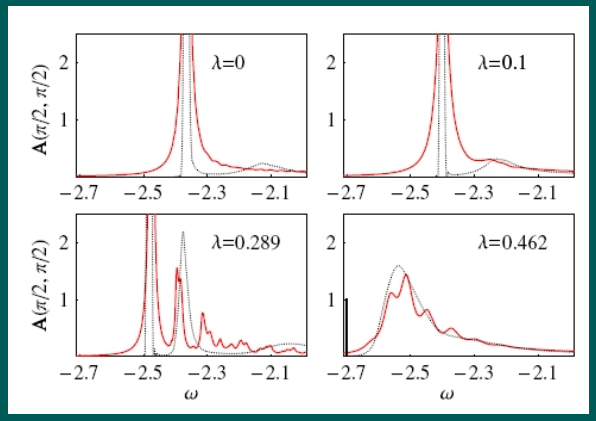


**Hybrid Dynamical Momentum Average Method (HDMAM)**

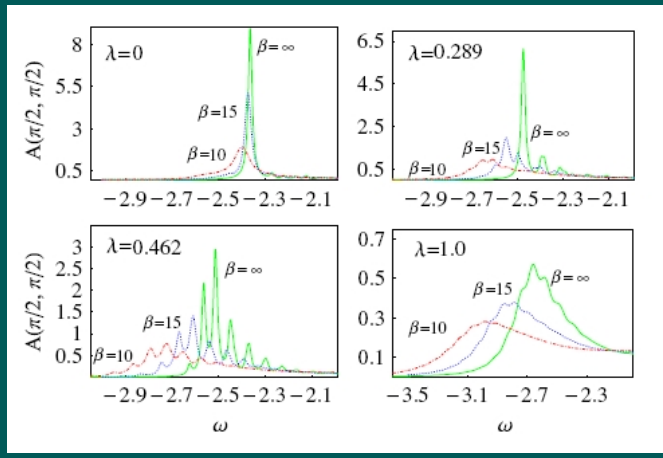


V. Cataudella et al, Phys. Rev. Lett. 99, 226402 (2007)

# Temperature dependence of ARPES

George Sawatzky

The linewidth, as seems, extrapolates to zero ……

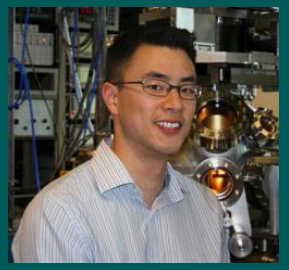

Kyle Shen and Z.-X. Shen et al

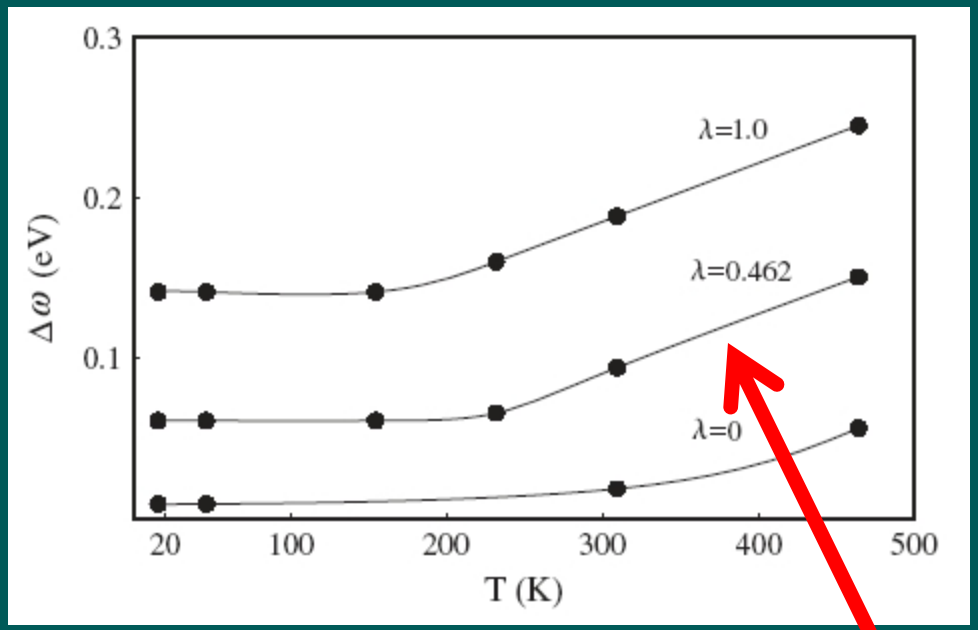


V. Cataudella et al, Phys. Rev. Lett. 99, 226402 (2007)

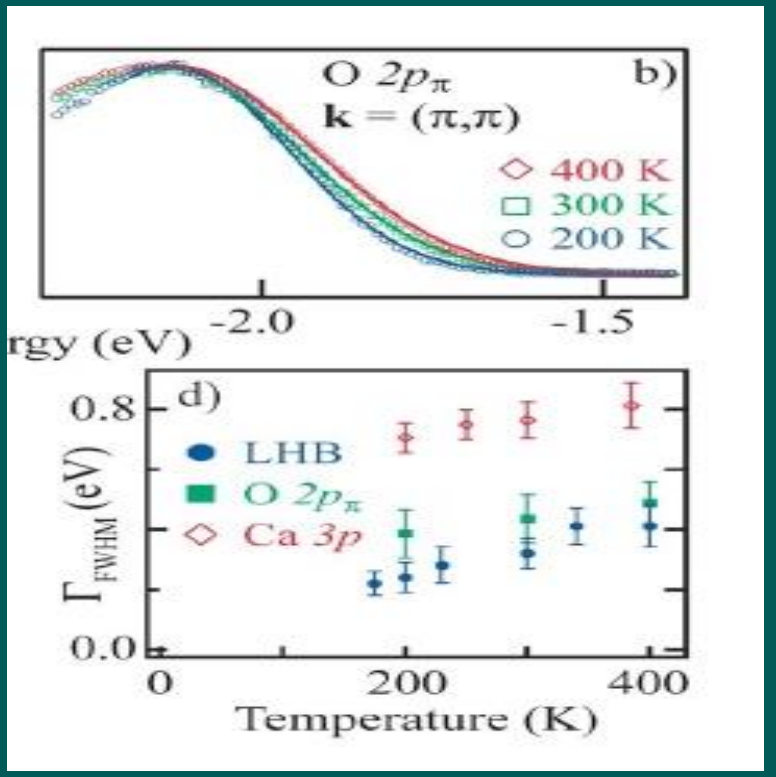


K.M. Shen, Phys. Rev. B 75, 075115 (2007)

λ>0.4 is already strong coupling

**Why we need additional electron-boson interaction on top of Hubbard model to explain**

# PUMP-PROBE PHENOMENA (undoped !!)

# Novel kind of pump-probe phenomenon

## Witnessing the formation and relaxation of dressed quasi-particles in a strongly correlated electron system

Fabio Novelli[1,2], Giulio De Filippis[3], Vittorio Cataudella[3], Martina Esposito[1], Ignacio Vergara[4], Federico Cilento[2], Enrico Sindici[1], Adriano Amaricci[5], Claudio Giannetti[6,7], Dharmalingam Prabhakaran[8], Simon Wall[9], Andrea Perucchi[2,10], Stefano Dal Conte[11], Giulio Cerullo[11], Massimo Capone[5], Andrey Mishchenko[12,13], Markus Grüninger[4], Naoto Nagaosa[12,14], Fulvio Parmigiani[1,2,4] & Daniele Fausti[1,2]

NATURE COMMUNICATIONS | 5:5112 | DOI: 10.1038/ncomms6112

# Pump-probe phenomena.

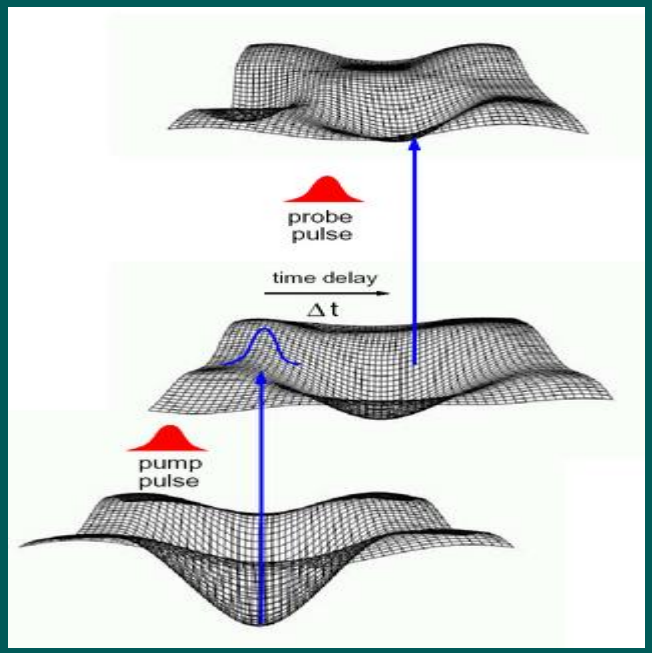


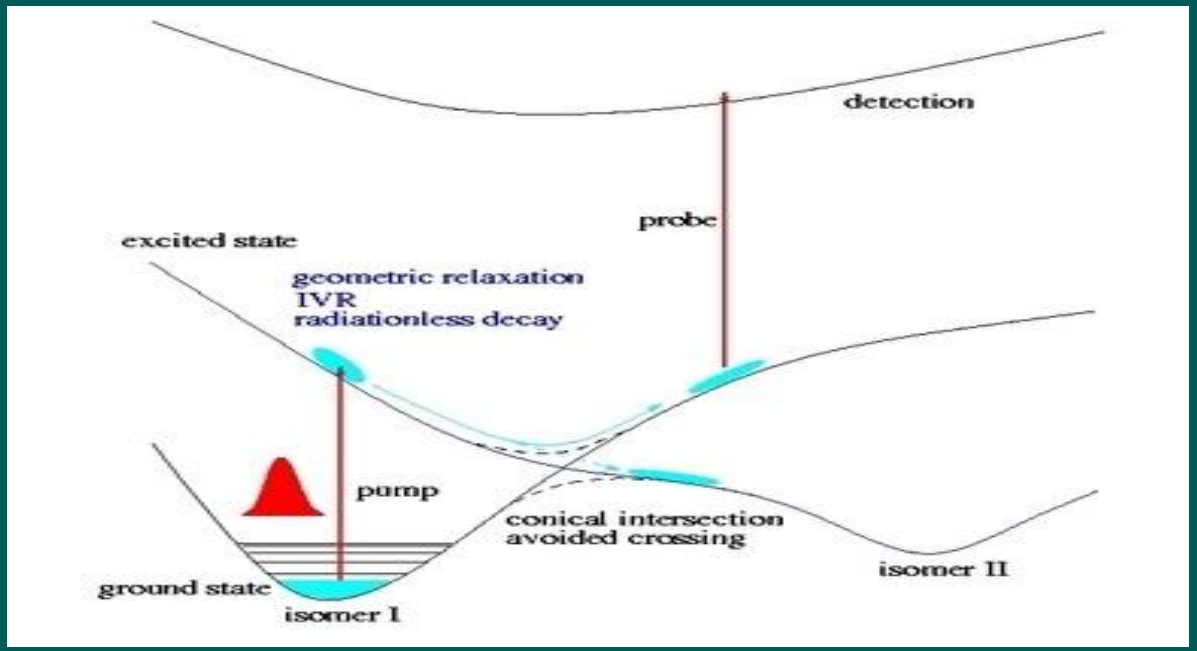


**General understanding:**
**To change the electronic state and watch how system evolves with time.**

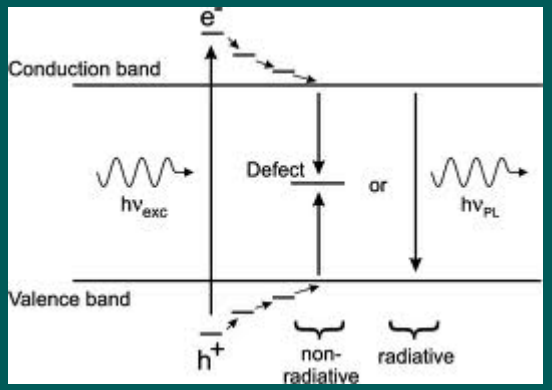

# Pump-probe phenomena.

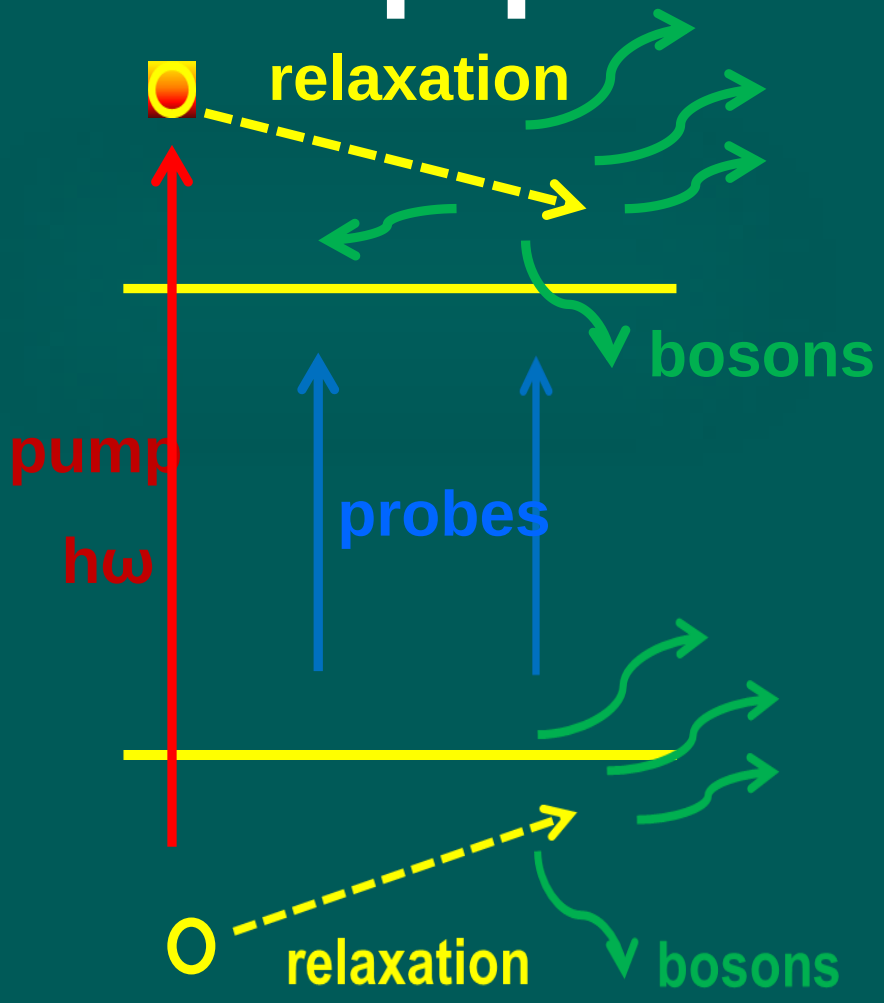


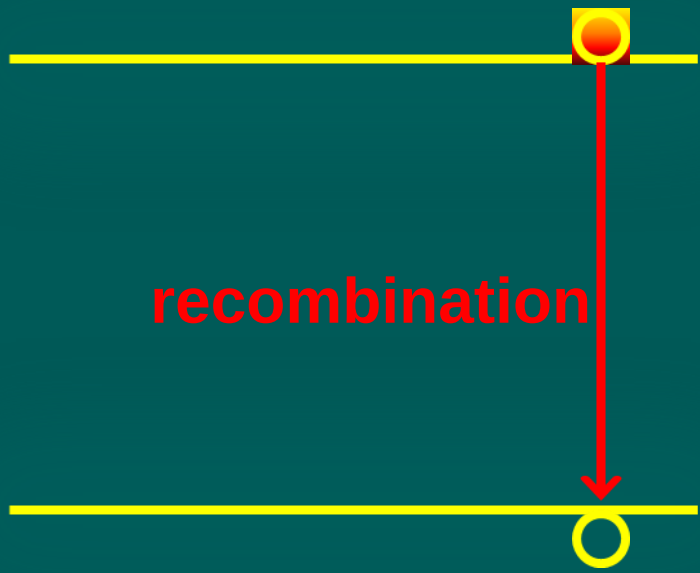


**The bottleneck is RECOMBNATION**

time

femtoseconds → picoseconds →

Witnessing the formation and relaxation of dressed quasi-particles in a strongly correlated electron system

Fabio Novelli[1,2], Giulio De Filippis[3], Vittorio Cataudella[3], Martina Esposito[1], Ignacio Vergara[4], Federico Cilento[2], Enrico Sindici[1], Adriano Amaricci[5], Claudio Giannetti[6,7], Dharmalingam Prabhakaran[8], Simon Wall[9], Andrea Perucchi[2,10], Stefano Dal Conte[11], Giulio Cerullo[11], Massimo Capone[5], Andrey Mishchenko[12,13], Markus Grüninger[4], Naoto Nagaosa[12,14], Fulvio Parmigiani[1,2,4] & Daniele Fausti[1,2]

NATURE COMMUNICATIONS | 5:5112 | DOI: 10.1038/ncomms6112

**Undoped $La_2CuO_4$**

**Novel pheno-menon**

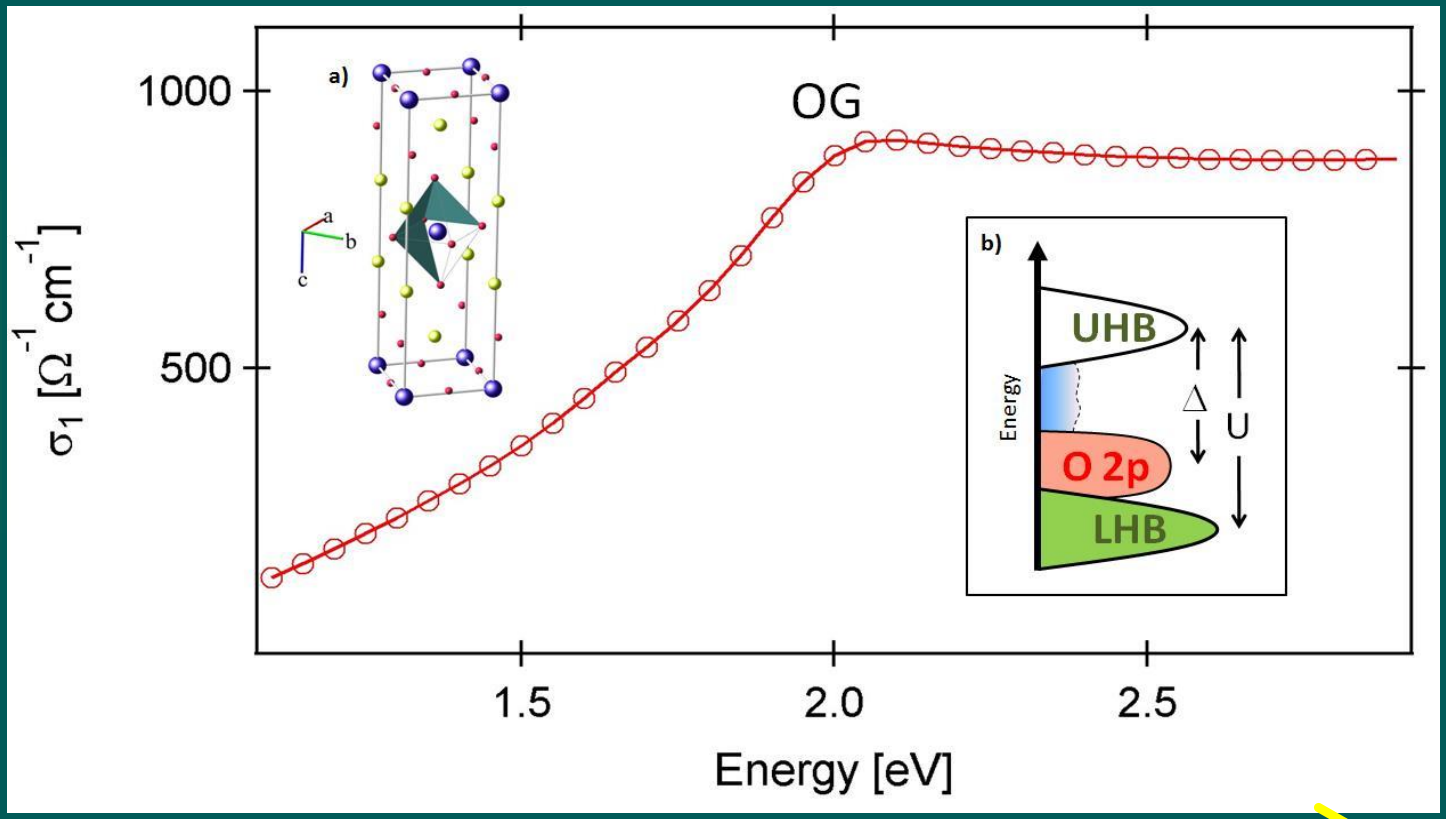


**Over-gap pulse**

**Sub-gap pulse**

**Daniel Fausti**

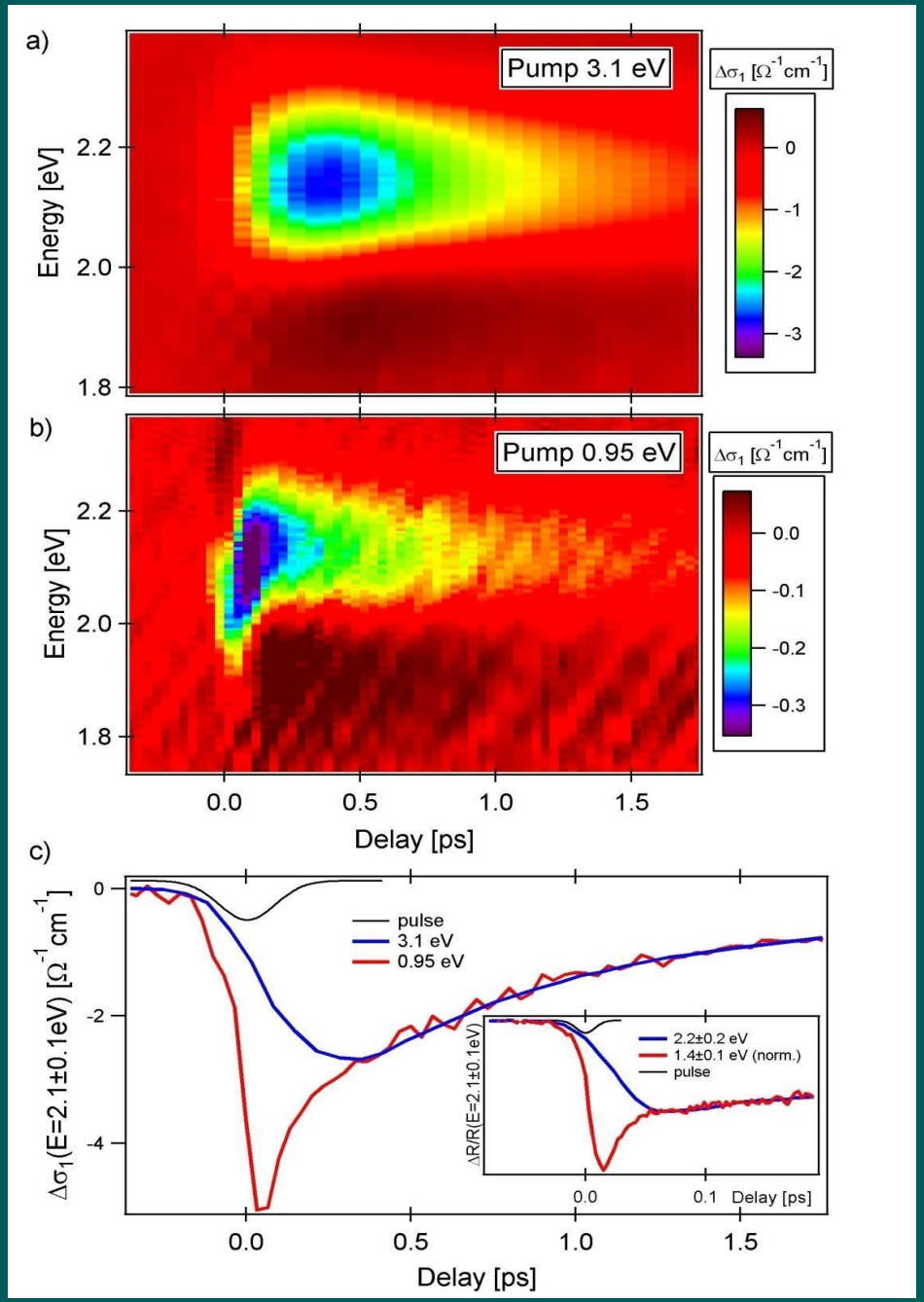


**Sub-gap pulse shows fast component in comparison with over-gap pulse.**

**Effect is normalized to the absorbed energy. Hence, fast component is not connected to absorption!**

**What is peculiarity of the sub-gap pulse?**

# Sub-gap pulse

No absorption of real energy
when the pulse is over!

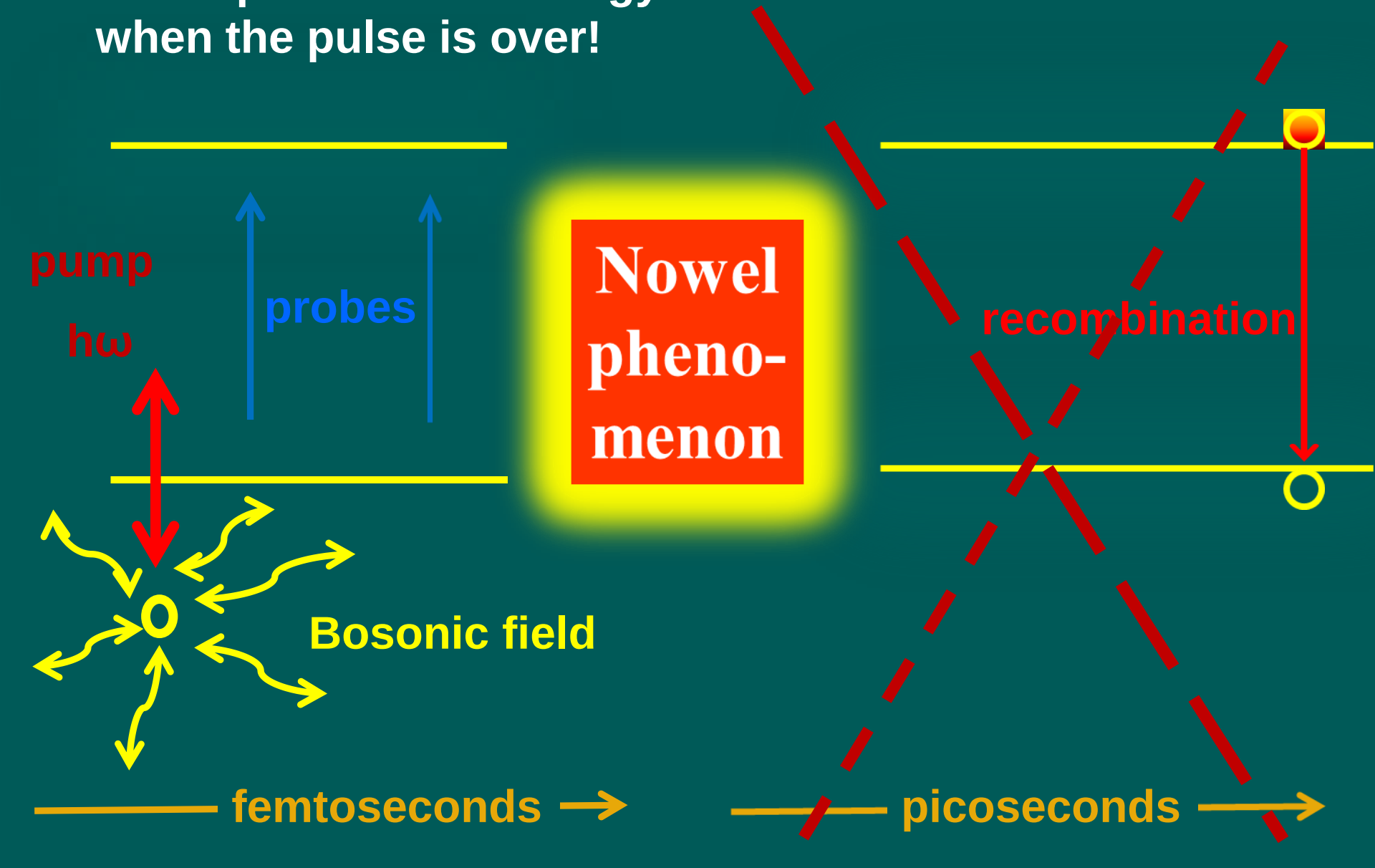

There is a red shift of the variation of the optical conductivity which survives only several tenth of femtoseconds after the pump pulse is over.

This effect is present in theoretical results ONLY if considerable electron-boson coupling is assumed in the Hubbard-Holstein model.

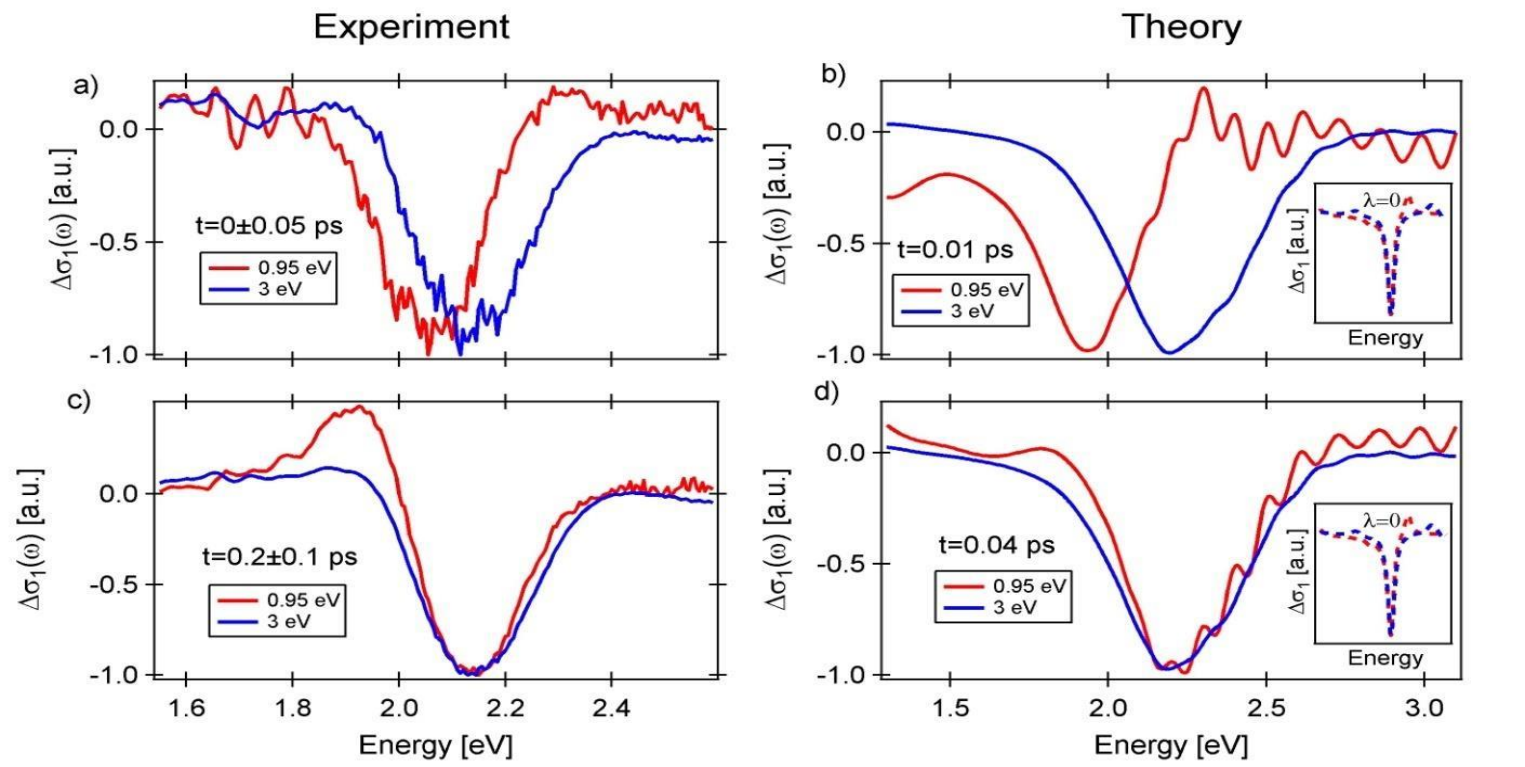

# Physical picture of fast component in sub-gap pulse.

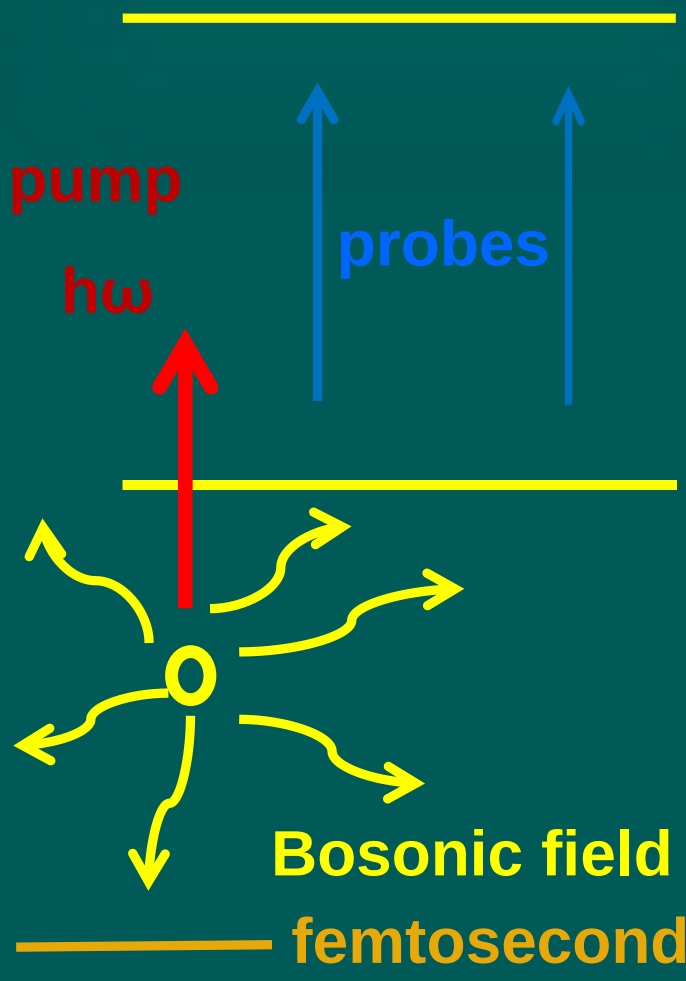


In the absence of electron-boson coupling the distortion of ground state by the electric field of pump exists only few femtoseconds after the pulse is over (electron characteristic times are h/t ~ 2 fs).

However, memory of slower bosonic filed prolongs the memory of the pulse and the red shift is observed for some time when the pump pulse is already over.

# Sub-gap pump-probe spectroscopy: A novel tool to probe electron-boson coupling.

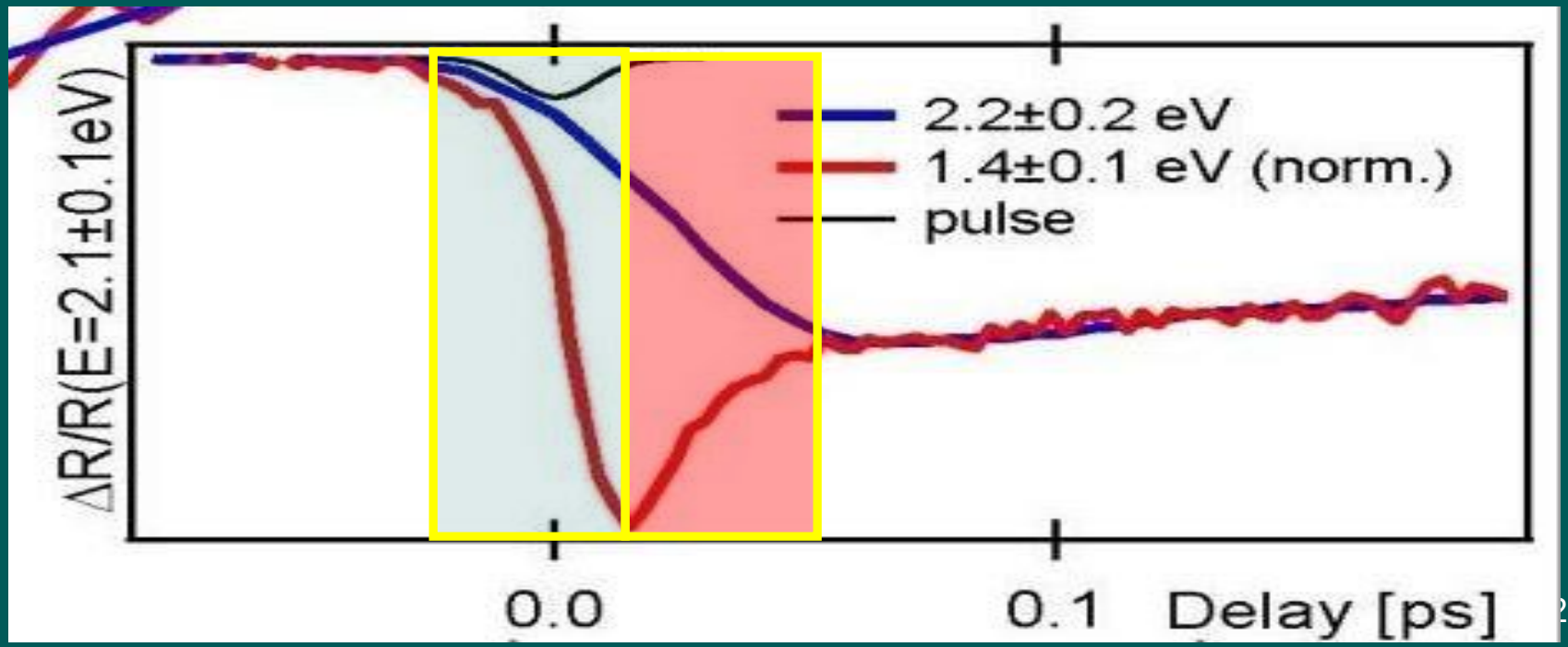

Why we need additional electron-boson interaction on top of Hubbard model to explain

# RAMAN and Optical conductivity (undoped !!)

# Joint description of RAMAN and optical conductivity: extended Hubbard versus Hubbard-Holstein

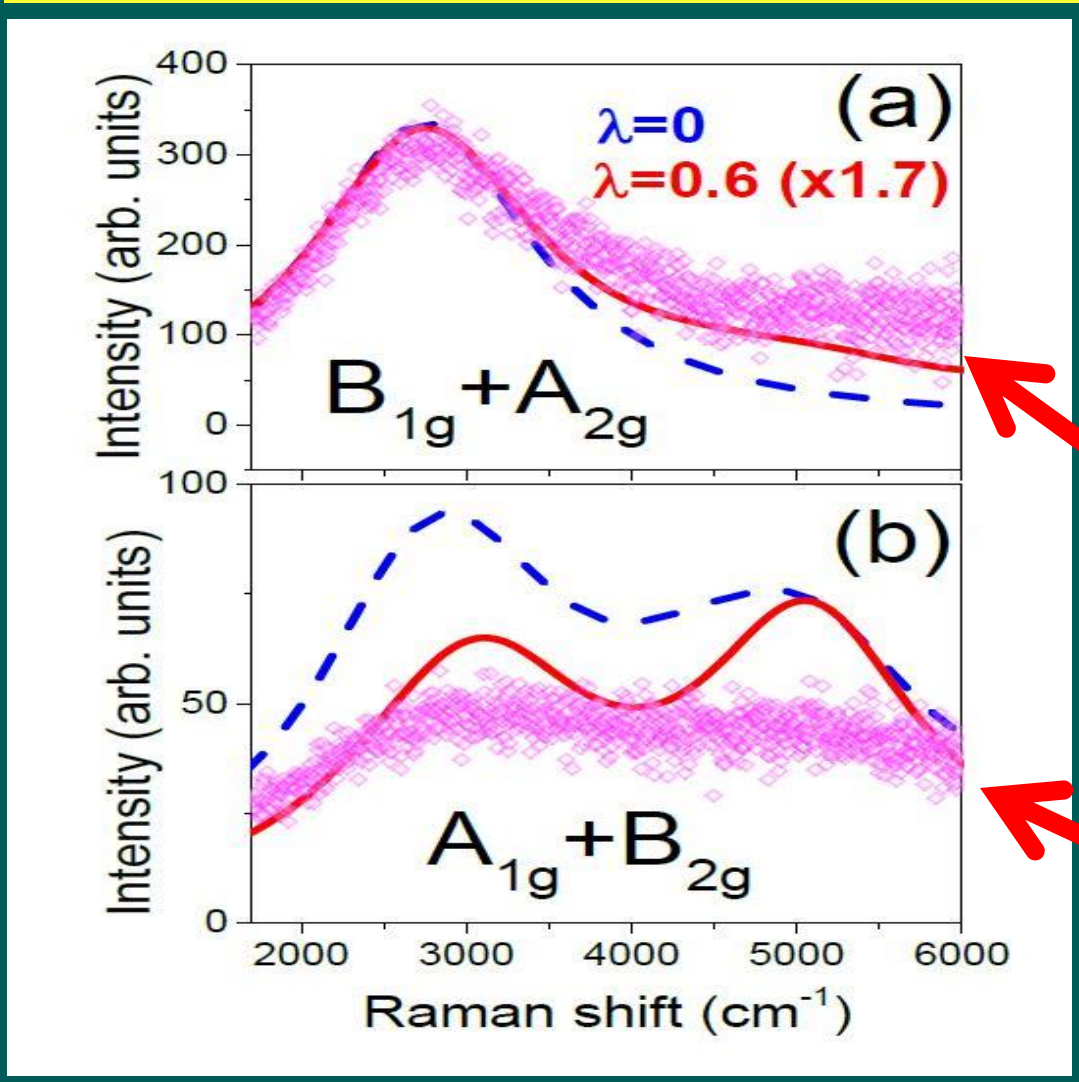


***2-magnon peak in Raman***

**Asymmetry with EPI**

**Flatness with EPI**

**Submitted**

# Joint description of RAMAN and optical conductivity: extended Hubbard versus Hubbard-Holstein

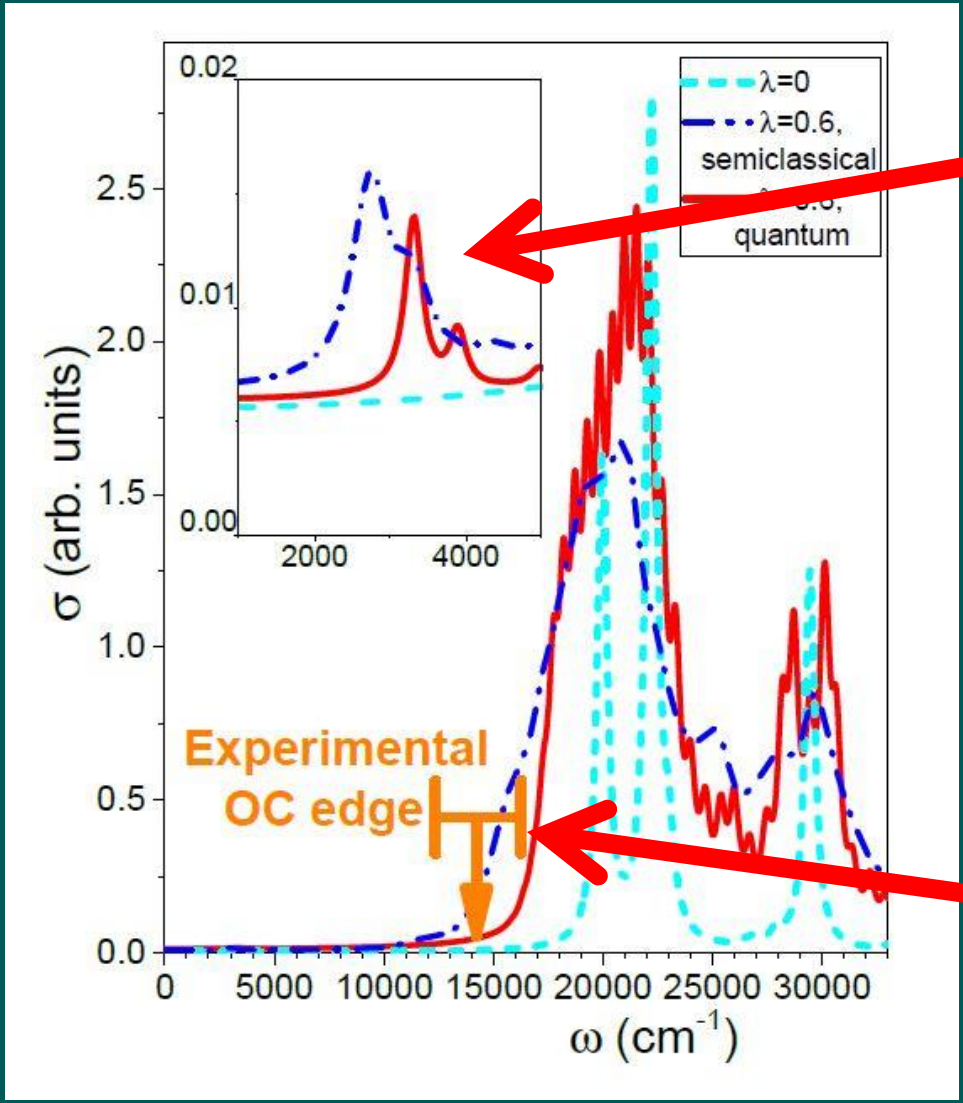


**2-magnon peak is visible in OC with EPI**

**Correct position of the OC edge with EPI**

We need considerable electron-boson coupling on top of the Hubbard model to explain **all spectroscopy** ***IN UNDERDOPED*** **compounds**

George Sawatzky, Vancouver

Naoto Nagaosa, Tokyo

Giulio de Filippis

and

Vittorio Cataudella

Napoli

Z.-X. Shen, Stanford

Jan Zaanen, Leiden

Christian Bernhard, Kyungwan Kim
Freiburg

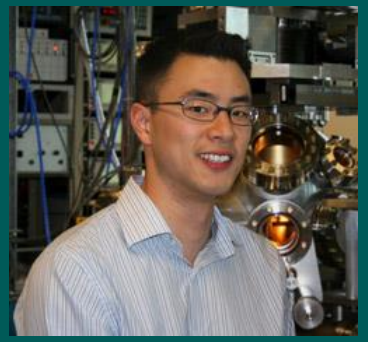

Kyle Shen,
Cornell University

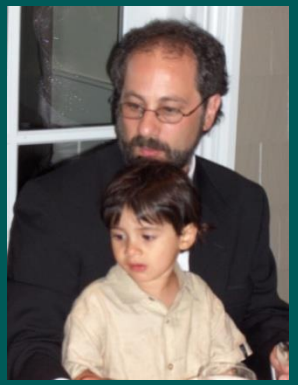

Tom Devereaux,
Stanford

RIKEN

Jan Zaanen, Leiden

Christian Bernhard, Kyungwan Kim
Freiburg

Kyle Shen,
Cornell University

Z.-X. Shen, Stanford

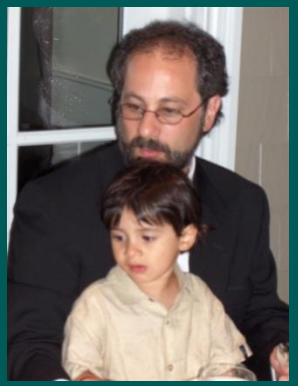

Tom Devereaux,
Stanford

RIKEN

# What happens with hole doping?

**It looks like in experiments that the manifestations of the electron-phonon coupling decreases with doping as if effective λ decreases when holes concentration increases.**

**Let us determine effective λ from:**

**1.Optical conductivity**
**2.ARPES**

# Dependence of effective electron-phonon coupling from MIR position in optical conductivity.

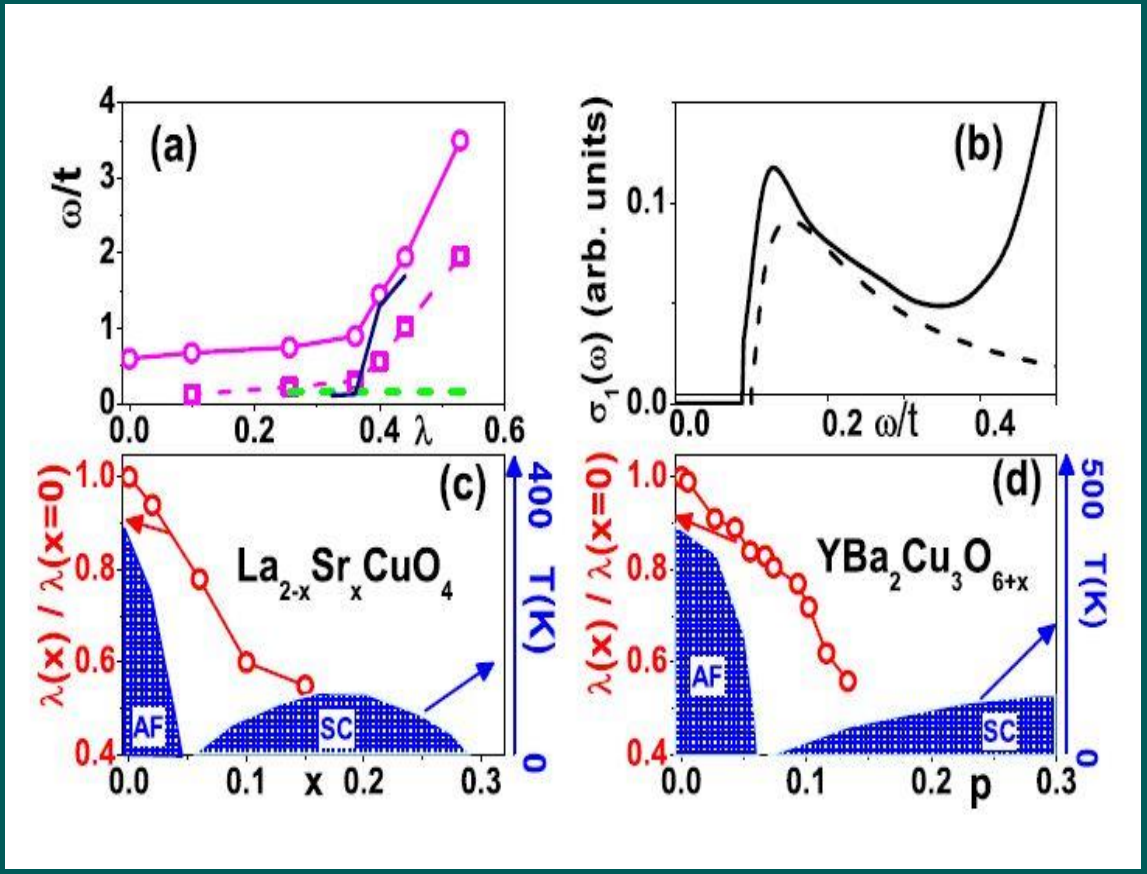


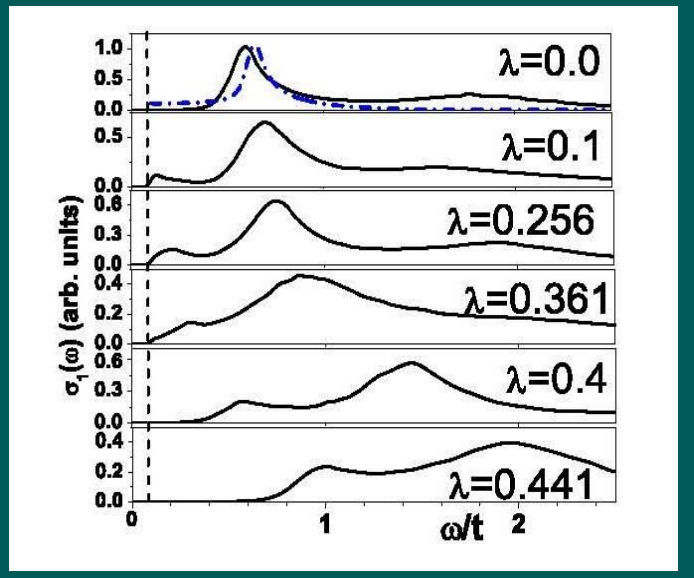


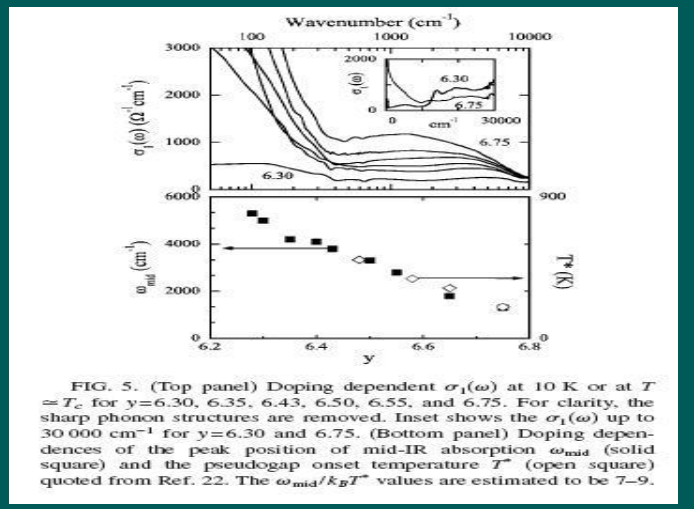


FIG. 5. (Top panel) Doping dependent $\sigma_1(\omega)$ at 10 K or at $T \simeq T_c$ for y=6.30, 6.35, 6.43, 6.50, 6.55, and 6.75. For clarity, the sharp phonon structures are removed. Inset shows the $\sigma_1(\omega)$ up to 30 000 $cm^{-1}$ for y=6.30 and 6.75. (Bottom panel) Doping dependences of the peak position of mid-IR absorption $\omega_{mid}$ (solid square) and the pseudogap onset temperature $T^*$ (open square) quoted from Ref. 22. The $\omega_{mid}/k_BT^*$ values are estimated to be 7–9.

ASM, N. Nagaosa, Z.-X. Shen, G. De Filippis, V. Cataudella, T. P. Devereaux, C. Bernhard, K.W. Kim, and J. Zaanen, Phys. Rev. Lett. 100, 166401 (2008)

Lee at al 2005

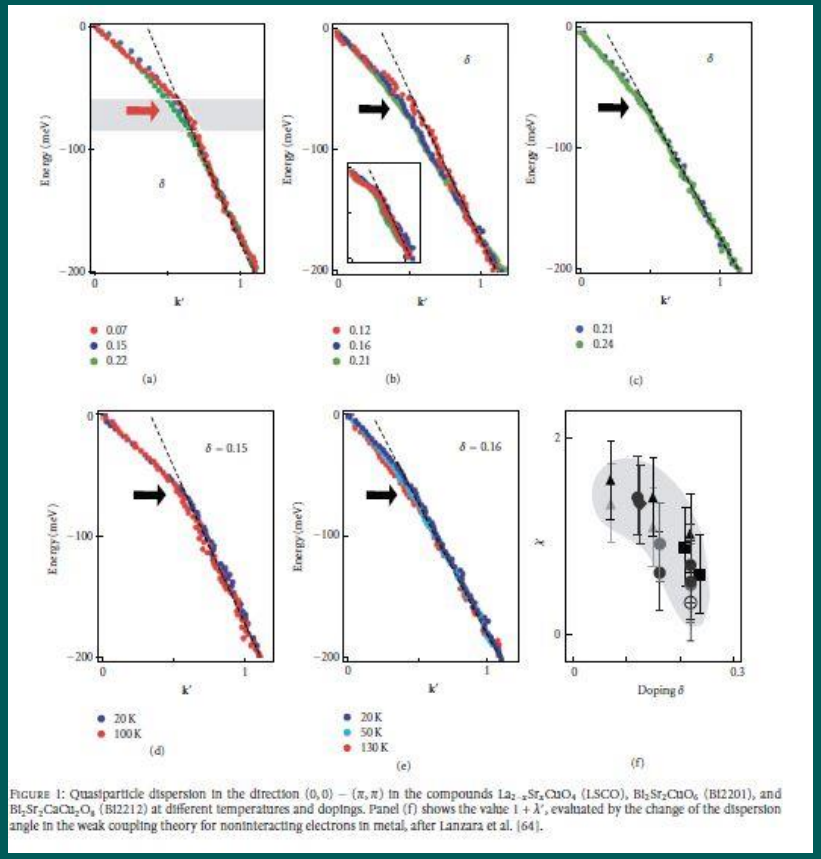


FIGURE 1: Quasiparticle dispersion in the direction $(0,0) - (\pi,\pi)$ in the compounds $La_{2-x}Sr_xCuO_4$ (LSCO), $Bi_2Sr_2CuO_6$ (Bi2201), and $Bi_2Sr_2CaCu_2O_8$ (Bi2212) at different temperatures and dopings. Panel (f) shows the value $1 + \lambda'$, evaluated by the change of the dispersion angle in the weak coupling theory for noninteracting electrons in metal, after Lanzara et al. [64].

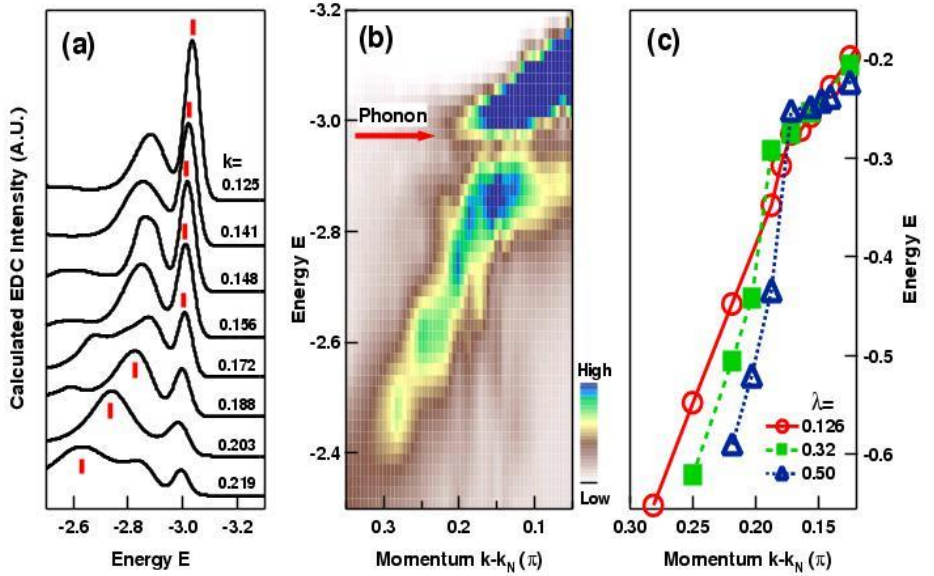


A. S. M., N. Nagaosa, K. M. Shen, Z.-X. Shen, X. J. Zhou, and T. P. Devereaux, EPL, 95 (2011) 57007

## Lanzara et al, 2001

**Effective EPI strength is defined from comparison of experimental and theoretical kink's angle.**

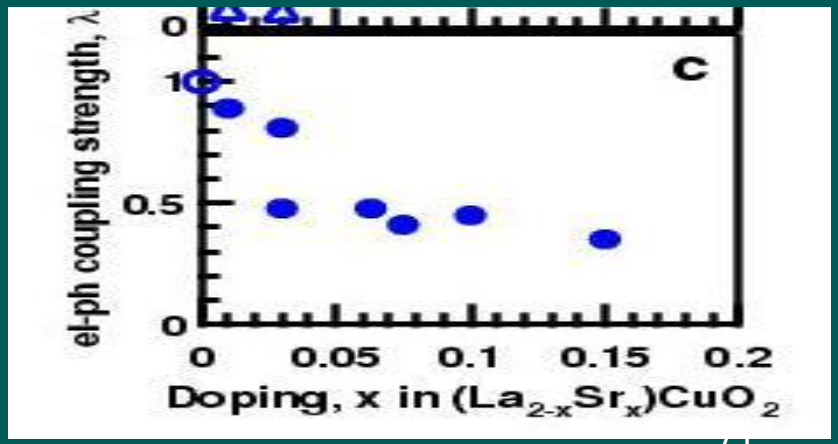

# Dependence of effective electron-phonon coupling:

## From MIR position

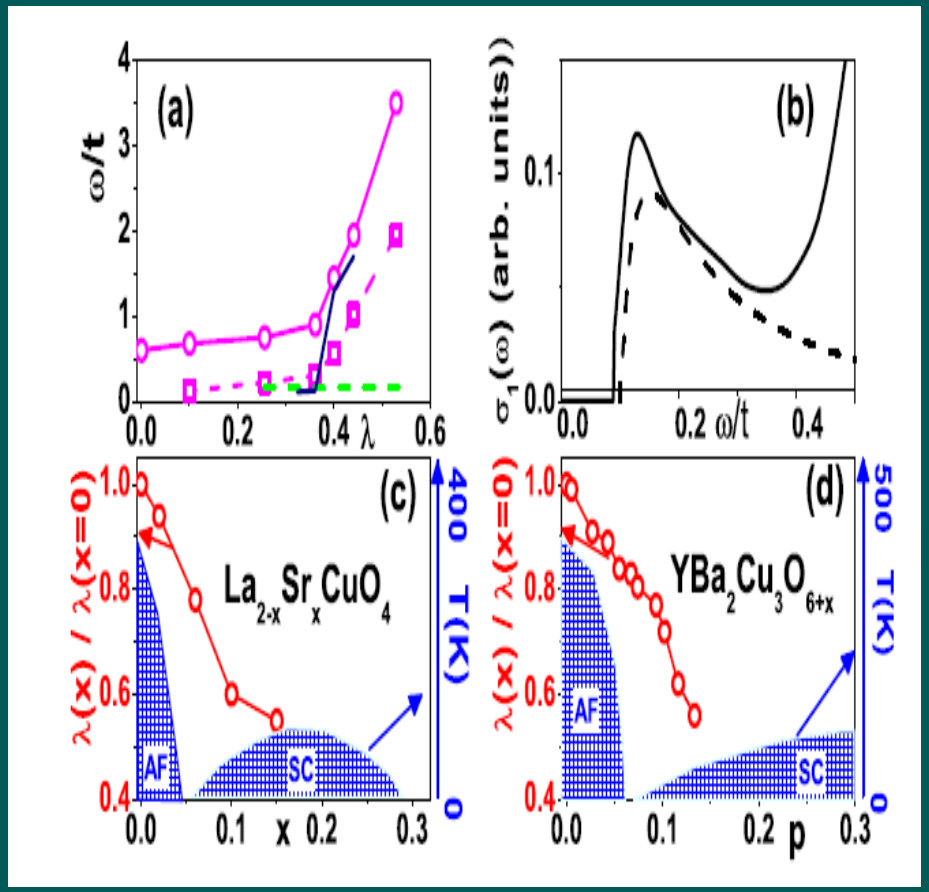


## From kink angle in ARPES

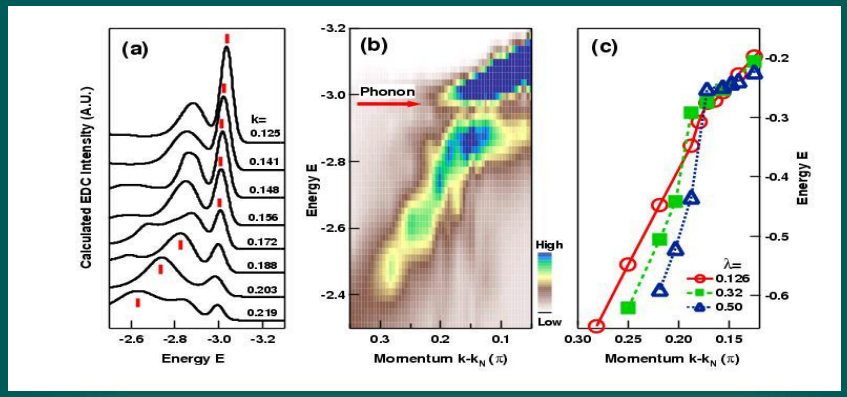


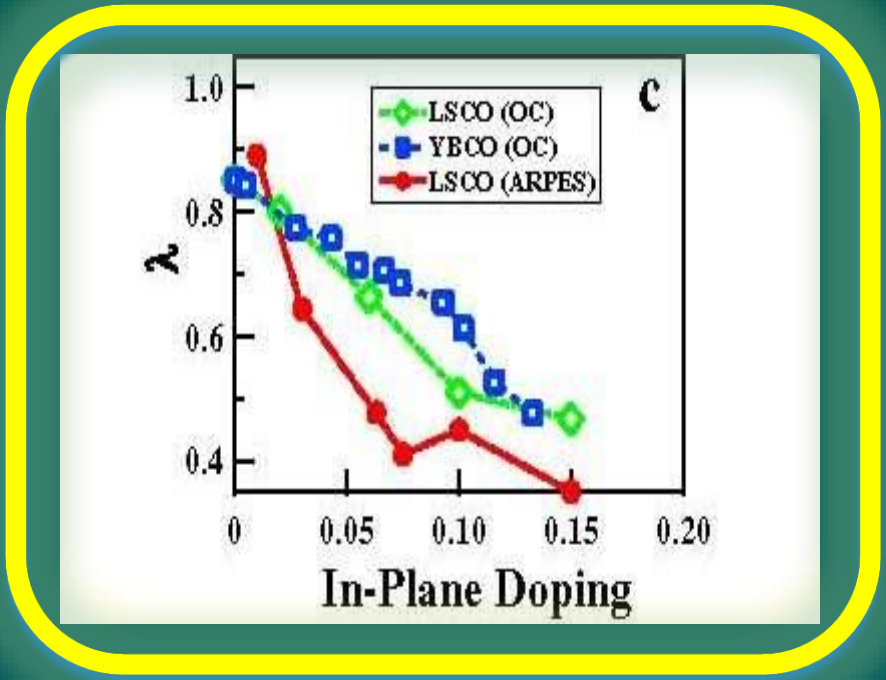

**Of course there is no decrease of material parameter λ with increase of doping.**

**However, one can show that manifestations of strong electron-phonon coupling in spectroscopy are suppressed with doping as if λ is small.**

$$H = \sum_p \varepsilon(p) a_p^+ a_p + \sum_q \omega(p)(b_q^+ b_q + 1/2) + \sum_{pq} \left( V_q a_{p-q}^+ a_p b_q^+ + h.c. \right)$$

electron

phonons

el.-ph. interaction

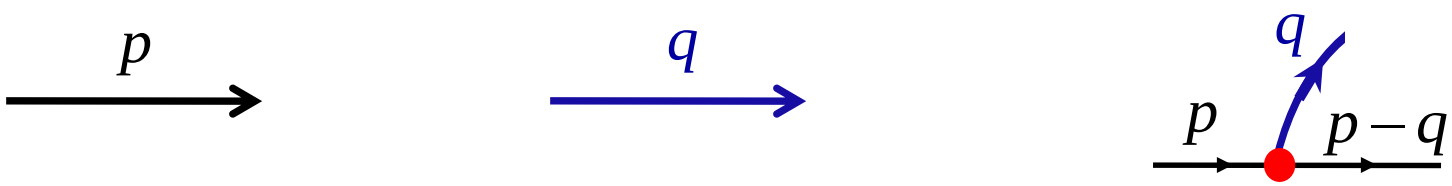


## Conventional Diagrammatic Monte Carlo

**Green function:** $G(p,\tau) = \langle a_p(0) a^+{}_p(\tau) \rangle = \langle a_p \; e^{-\tau H} \; a^+{}_p \; e^{\tau H} \rangle$

$=$ **Sum of all Feynman diagrams**

**Positive definite series in the** $(\vec{p},\tau)$ **representation**

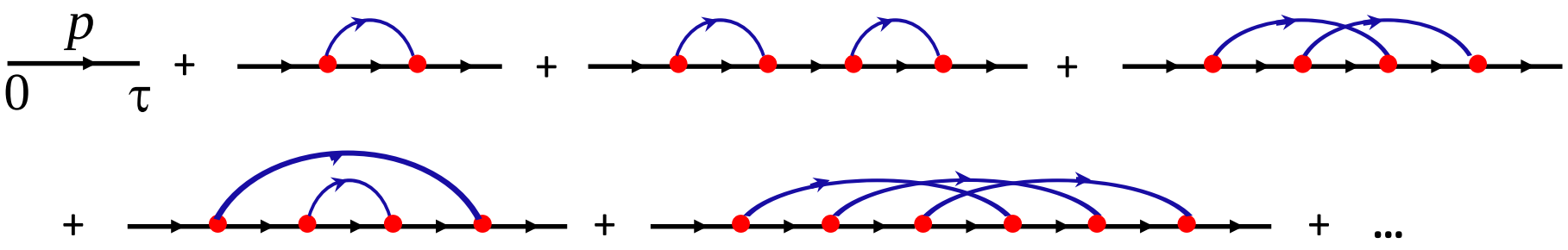

$$G(p,\tau) = \sum$$

Feynman digrams

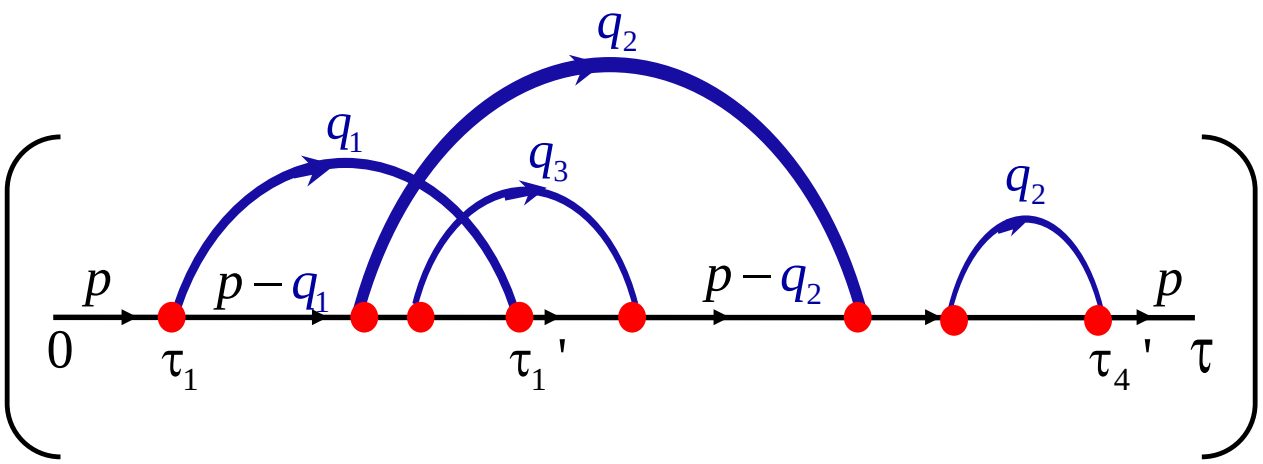


**Graph-to-math correspondence:**

$$G\left(\vec{p},\tau\right) = \sum_{n=0}^{\infty} \sum_{\xi} \iiint d\vec{x}_1 d\vec{x}_2 \ldots d\vec{x}_n \; D_n\left(\xi; \vec{x}_1, \vec{x}_2, \ldots \vec{x}_n, \vec{p}, \tau\right) \text{ where } \vec{x}_i = (\vec{q}_i, \tau_i, \tau_i')$$

**is a product of**

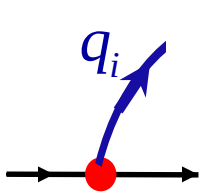


$V_{q_i}$

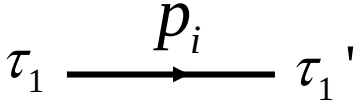


$e^{-\varepsilon(p_i)(\tau_i'-\tau_i)}$

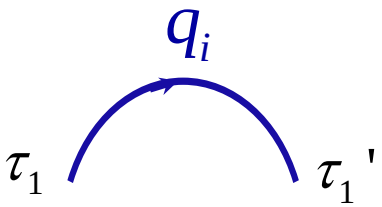


$e^{-\omega(q)(\tau_i'-\tau_i)}$

**Positive definite series in the $(\vec{p},\tau)$ representation**

One polaron

↓

Finite density

Sign problem

↓

Sign blessing

# Bold Line DMC

*Sceleton*
*Ireducible*

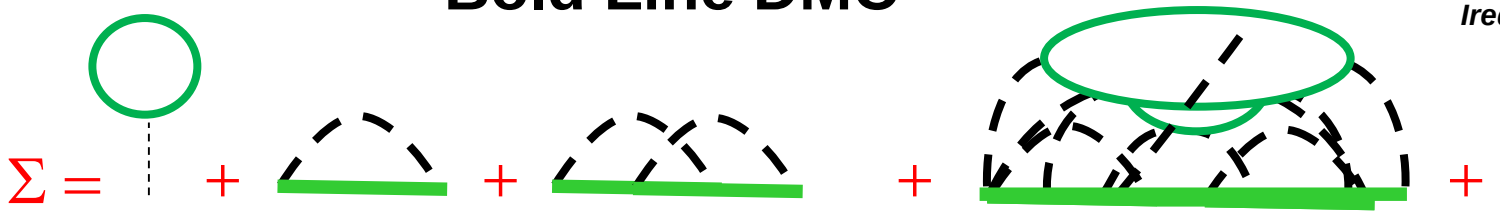


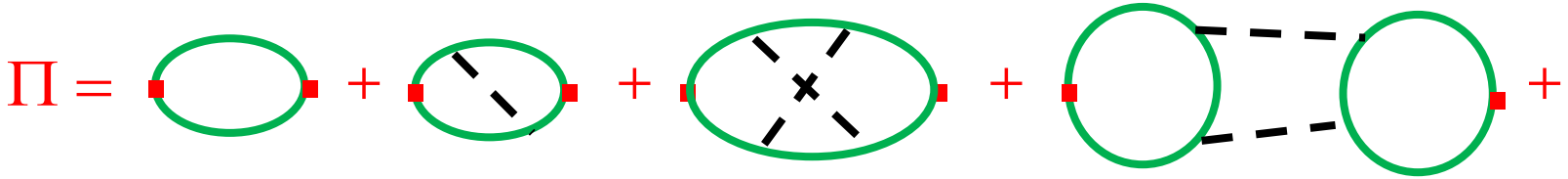


**In terms of "exact" propagators**

**Dyson Equation:**

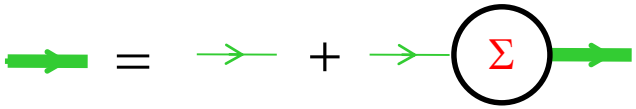


**Screening:**

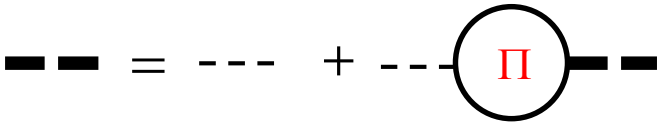


**ASM, N. Nagaosa and N. Prokof'ev, Phys. Rev. Lett. 113, 166402 (2014) –**
**finite density polaron gas**

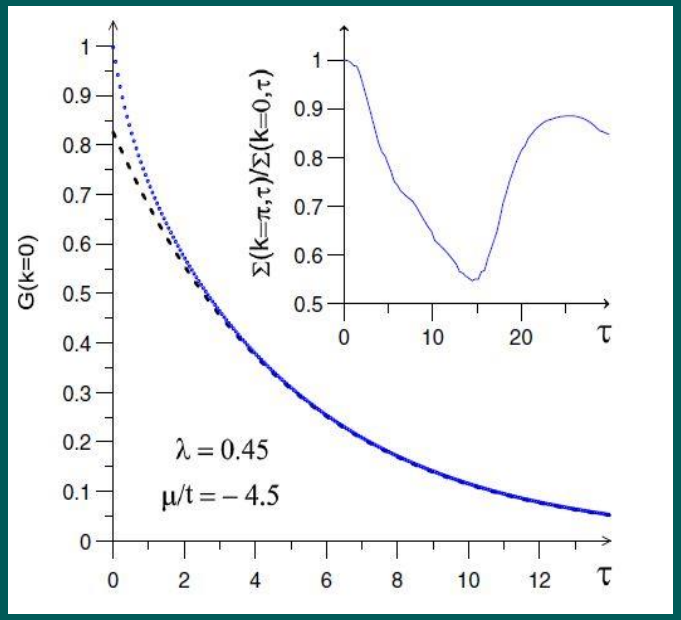


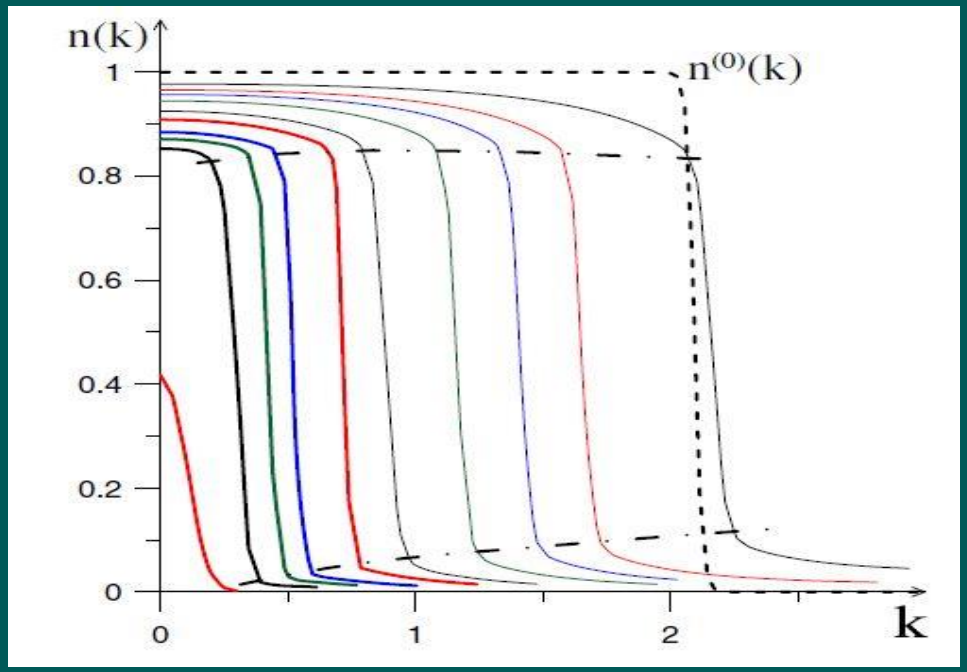


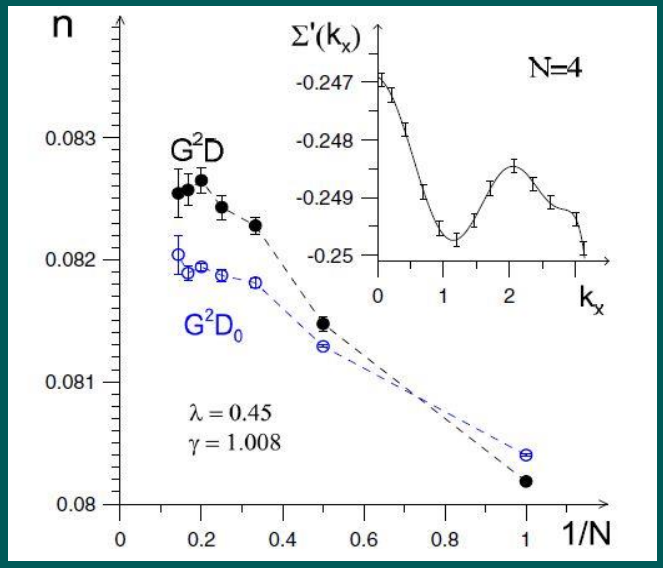


**Holstein, λ=0.45, 2D, 128x128**

$\gamma = \omega_0 / \varepsilon_F$

1. Converge even for γ≈1
2. On-site DMFT good for GS large density
3. Not good for excited states

ASM, N. Nagaosa and N. Prokof'ev, Phys. Rev. Lett. 113, 166402 (2014)

# Strong coupling.

## Spin-polarized fermion gas = holes in t-J model

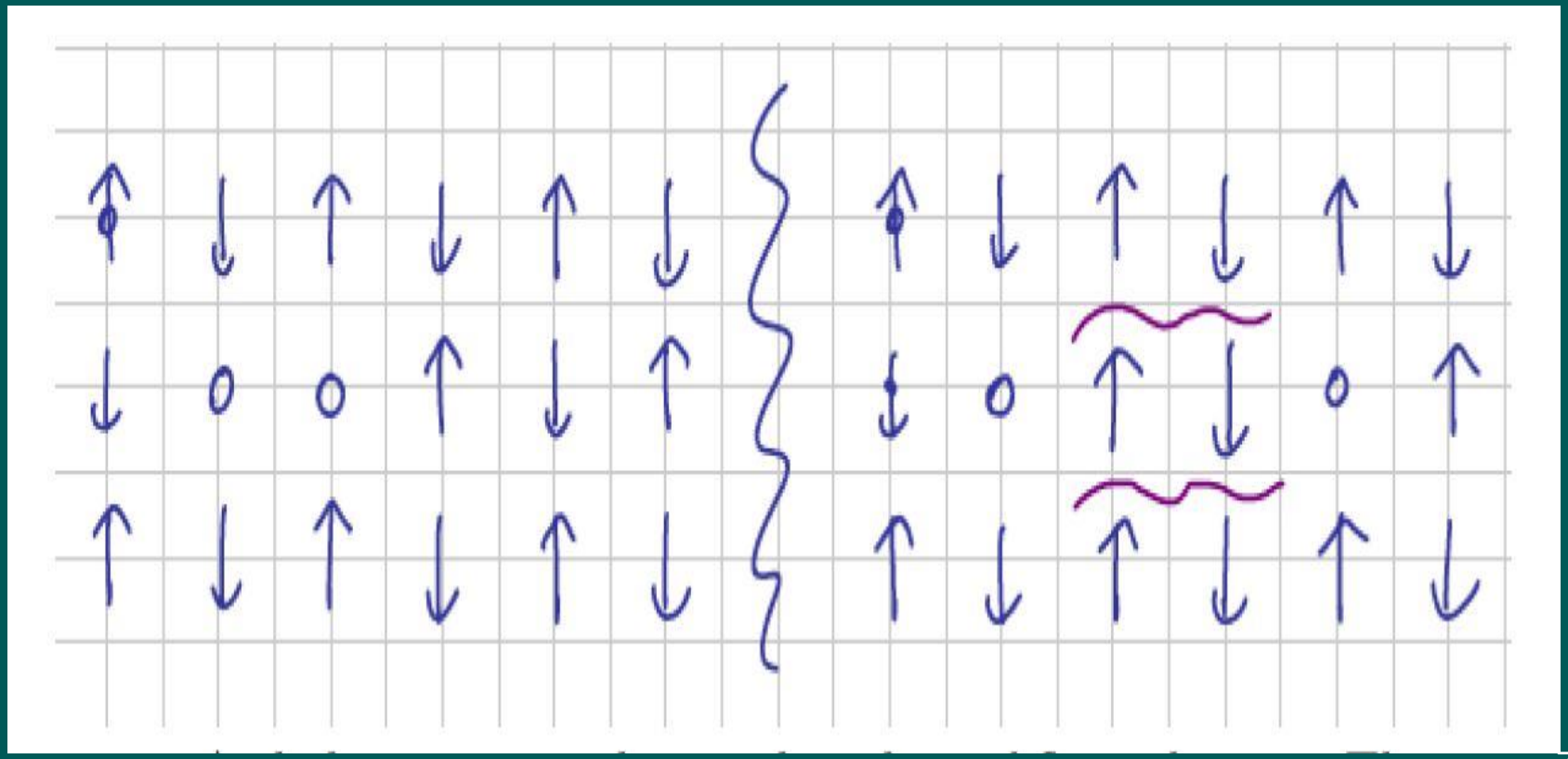

# Polaronic spectral function: Z-factor

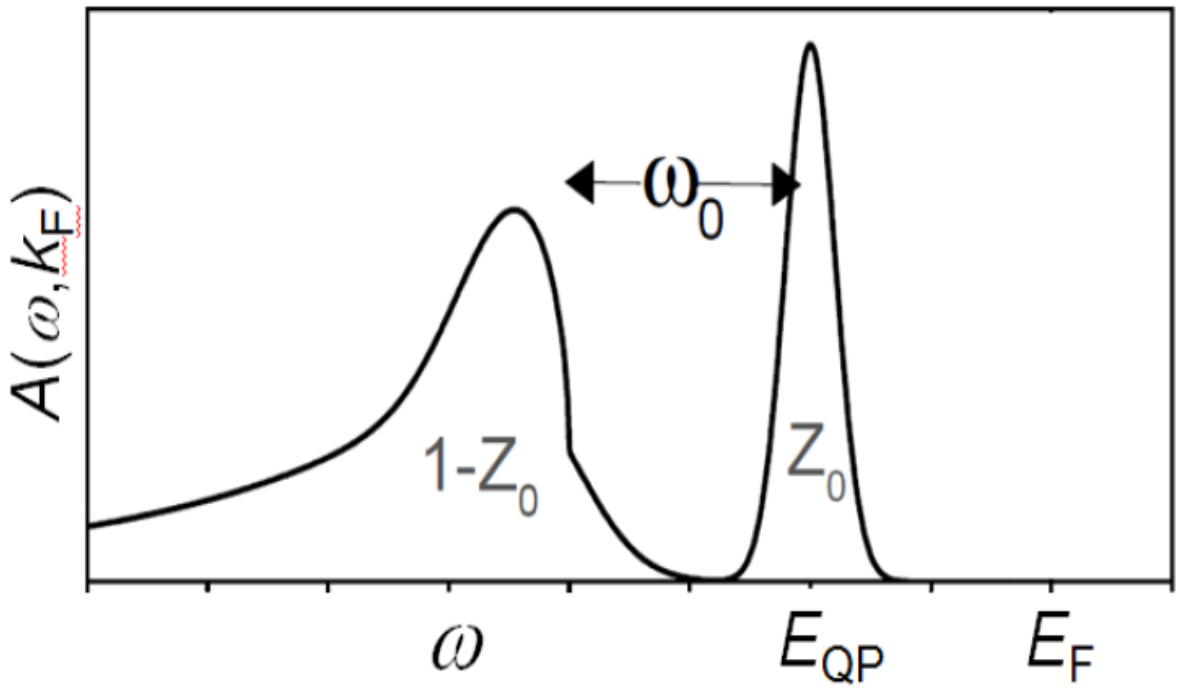


**Fig. 10.** Sketch of the polaron spectral function $A(\omega,\mathbf{k})$ at low electron excitation energy $E(\mathbf{k}) - E_F$. The characteristic peak-dip-hump (PDH) spectral shape is formed by the quasiparticle (QP) peak followed by the phonon sideband tail corresponding to a sequence of optical phonons with frequency $\omega_0$.

1. Explanation of
   (a) ARPES;
   (b) optical conductivity;
   (c) T-dependence of the spectral properties;
   (d) pump-probe evolution of the optical conductivity
   (e) Raman
   in underdoped cuprates
   requires considerable electron-boson coupling

2. Naively, experimental data indicate that increase of doping decreases manifestations of the electron-boson coupling in specroscopy

3. We solve famous sign-problem in Mote Carlo for many-particle Fermi-polarons system and explain what happens with electron-boson coupling when doping in high $T_c$ cuprates increases.

## PART I: Further reading for details:

Phys. Rev. Lett., vol. 86, 4624 (2001) : Pseudo-Jahn-Teller polaron
Phys. Rev. Lett., vol. 91, 236401 (2003) : Optical cond-ty of Frohlich polaron
Phys. Rev. Lett., vol. 93, 036402 (2004) : ARPES in high $T_c$ cuprates
Phys. Rev. Lett., vol. 99, 146405 (2007) : Nonlocal el-ph in high $T_c$ cuprates
Phys. Rev. Lett., vol. 99, 226402 (2007) : ARPES in high $T_c$ cuprates
Phys. Rev. Lett., vol. 100, 166401 (2008) : Optical cond-ty in high $T_c$ cuprates
Phys. Rev. Lett., vol. 107, 076403 (2011) : Optical cond-ty of Holstein polaron
Phys. Rev. Lett., vol. 109, 176402 (2012) : Time dependent Holstein-Hubbard
Nature Commun. 5:5112 (2014) : Pump-probe in optics of LaCuO4
Phys. Rev. Lett., vol. 113, 166402 (2014) : Finite density polaron gas
Phys. Rev. Lett., vol. 114, 146401 (2015) : Unbiased mobility of Holstein polaron
Nature Commun. 7:10386 (2016) : Polarons in LAO-STO interface
……..

# New advances in analytic continuation method: well posed answers to ill posed questions.

Andrey S. Mishchenko
RIKEN CEMS
(Center for Emergent Matter Science)

1. Analytic continuation.
2. Why difficult.
3. Why SOM successful and what are drawbacks.
4. Consistent constraints cure.
5. Playing with linear combinations of solutions.
6. Which additional information we can get with new ideology.

*Physical properties under interest: absorption by polaron.*

Such relation between imaginary-time function and spectral properties is rather general:

$$G_{\mathbf{k}}(\tau) = \int_0^\infty d\omega\, L_{\mathbf{k}}(\omega)\, e^{-\omega\tau}$$

**ARPES**

Current–current corelation function is related to optical absorption by polarons by the same expression:

$$\langle J_\beta(\tau) J_\delta \rangle$$

$$\sigma_{\beta\delta}(\omega) = \pi \hat{\mathcal{F}}_\omega^{-1} \left[ \langle J_\beta(\tau) J_\delta \rangle \right] / \omega$$

**Optical absorption**

**μ = σ (ω→0)/en**

**Mobility**

$$G(m) = \int_{-\infty}^{\infty} d\omega \; K(m,\omega) \; A(\omega)$$

**There are a lot of problems where one has to solve Fredholm integral equation of the first kind**

# Optical conductivity at finite T in imaginary times representation

$$G(m) = \int_{-\infty}^{\infty} d\omega \; \mathcal{K}(m,\omega) \; A(\omega)$$

$$\mathcal{G}(i\omega_m) = \int_0^{\beta} d\tau \; e^{i\omega_m \tau} \; G(\tau)$$

$$G(\tau) = \frac{1}{\beta} \sum_{\omega_m} e^{-i\omega_m \tau} \; \mathcal{G}(i\omega_m)$$

$$\mathcal{K}(\tau_m,\omega) = \frac{1}{\pi} \frac{\omega \exp(-\tau_m \omega)}{1 - \exp(-\beta\omega)}$$

# Equation for many problems

# Image deblurring with e.g. known 2D noise K(m,ω)

$$G(m) = \int_{-\infty}^{\infty} d\omega \; K(m,\omega) \; A(\omega)$$

**m and ω are 2D vectors**

**K(m,ω) is a 2D x 2D noise distributon function**

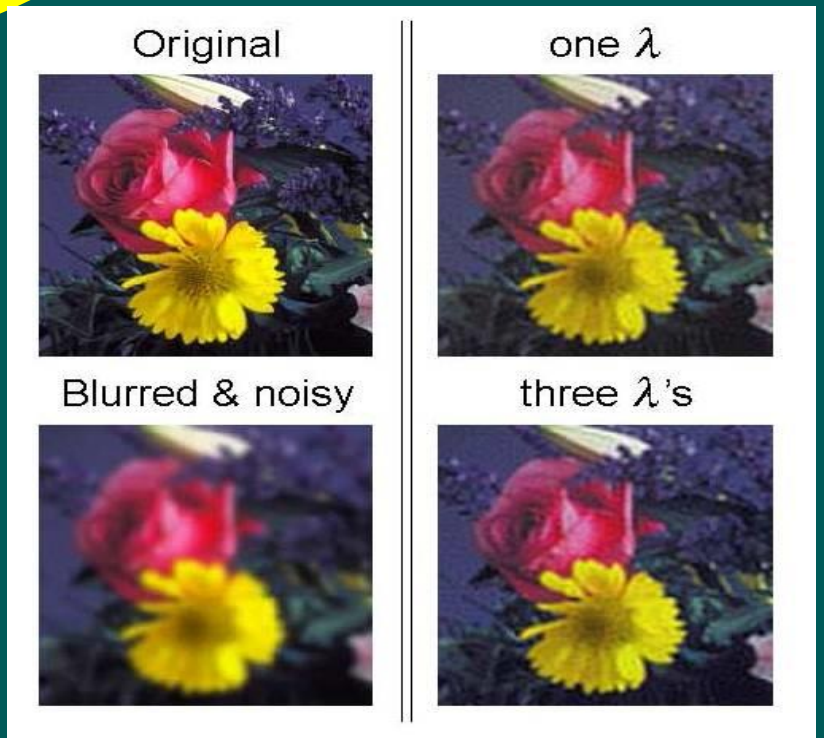

# Tomography image reconstruction (CT scan)

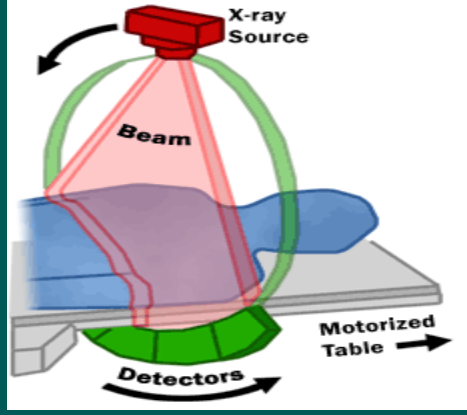


$$G(m) = \int_{-\infty}^{\infty} d\omega \; K(m,\omega) \; A(\omega)$$

**m and ω are 2D vectors**

**K(m,ω) is a 2D x 2D distribution function**

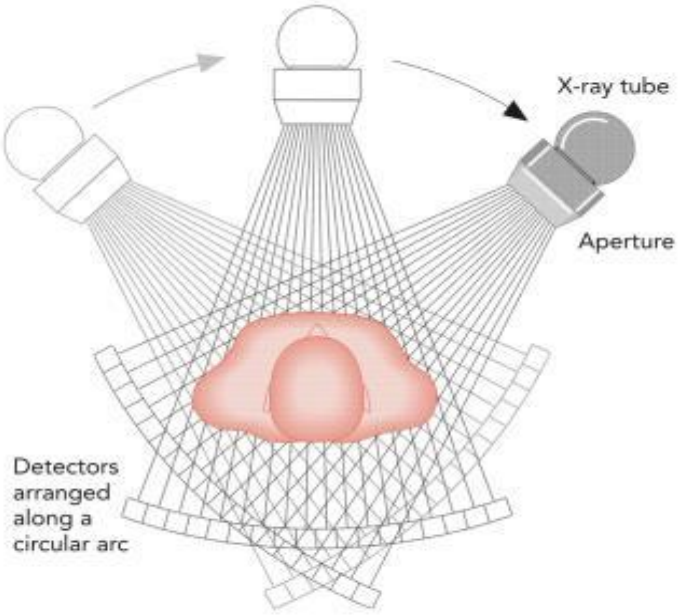


Figure 7-10 Computer tomography

$$G(m) = \int_{-\infty}^{\infty} d\omega \; K(m,\omega) \; A(\omega)$$

Aircraft stability

Nuclear reactor operation

Image deblurring

A lot of other…

**What is dramatic in the problem?**

*Ill-posed!*

$$G(m) = \int_{-\infty}^{\infty} d\omega \; K(m,\omega) \; A(\omega)$$

**Aircraft stability**

**Nuclear reactor operation**

**Image deblurring**

**A lot of other…**

**What is dramatic in the problem?**

# *Ill-posed!*

$$G(m) = \int_{-\infty}^{\infty} d\omega \; K(m,\omega) \; A(\omega)$$

**We cannot obtain an exact solution not because of some approximations of our approaches.**

**Instead, we have to admit that the exact solution does not exist at all!**

# Ill-posed!

$$G(m) = \int_{-\infty}^{\infty} d\omega \; K(m,\omega) \; A(\omega)$$

1. ***No unique solution in mathematical sense***
   ***No function A to satisfy the equation***

***2. Some additional information is required which specifies which kind of solution is expected. In order to chose among many approximate solutions.***

*Ill-posed!*

***Next player:***
***stochastic methods***

$$G(m) = \int_{-\infty}^{\infty} d\omega \; K(m,\omega) \; A(\omega)$$

**Physics department:**
**Max Ent.**

**Statistical department:**
**ridge regression**

**Engineering department:**
**Tikhonov Regularization**

*Ill-posed!*

**Another players:**
**CC, Pade, ….**

***Next player:***
***stochastic methods***

$$G(m) = \int_{-\infty}^{\infty} d\omega \; K(m,\omega) \; A(\omega)$$

**Physics department:**
**Max Ent.**

**Statistical department:**
**ridge regression**

**Engineering department:**
**Tikhonov Regularization**

*Ill-posed!*

$$G(m) = \int_{-\infty}^{\infty} d\omega \; \mathcal{K}(m,\omega) \; A(\omega)$$

$$G(m) = \sum_{n=1}^{N} \mathcal{K}(m,\omega_n) A(\omega_n) \; , \; m = 1, \ldots, M$$

**Because of noise present in the input data G(m) there is no unique $A(\omega_n)=A(n)$ which exactly satisfies the equation.**

**Hence, one *can* search for the *least-square* fitted solution A(n) which minimizes:**

$$\| \; \widehat{\mathcal{K}}\vec{A} - \vec{G} \; \|^2 = \sum_{m=1}^{M} \left| \sum_{n=1}^{N} \mathcal{K}(m,\omega_n) A(\omega_n) - G(m) \right|^2$$

$$\| \hat{\mathcal{K}}\vec{A} - \vec{G} \|^2 = \sum_{m=1}^{M} \left| \sum_{n=1}^{N} \mathcal{K}(m,\omega_n) A(\omega_n) - G(m) \right|^2$$

# *Ill-posed!*

## *Saw tooth noise*

**instability due to small singular values.**

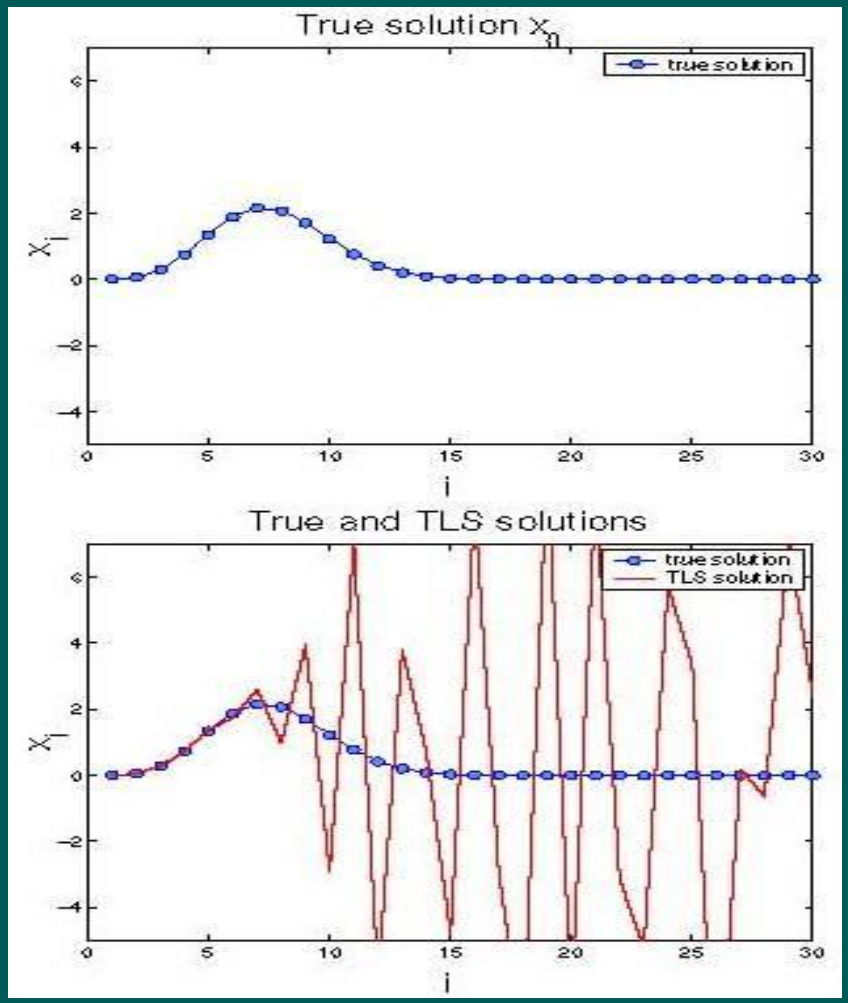


**Explicit expression:**

$$\vec{A} = \sum_{i=1}^{r} \frac{\vec{u}_i^{\dagger} \otimes \vec{v}_i}{\sigma_i} \vec{G}$$

$$\| \hat{\mathcal{K}}\vec{A} - \vec{G} \|^2 = \sum_{m=1}^{M} \left| \sum_{n=1}^{N} \mathcal{K}(m,\omega_n) A(\omega_n) - G(m) \right|^2$$

*Ill-posed!*

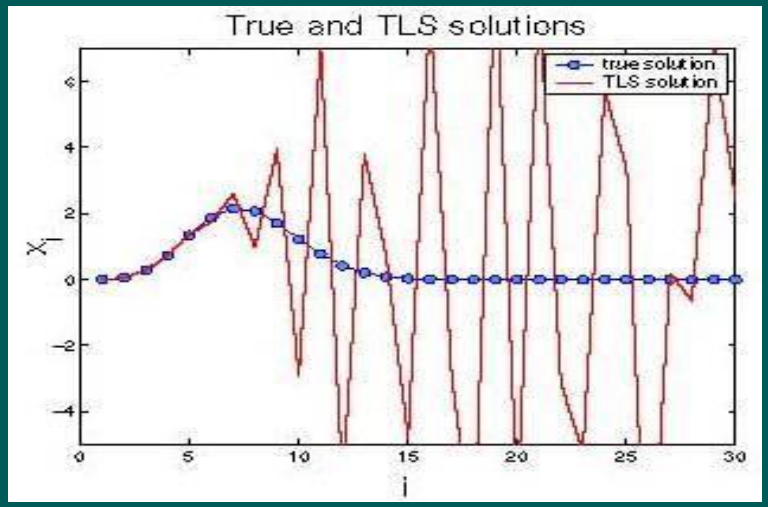


**Tikhonov regularization to fight with the saw tooth noise instability.**

**TIKHONOW-SAMARSKY**

$$\vec{A} = \sum_{i=1}^{r} \frac{\vec{u}_i^{\dagger} \otimes \vec{v}_i}{\sigma_i} \vec{G}$$

$$\vec{A} = \sum_{i=1}^{r} \left\{ \frac{\sigma_i^2}{\sigma_i^2 + \lambda^2} \right\} \frac{\vec{u}_i^{\dagger} \otimes \vec{v}_i}{\sigma_i} \vec{G}$$

All existing methods are biased and over-smoothing!

# New player:

# Stochastic optimization method

# Stochastic Optimization method.

- Particular solution $L^{(i)}(\omega)$ for LSF is presented as a sum of a number K of rectangles with some width, height and center.

**Continuous-ω parametrization !!**

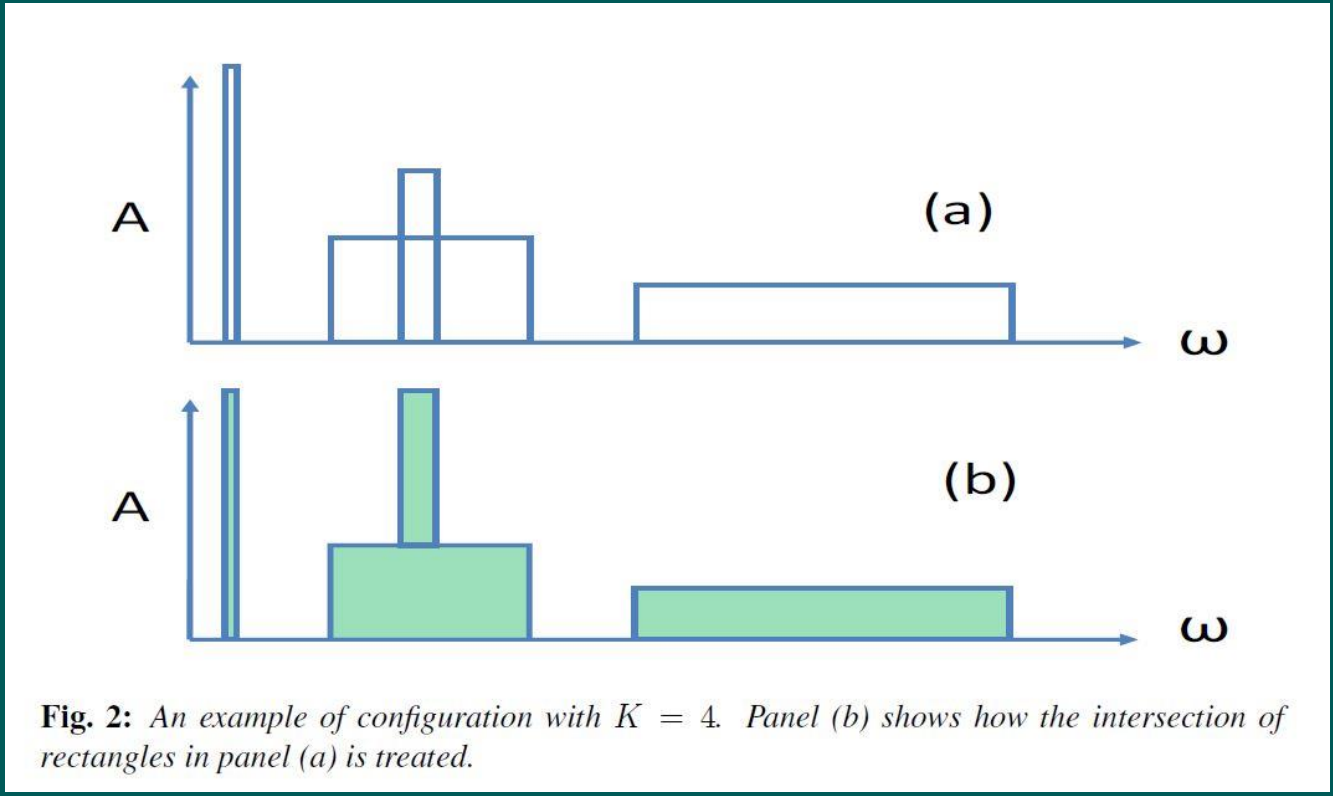


**Fig. 2:** *An example of configuration with $K = 4$. Panel (b) shows how the intersection of rectangles in panel (a) is treated.*

# Stochastic Optimization method.

- Particular solution $L^{(i)}(\omega)$ for LSF is presented as a sum of a number K of rectangles with some width, height and center.
- Initial configuration of rectangles is created by random number generator (i.e. number K and all parameters of of rectangles are randomly generated).

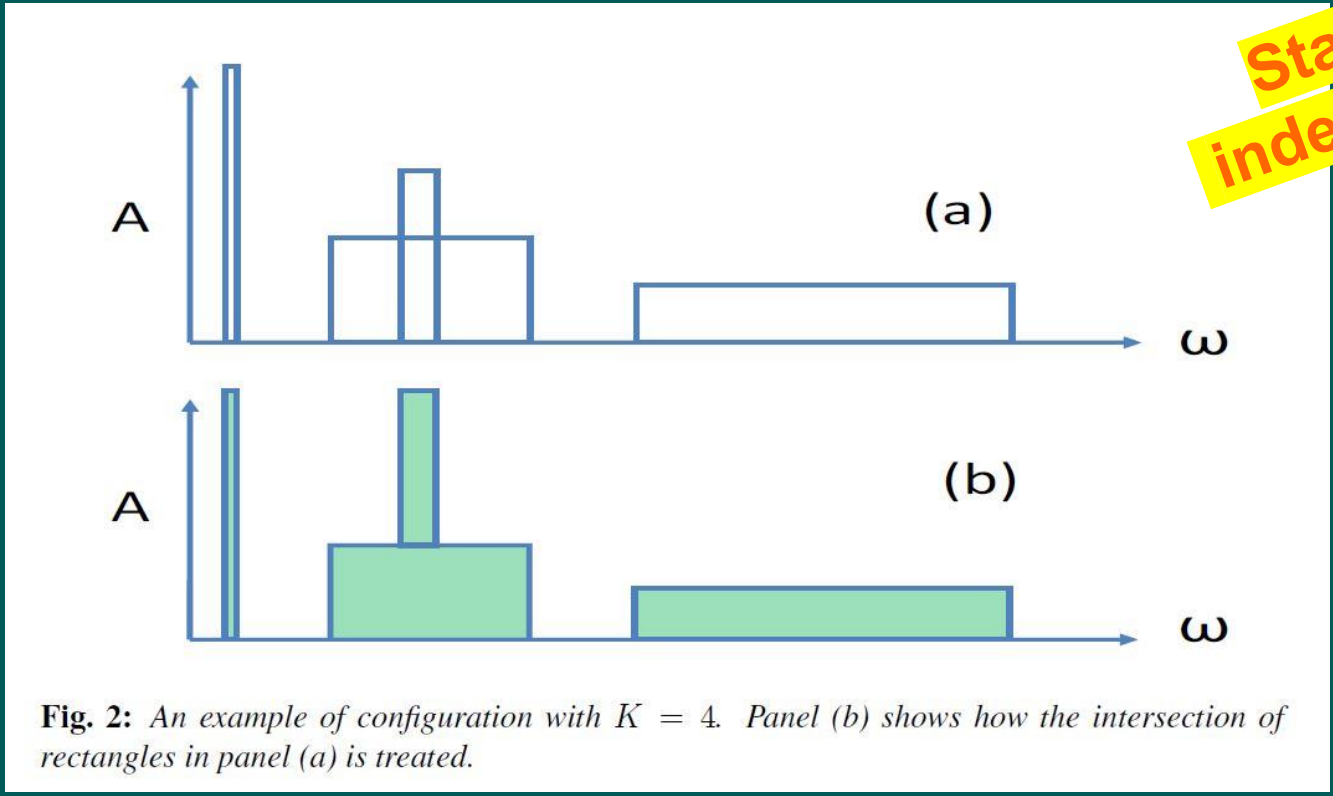


**Fig. 2:** *An example of configuration with $K = 4$. Panel (b) shows how the intersection of rectangles in panel (a) is treated.*

**Statistical independence**

# Stochastic Optimization method.

- Particular solution $L^{(i)}(\omega)$ for LSF is presented as a sum of a number K of rectangles with some width, height and center.
- Initial configuration of rectangles is created by random number generator (i.e. number K and all parameters of of rectangles are randomly generated).
- Each basic solution $L^{(i)}(\omega)$ is obtained by a naïve method without regularization (though, varying number K).

**Abandon Tikhonov regularization**

# Stochastic Optimization method.

- Particular solution $L^{(i)}(\omega)$ for LSF is presented as a sum of a number K of rectangles with some width, height and center.
- Initial configuration of rectangles is created by random number generator (i.e. number K and all parameters of of rectangles are randomly generated).
- Each basic solution $L^{(i)(}\omega)$ is obtained by a naïve method without regularization (though, varying number K).

- Final solution is obtained after M steps of such procedure

$$L(\omega) = M^{-1} \sum_i \alpha(i) L^{(i)(}\omega)$$

# Stochastic Optimization method.

- Particular solution $L^{(i)}(\omega)$ for LSF is presented as a sum of a number K of rectangles with some width, height and center.

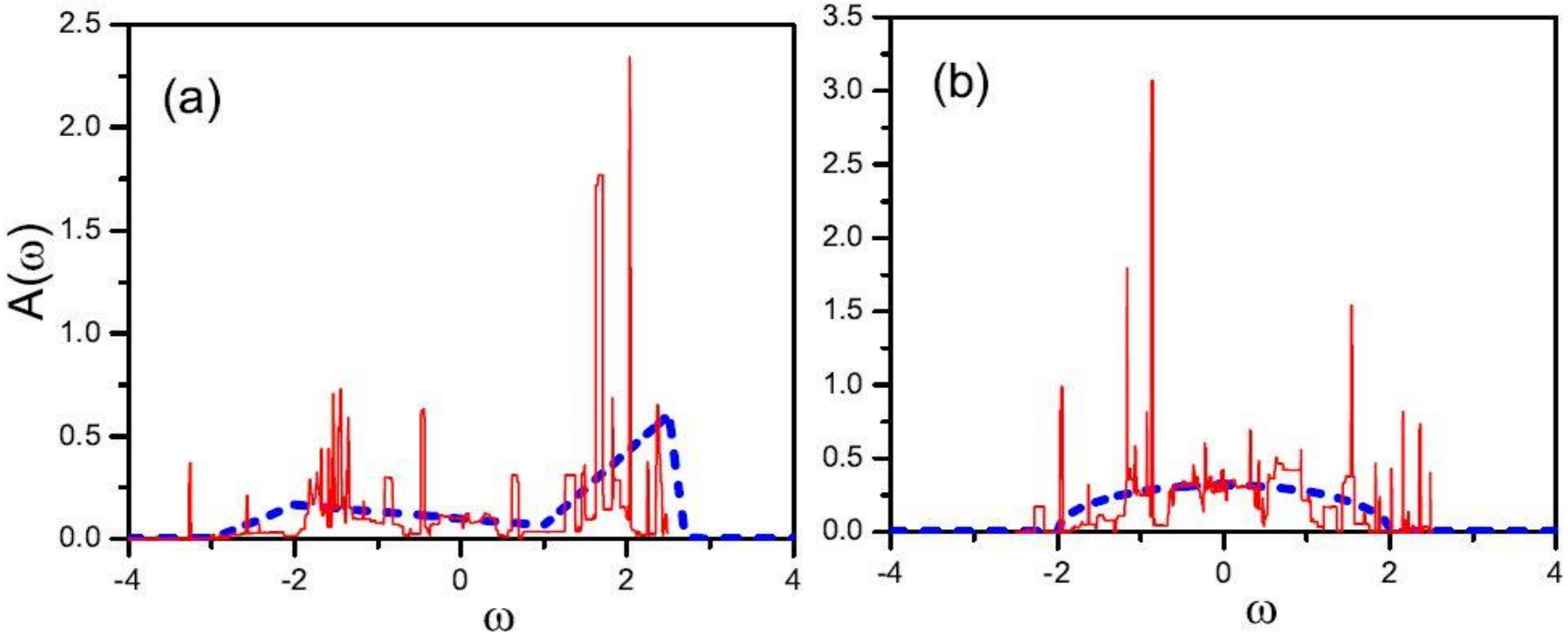


- Each particular basic solution has saw tooth noise

**Abandon Tikhonov regularization**

**Expected**

# Stochastic Optimization method.

- Particular solution $L^{(i)}(\omega)$ for LSF is presented as a sum of a number K of rectangles with some width, height and center.
- Initial configuration of rectangles is created by random number generator (i.e. number K and all parameters of of rectangles are randomly generated).
- Each basic solution $L^{(i)}(\omega)$ is obtained by a naïve method without regularization (though, varying number K).

- Final solution is obtained after M steps of such procedure

$$L(\omega) = M^{-1} \sum_i \alpha(i) L^{(i)}(\omega)$$

- Each particular basic solution has saw tooth noise
- Final averaged solution L(ω) has no saw tooth noise though not regularized with sharp peaks/edges!!!!

# Self-averaging of the saw-tooth noise.

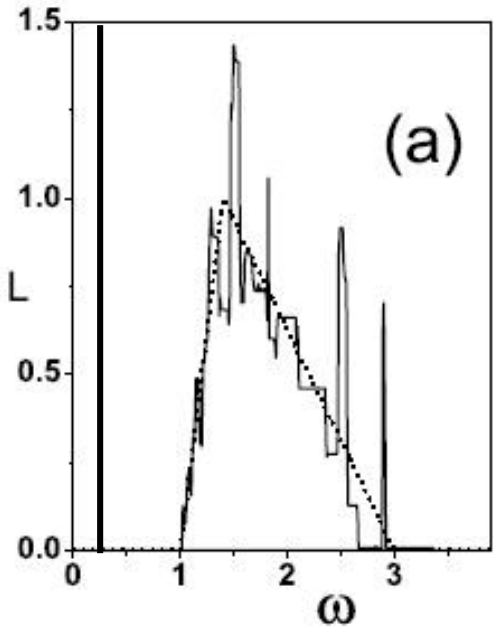


**Fig. 7.** Comparison of the actual spectral function (dashed line) with the results of spectral analysis after averaging over (a) $M = 4$, (b) $M = 28$, and (c) $M = 500$ particular solutions.

# Self-averaging of the saw-tooth noise.

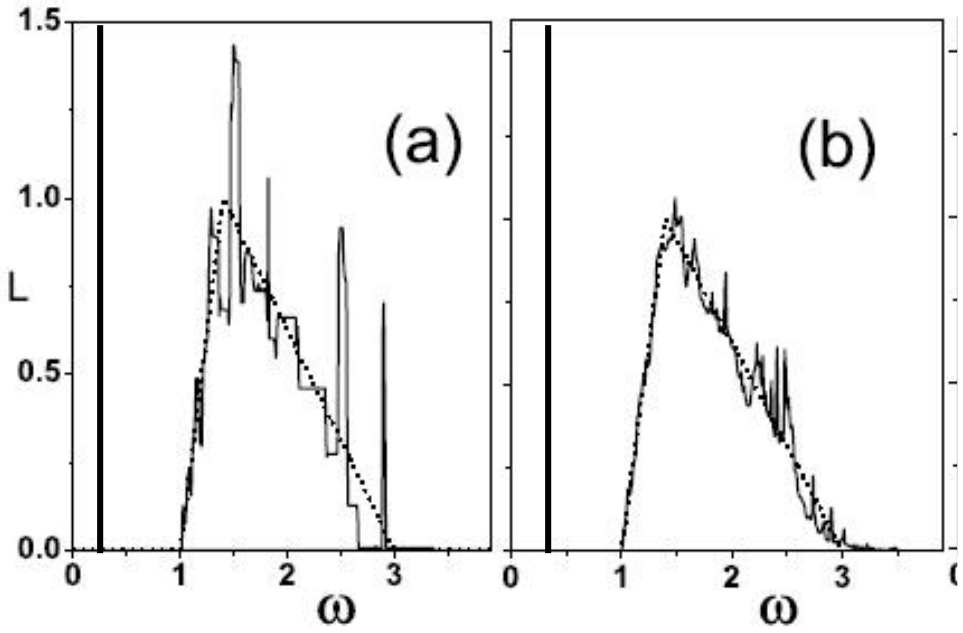


**Fig. 7.** Comparison of the actual spectral function (dashed line) with the results of spectral analysis after averaging over (a) $M = 4$, (b) $M = 28$, and (c) $M = 500$ particular solutions.

# Self-averaging of the saw-tooth noise.

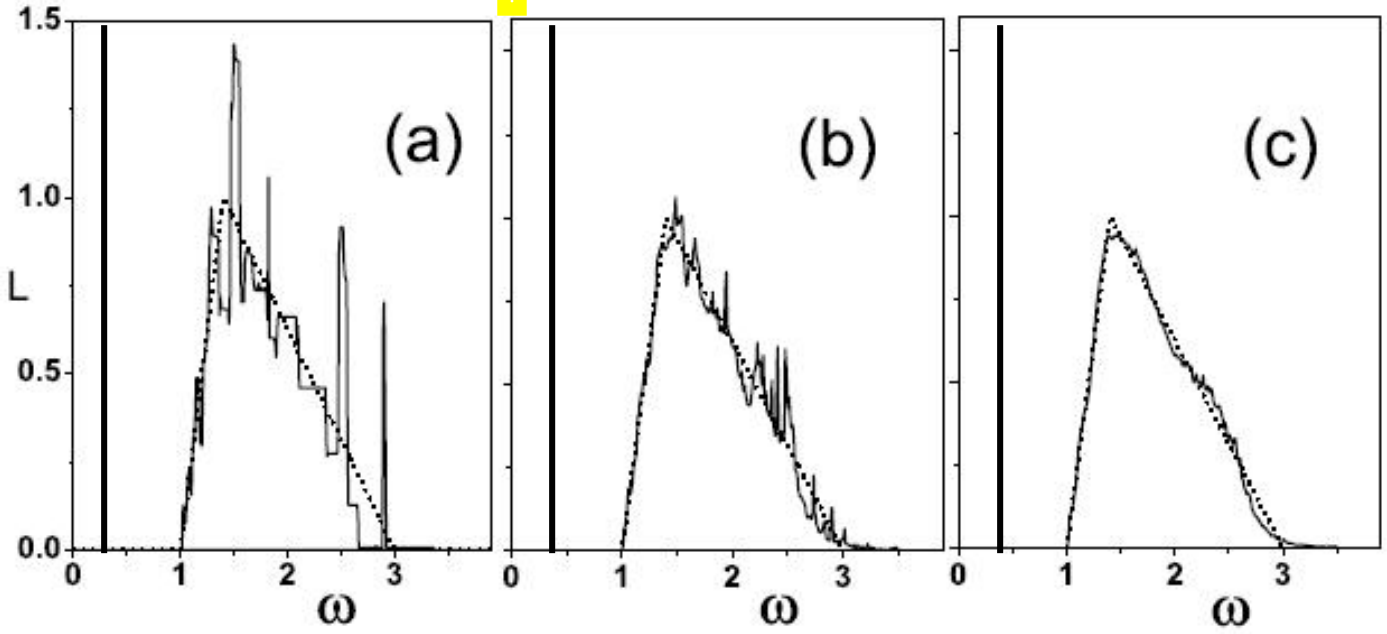


**Fig. 7.** Comparison of the actual spectral function (dashed line) with the results of spectral analysis after averaging over (a) $M = 4$, (b) $M = 28$, and (c) $M = 500$ particular solutions.

# Stochastic Optimization method: update procedures.

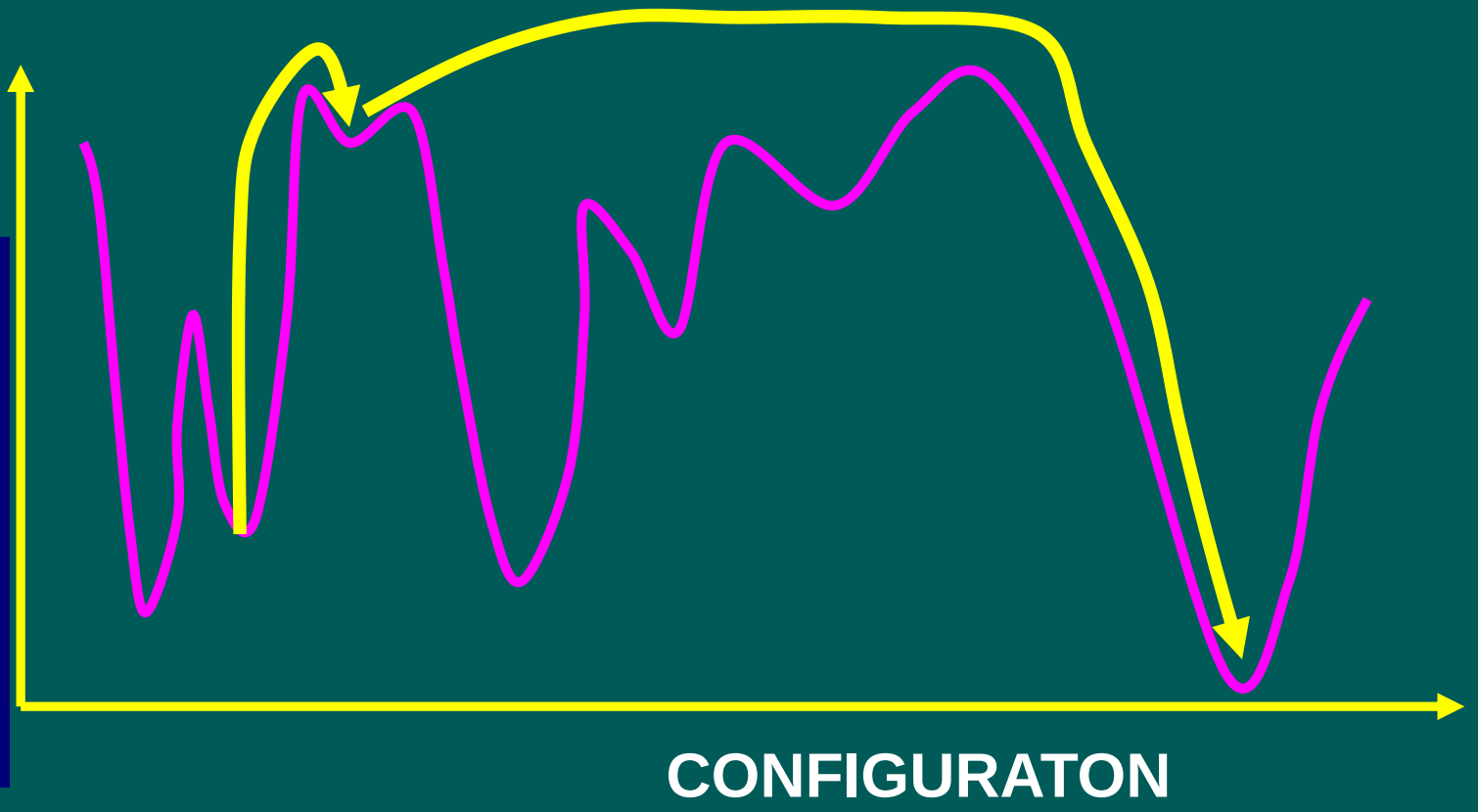


**K+M chain is accepted if final objective is smaller than initial**

**Shake-off two-step strategy:**

**Step 1: Increase of objective function is allowed during M steps with high probability**

**Step 2: Only decrease of objective function is allowed during last K steps.**

# Errorbars estimate

**Expectation and standard deviation in every selected bin**

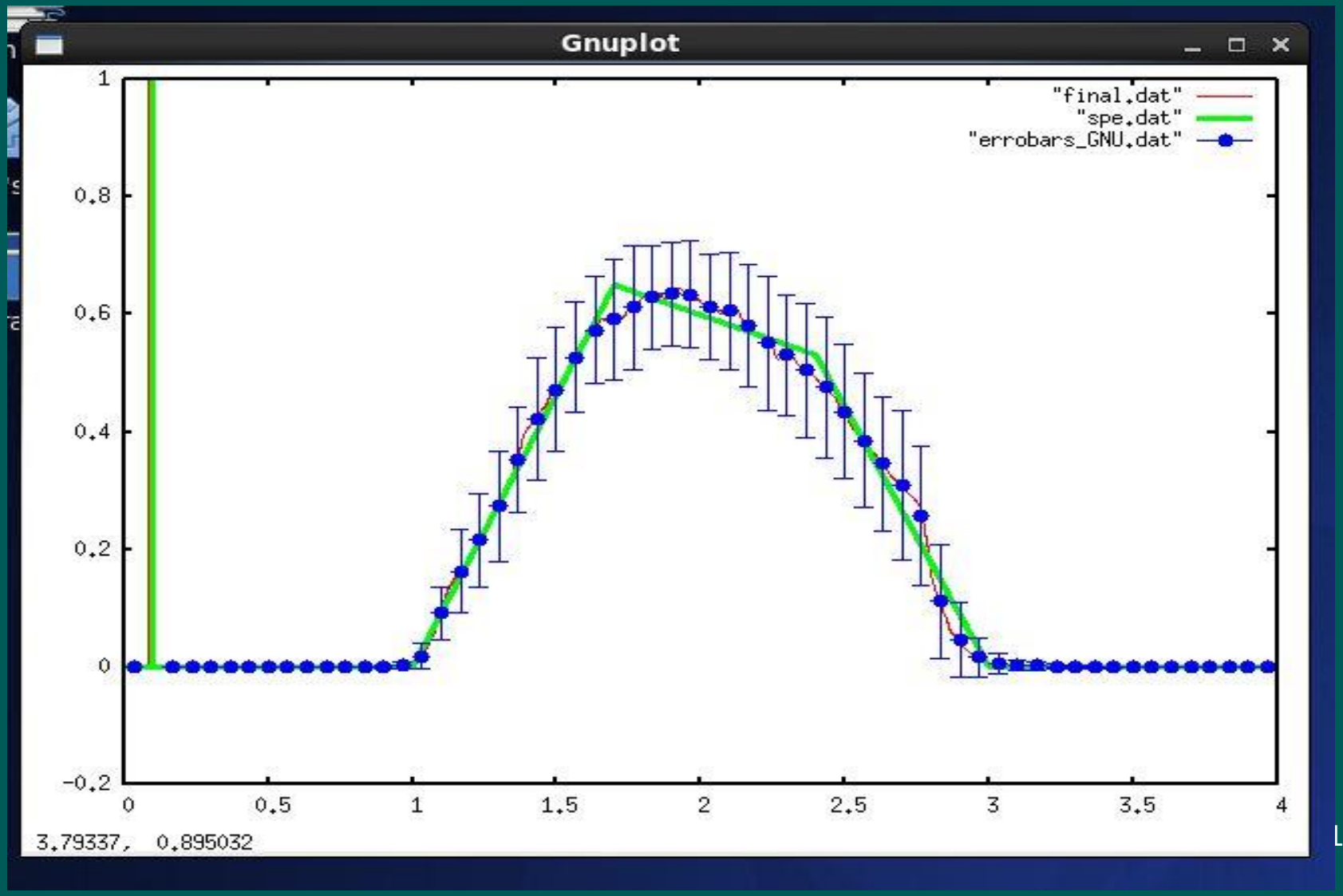

# Preparing final solutions

# Self-averaging of the saw-tooth noise.

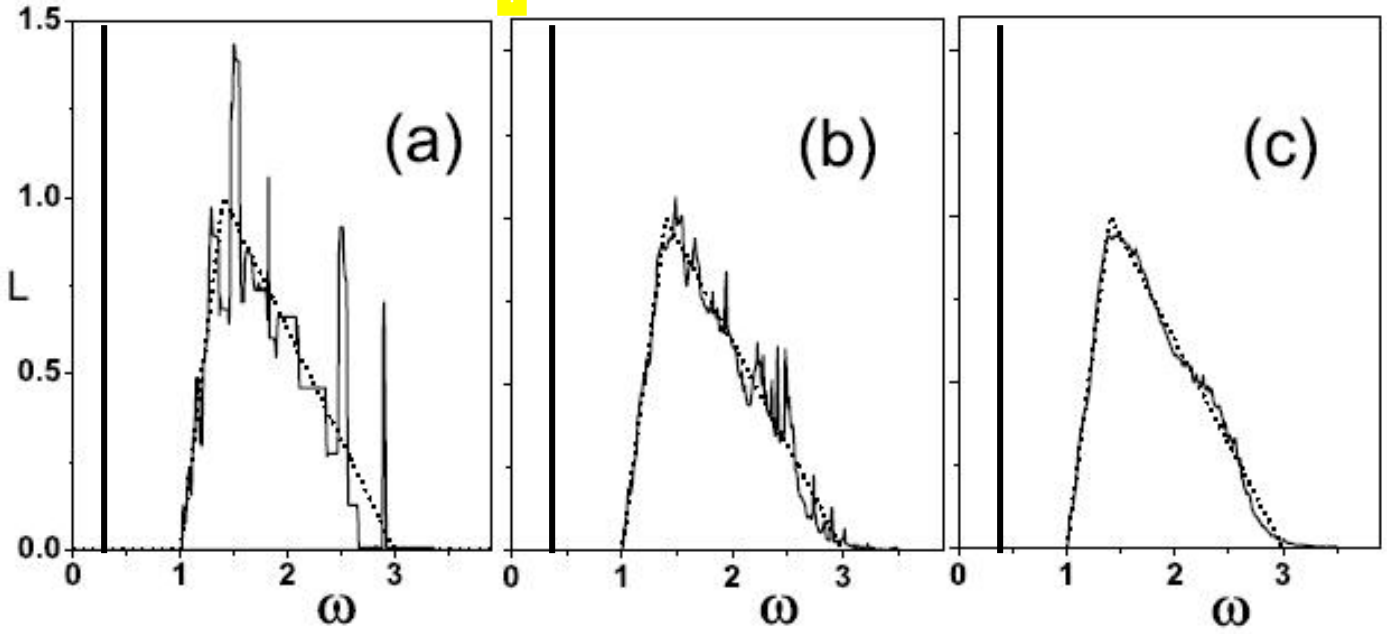


**Fig. 7.** Comparison of the actual spectral function (dashed line) with the results of spectral analysis after averaging over (a) $M = 4$, (b) $M = 28$, and (c) $M = 500$ particular solutions.

The formulation of the SOCC method :

1. Finding a large set of solutions $A_j(z)$ $[j = 1, \ldots, J \gg 1]$ to Eq. (1) that satisfy the input data within their error bounds. In what follows we call them "basic" solutions. Basic solutions are not biased in any way to be smooth or to satisfy any other requirements based on knowledge about the problem outside of Eq. (1).

2. Using the basic solutions $A_j(z)$ to determine the final solution by selecting a superposition of basic solutions

$$A_{\text{fin}}(z) = \sum_{j=1}^{J} c_j A_j(z), \qquad \sum_{j=1}^{J} c_j = 1\,, \tag{2}$$

such that $A(z)$ remains non-negative and the coefficients $c_j$ are optimized to impose smooth behavior or any other "conditional knowledge". Formally, the simplest interpretation corresponds to $c_j = 1/J$.

The search for basic solutions relies on the minimization of

$$\chi^2 = N^{-1} \sum_{n=1}^{N} \left( \frac{g_n - G[n, A]}{\delta_n} \right)^2 \qquad (3)$$

where $\delta_n$ is the error of the $g_n$ value. We choose a maximal tolerance $\chi_c$ of order unity and search for functions $A(z) > 0$ with $\chi^2 < \chi_c^2$, which are then added to the set of basic solutions for further processing.

Information about the input data is limited to the objective function (3). Truly unbiased methods should not assume anything about $A(z)$ that is not part of exact knowledge, such as the predetermined grid of points, and the number and parameters of peaks/gaps.

2. Using the basic solutions $A_j(z)$ to determine the final solution by selecting a superposition of basic solutions

$$A_{\text{fin}}(z) = \sum_{j=1}^{J} c_j A_j(z), \qquad \sum_{j=1}^{J} c_j = 1\,, \tag{2}$$

such that $A(z)$ remains non-negative and the coefficients $c_j$ are optimized to impose smooth behavior or any other "conditional knowledge". Formally, the simplest interpretation corresponds to $c_j = 1/J$.

$$\chi^2 = N^{-1} \sum_{n=1}^{N} \left( \frac{g_n - G[n, A]}{\delta_n} \right)^2$$

**Quadratic form with respect to $\{c_j\}$**

$$\chi^2 = \sum_{j,j'=1}^{J} c_j c_{j'} \chi_{jj'} \le \bar{C}^2 \chi_c^2, \quad \text{with} \quad \bar{C} = \sum_{j=1}^{J} |c_j|, \tag{10}$$

$$\chi_{jj'} = N^{-1} \sum_{n=1}^{N} \frac{(g_n - G[n, A_j])(g_n - G[n, A_{j'}])}{\delta_n^2}\,. \tag{11}$$

If some $c$-coefficients are negative, the accuracy of the final solution is guaranteed only if $\bar{C}$ is not large. One may argue that the upper bound $\chi^2 \le \bar{C}^2 \chi_c^2$ is substantially overestimating deviations, and the actual accuracy is better. Finally, Eq. (10) is only an upper bound, and superpositions with $\bar{C}$ as large as 2 may still have $\chi^2 < \chi_c^2$.

# What is to minimize?

• To suppress large derivatives we consider the following form

$$O_1 = \sum_{k=2}^{K} \left\{ D_k^2 [A'(z_k)]^2 + B_k^2 [A''(z_k)]^2 \right\} , \qquad (12)$$

where $\{z_k\}$ is the grid of points used to define the first and second discrete derivatives of the function $A(z)$. The sets of coefficients $D_k$ and $B_k$ are adjusted under iterations self-consistently in such a way that contributions of all $z_k$-points to $O_1$ are similar.

• The unity-sum constraint on the sum of all coefficients in the superposition is expressed as

$$O_2 = \mathcal{U} \left( \sum_{j=1}^{J} c_j - 1 \right)^2 , \qquad (13)$$

with a large constant $\mathcal{U}$.

• Since $O_1 + O_2$ does not constrain the amplitudes and signs of all $c_j$ the minimization cannot proceed by matrix inversion. To improve matrix properties we add a "soft" penalty for large deviations of $c_j$ from the equal-weight superposition

$$O_3 = \sum_{j=1}^{J} (c_j - 1/J)^2 \ . \qquad (14)$$

• To ensure that the spectral function is non-negative (with high accuracy) we need $z$-dependent penalties (to be set self-consistently) that suppress the development of large negative fluctuations:

$$O_4 = \sum_{k=1}^{K} Q_k A(z_k)^2 \ . \qquad (15)$$

# Main ingredient: Target function points

- Finally, we can introduce a penalty for the solution to deviate from some "target" function (or "default model") $A_T(z_k)$:

$$O_5 = \sum_{k=1}^{K} T_k \left[A(z_k) - A_T(z_k)\right]^2 . \qquad (16)$$

The main purpose of $O_5$ is to address subtle multi-point correlations between allowed shapes: by forcing the solution to be close to a certain target function one can monitor how the solution starts developing additional sawtooth-instability-related features or violates the unity-sum constraint. This penalty is zero when preparing $A_{\rm fin}$ in the absence of any target function.

# Self-consistent protocol.

After the quadratic form for the objective function $O$ is minimized, the new set of $c$-coefficients is used to define a new solution $A(z)$, penalties for derivatives are increased, $\mathcal{D} \to f\mathcal{D}$, $D_k \to fD_k$, $B_k \to fB_k$ by some factor $f > 1$, and then all penalties in in $O_1$ and $O_4$ are adjusted self-consistently as follows:

- If $D_k|A'(z_k)| > \mathcal{D}$, we assign $D_k = \mathcal{D}/|A'(z_k)|$;
- If $B_k|A''(z_k)| > \mathcal{D}$, we assign $B_k = \mathcal{D}/|A''(z_k)|$;
- If $A(z_k) < 0$, we assign a large penalty suppressing the amplitude of the solution at this point, $Q_k = \mathcal{Q}$, where $\mathcal{Q}$ is a large constant; otherwise the value of $Q_k$ is increased by two orders of magnitude.

In this work we use $\mathcal{U} = 10^6$, $\mathcal{Q} = 10^6$, and $f = 2$. This sets the stage for the next iteration of the $O$-optimization protocol. The final solution (2) is based on the last set of $c$-coefficients that satisfied the condition $\chi^2 < \chi^2_c$.

A

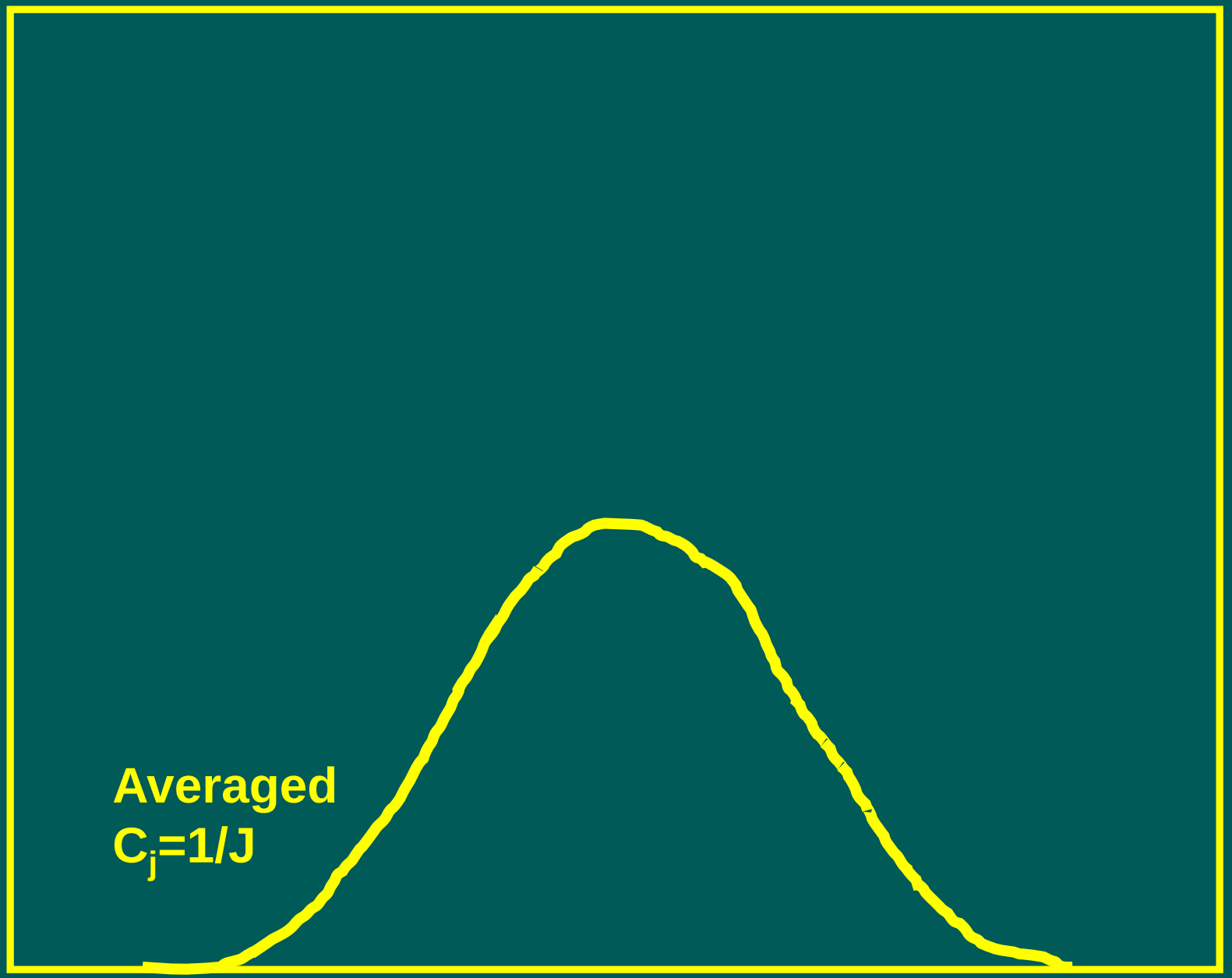

A

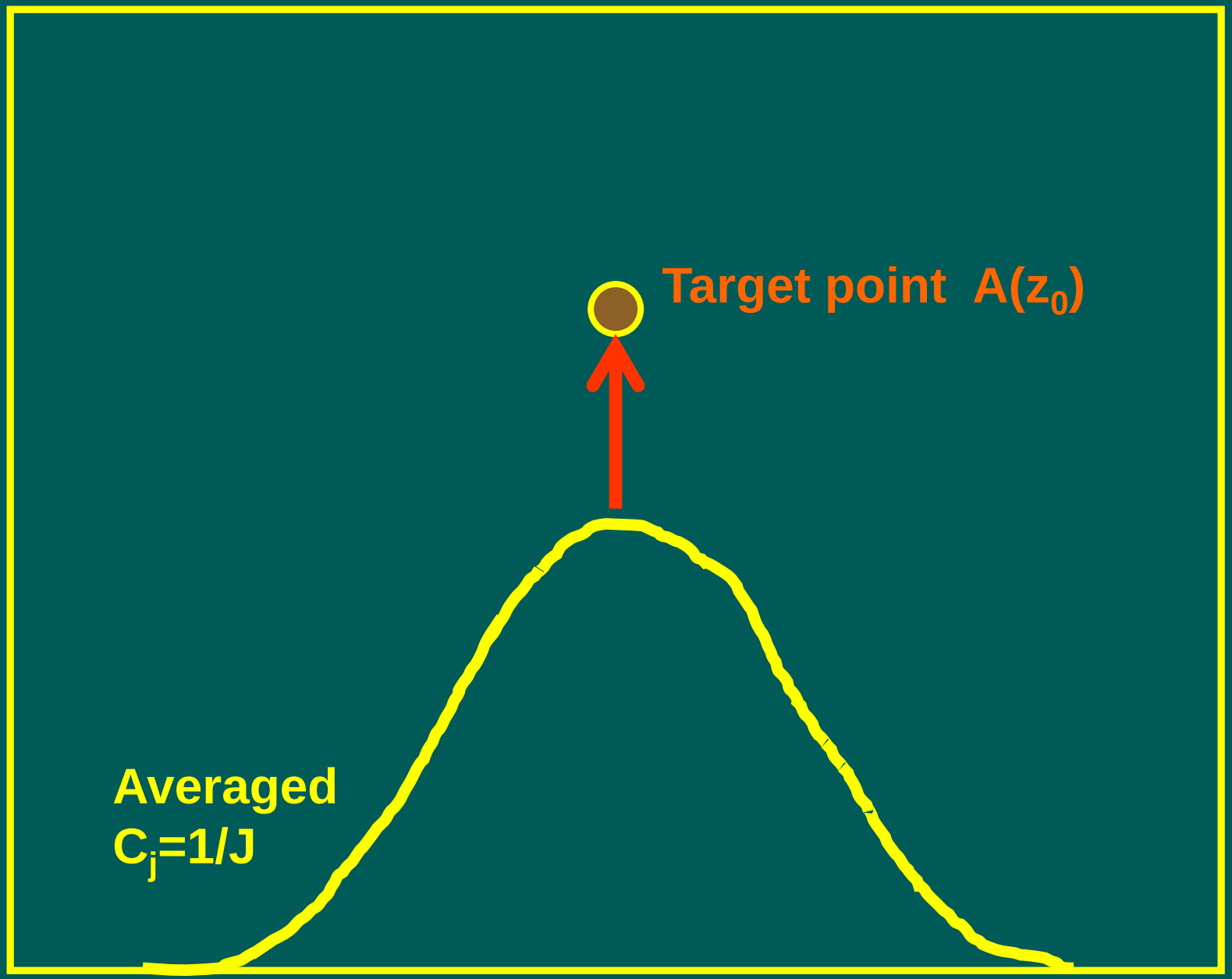

A

Valid
Transformation?

YES!

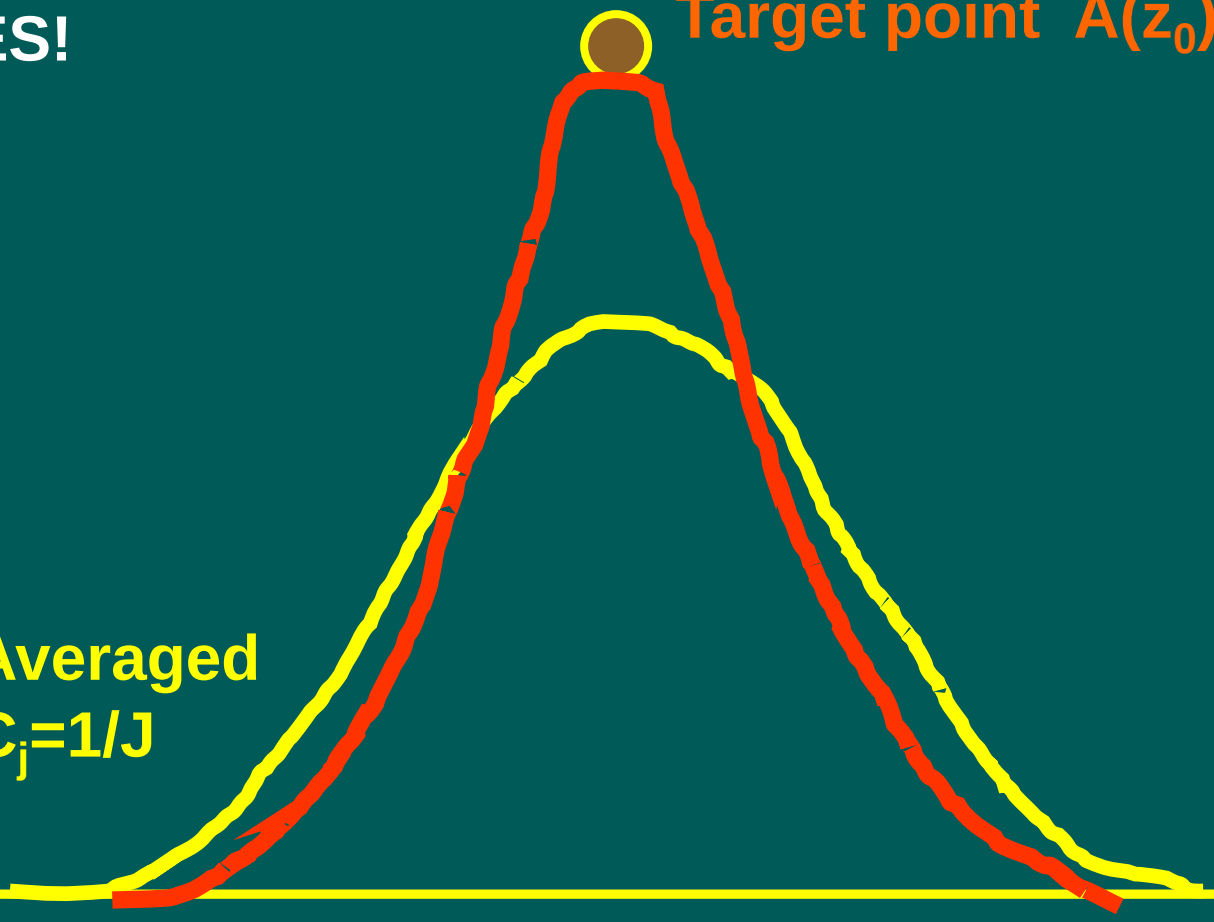

A

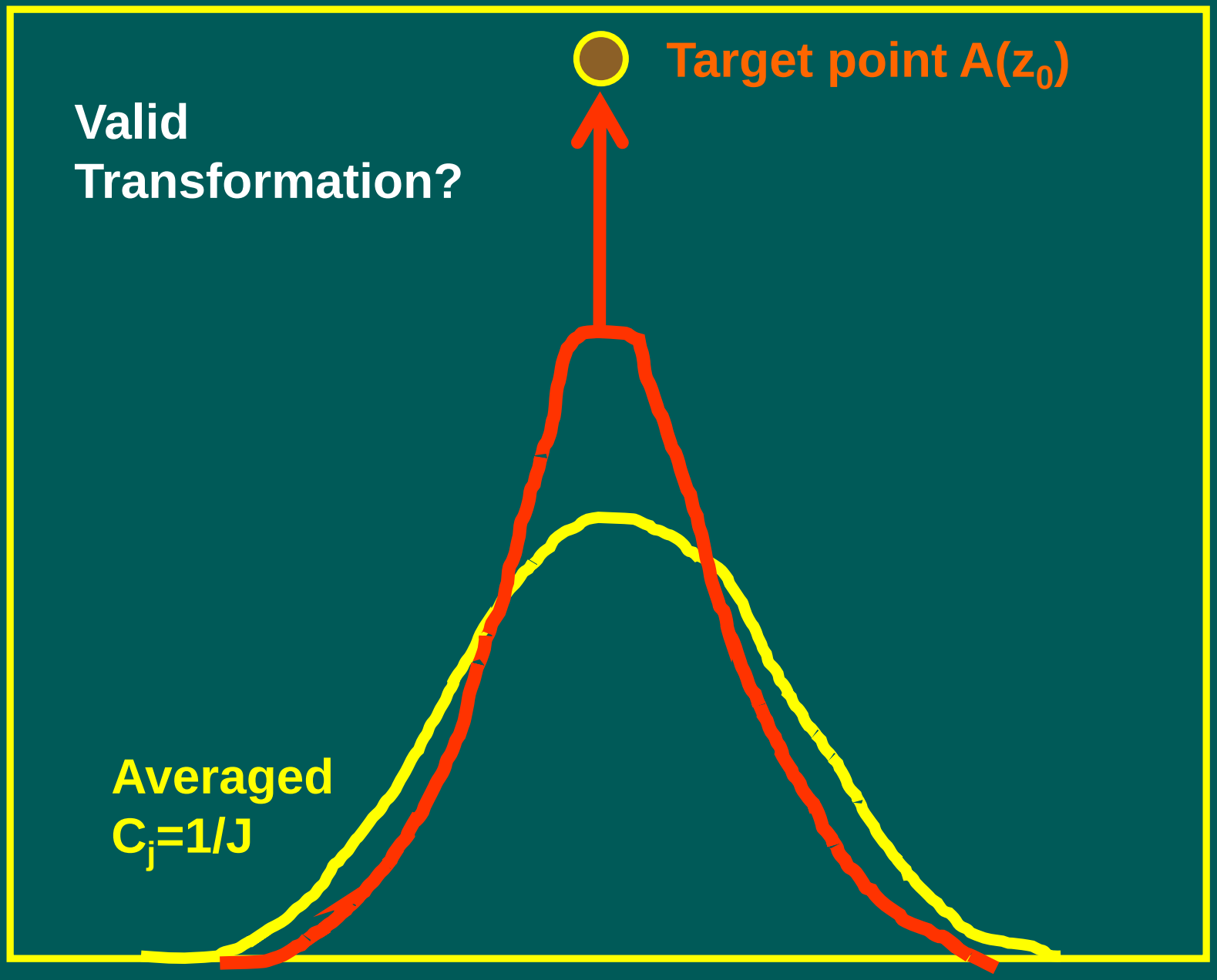

A

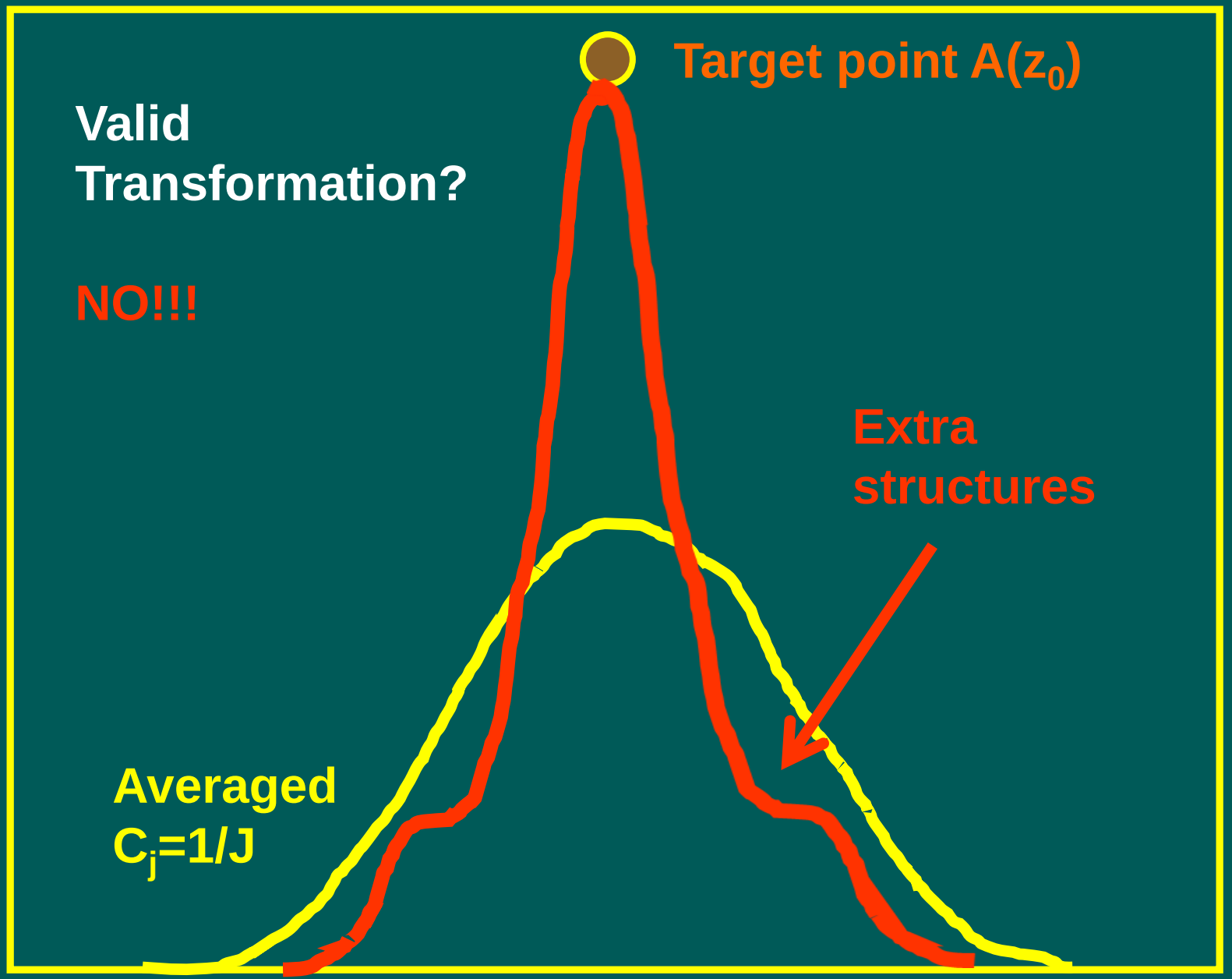
Target point A($z_0$)
Valid Transformation?
NO!!!
Extra structures
Averaged $C_j$=1/J

# Blind tests: how much we can say about second peak

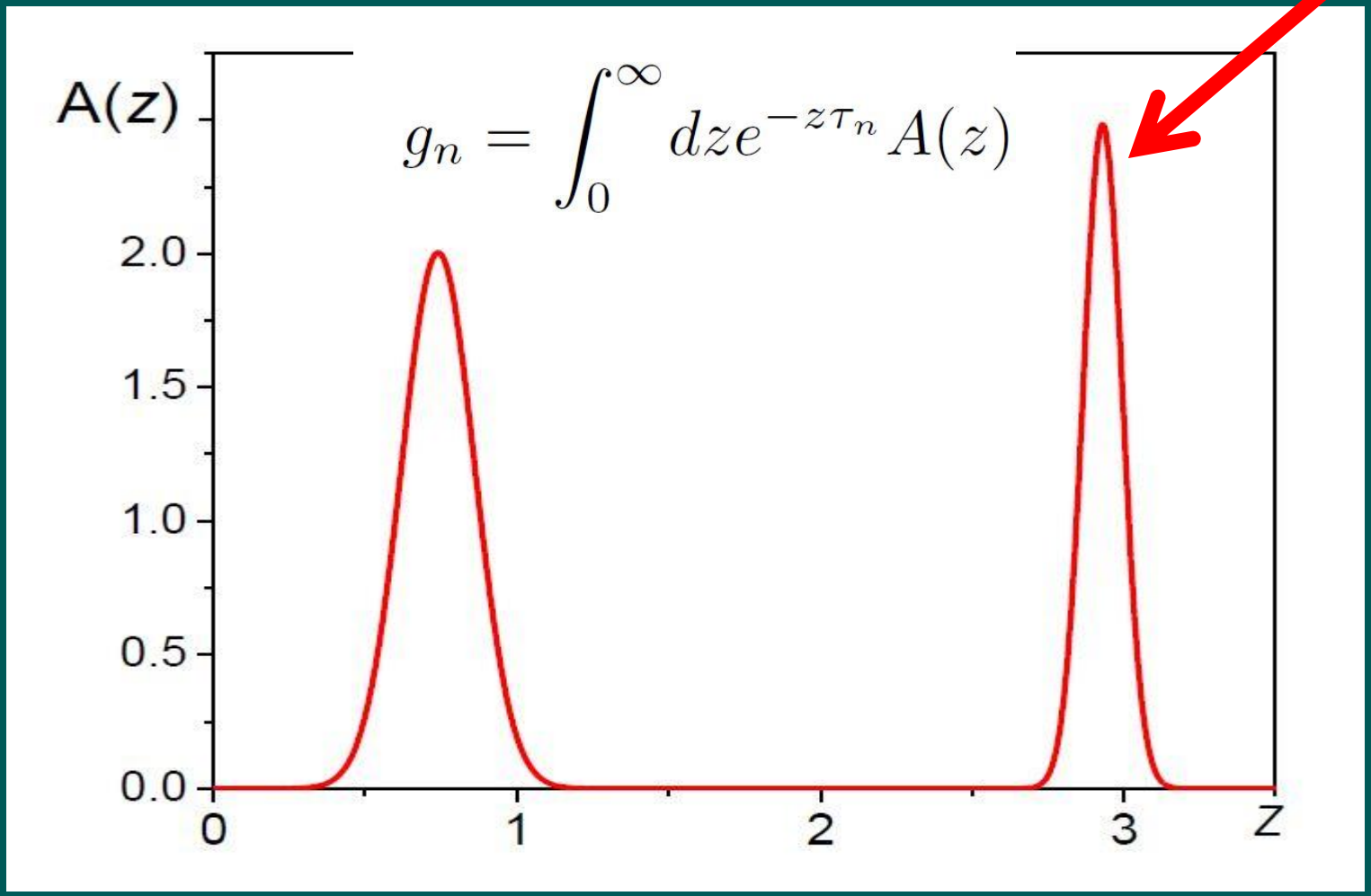


O. Goulko et al, Phys. Rev. B **95**, 014102 (2017)

# Noise level $\delta=10^{-3}$

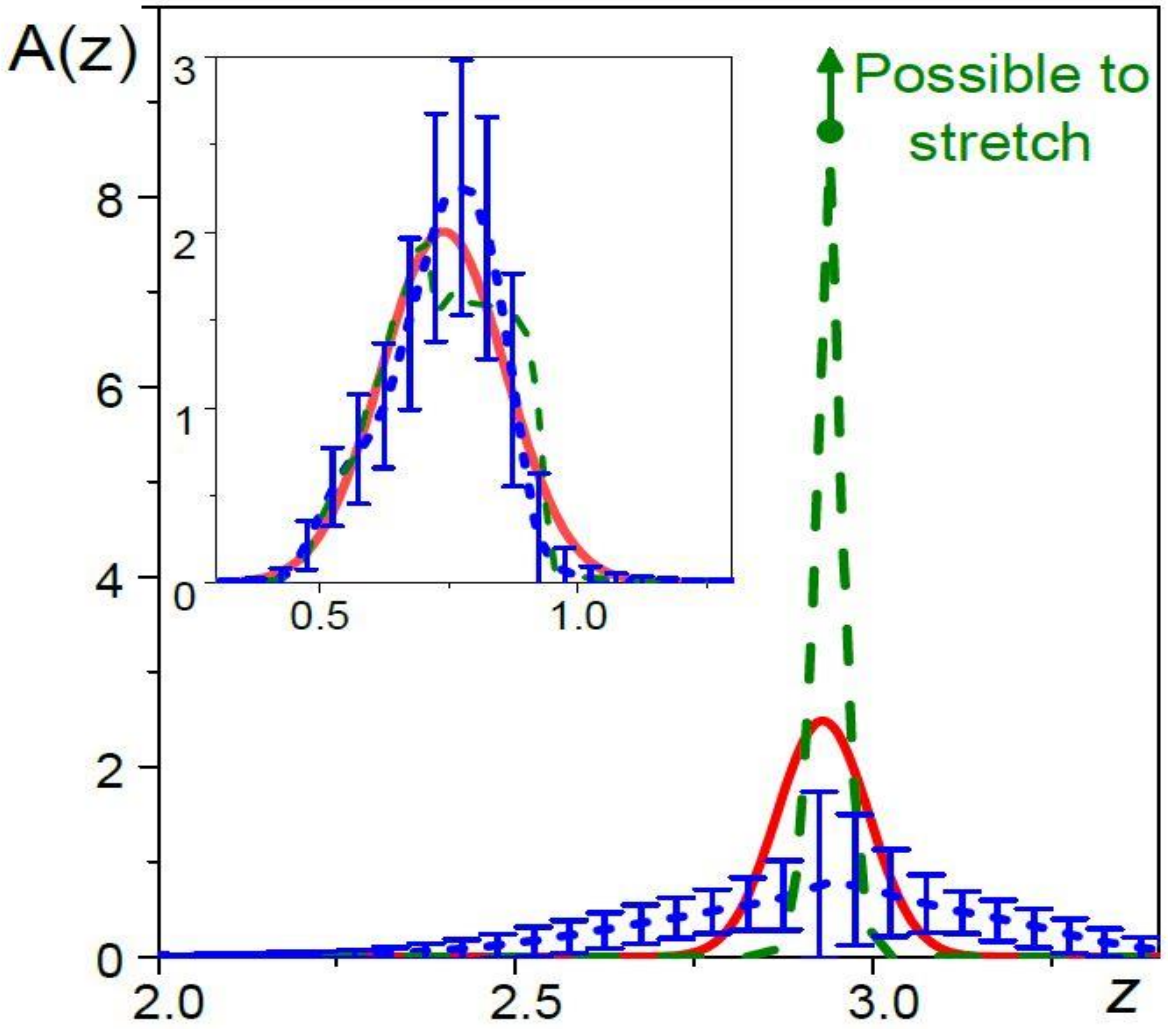


FIG. 3. (Color online.) Results for test 1, featuring two peaks of finite width with noise level $10^{-3}$. Shown is the compari-

# Noise level $\delta=10^{-5}$

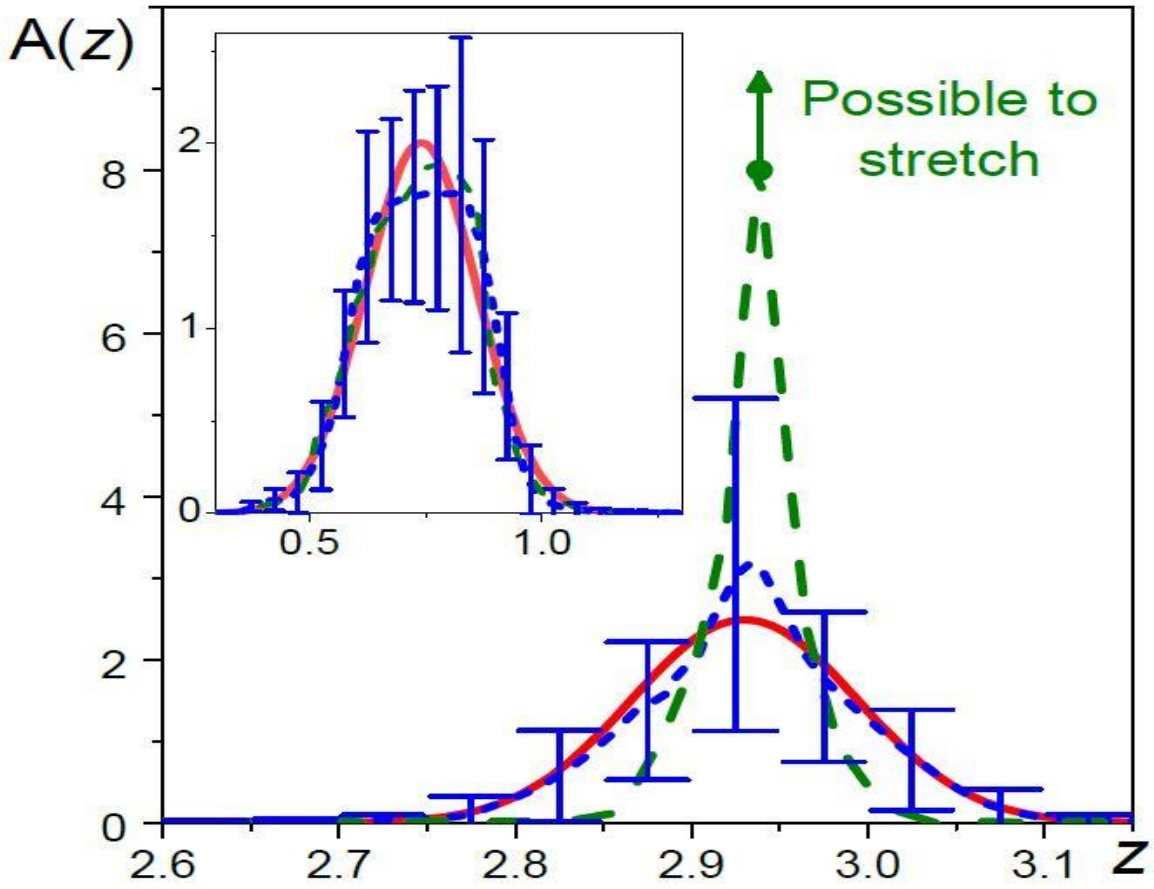


FIG. 6. (Color online.) Results for test 2, featuring two peaks of finite width with noise level $10^{-5}$. Shown is the com-

# Noise level $\delta=10^{-5}$
# First peak -> δ function

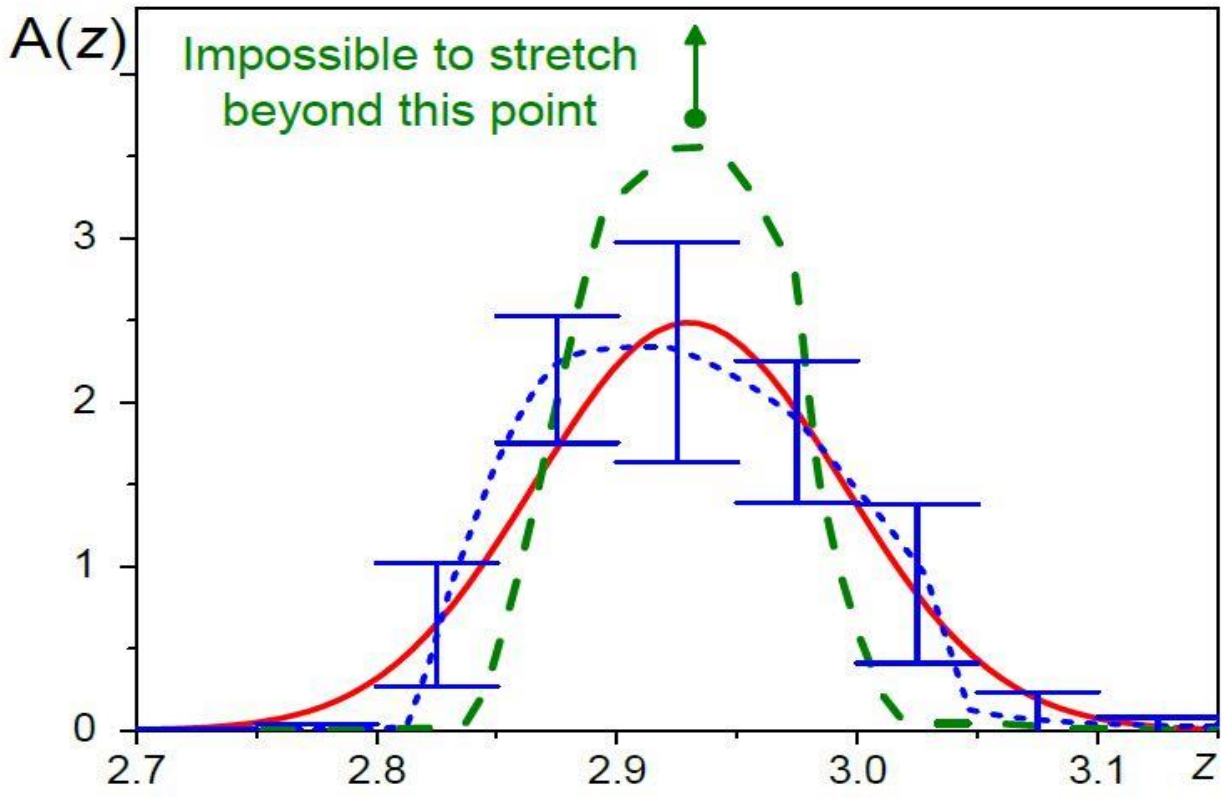


FIG. 8. (Color online.) Results for test 3, characterized by a $\delta$-function at low frequency and a peak of finite width at high frequency with noise level $10^{-5}$. Shown is the comparison be-

# Conclusions. Numeric analytic continuation :

## well posed answers to the ill posed problems.

$g_n$ – given MC data,
K[n,z] – known kernel

$$G[n,A] = \int dz\, K[n,z]\, A(z)$$

A(z) – spectral function to find

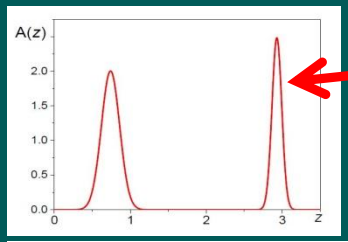


High energy peak

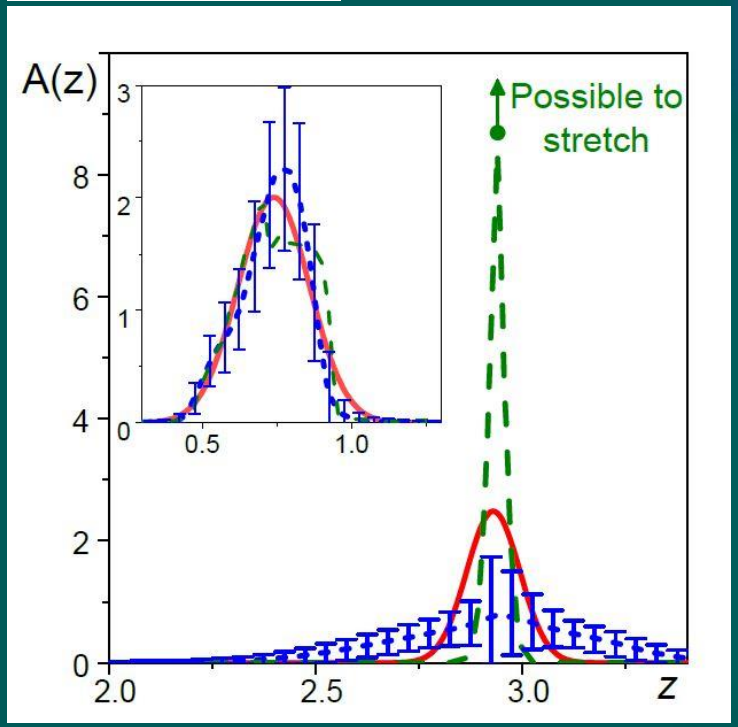


## Objectives:

1.Stochastic optimization method (SOM) can quickly find a lot of [J>1000] solutions $\{A_j(z)\}$ each having good objective function ($\delta_n$ – error bars)

$$.. O_1 = \chi^2 = N^{-1}\sum_{n=1}^{N} [\,(g_n - G[n,A_j])/\,\delta_n\,]^2 < \chi_c^2 = 1$$

Usually, final solution is obtained as average

$$\langle A(z)\rangle = J^{-1}\sum_{j=1}^{J} A_j$$

which removes saw tooth instability. However, one can search solution as

$$A_{fin}(z) = J^{-1}\sum_{j=1}^{J} c_j\, A_j \quad \text{where} \quad \sum_{j=1}^{J} c_j = 1$$

where Cj<0 are possible untill $\chi^2 < \chi_c^2$.

## Results

1. One can introduce one more part of objective function

$$O_5 = \sum_k T(k)[A_{fin}(z_k) - A_T(z_k)]^2$$

which characterizes deviation from target function $A_T(z)$.

2. It is legal to satisfy $O_5$ until $\chi^2 < \chi_c^2$.

3. This approach can verify which features of result are robust and which can be an artefact at given error bars $\delta_n$. (see example where high energy peak can be made very narrow (green) or very wide (blue) in comparison with actual peak (red) without compromising the error bars). Hence, peak width is undefined.

O. Goulko et al, arXiv: 1609.01260

# Polaron mobility:

5
different
regimes

$$\mu = \sigma(\omega \rightarrow 0) / eN$$

A.S.M., N. Nagaosa, G. De Filippis, A. de Candia, and V. Cataudella,
**Phys. Rev. Lett., vol. 114, 146401 (2015)**

## Hamiltonian

$$\mathcal{H} = \sum_k \left( \varepsilon_k c_k^\dagger c_k + \omega_0 b_k^\dagger b_k \right) + \frac{g}{\sqrt{N}} \sum_{k,q} c_{k-q}^\dagger c_k \left( b_q^\dagger + b_{-q} \right)$$

Analytic continuation

$$\Pi(\tau) = \int_{-\infty}^{\infty} d\omega \, \frac{1}{\pi} \frac{\omega \exp[-\tau\omega]}{1 - \exp[-\beta\omega]} \, \sigma(\omega) \equiv \mathcal{F}[\tau, \sigma(\omega)]$$

## Regimes

### Metallic

$$\mu_{\text{metal}}(T) \sim T^{-\delta}$$

### Activation

$$\mu_{\text{hop}}(T) \sim T^{-\kappa} \exp(-\varepsilon_a / T)$$

$$\varepsilon_a = E_b/2 - t'$$

# Mobility of 1D Holstein polaron

$$\mu_\lambda(\omega, T) = \sigma_\lambda(\omega, T)/(eN_e)$$

**λ=0.5, weak copling**

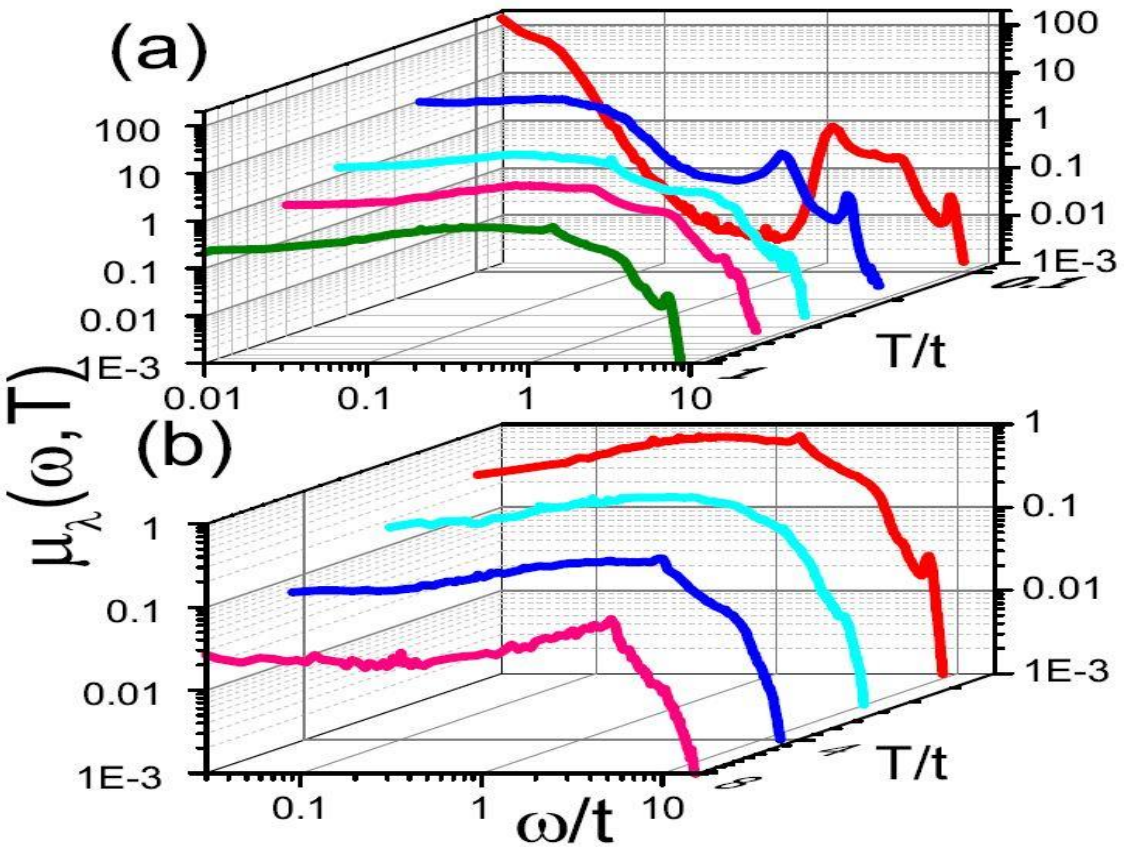

# Mobility of 1D Holstein polaron

$$\mu_\lambda(\omega, T) = \sigma_\lambda(\omega, T)/(eN_e)$$

**λ=4.0, strong coupling**

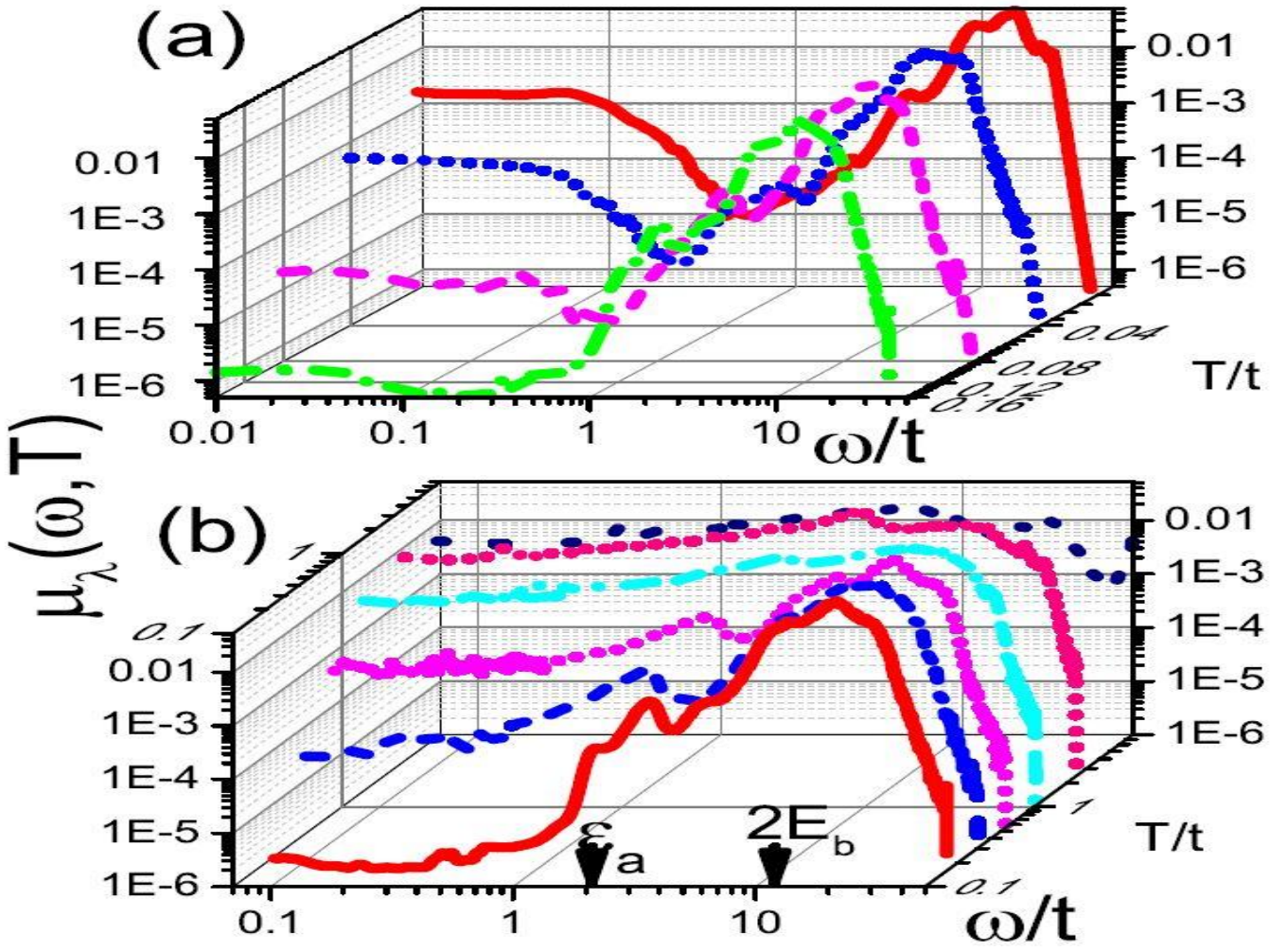

# Mobility of 1D Holstein polaron

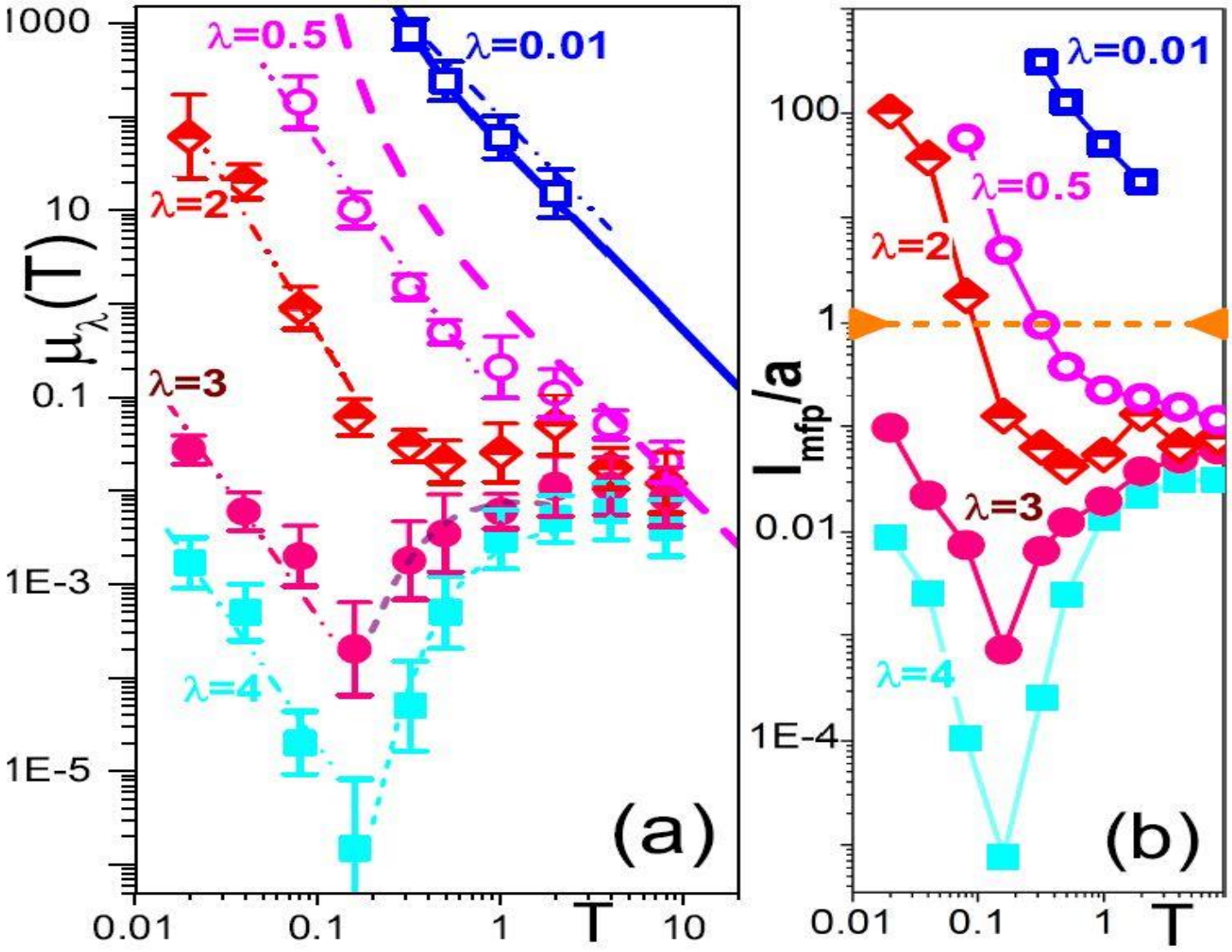

# Mobility of 1D Holstein polaron

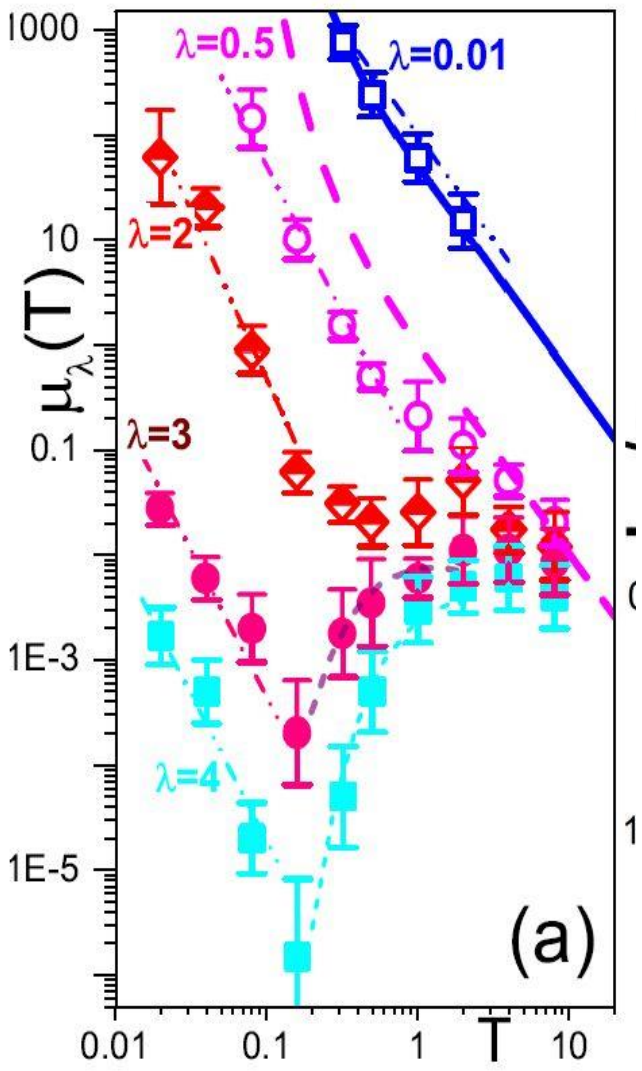


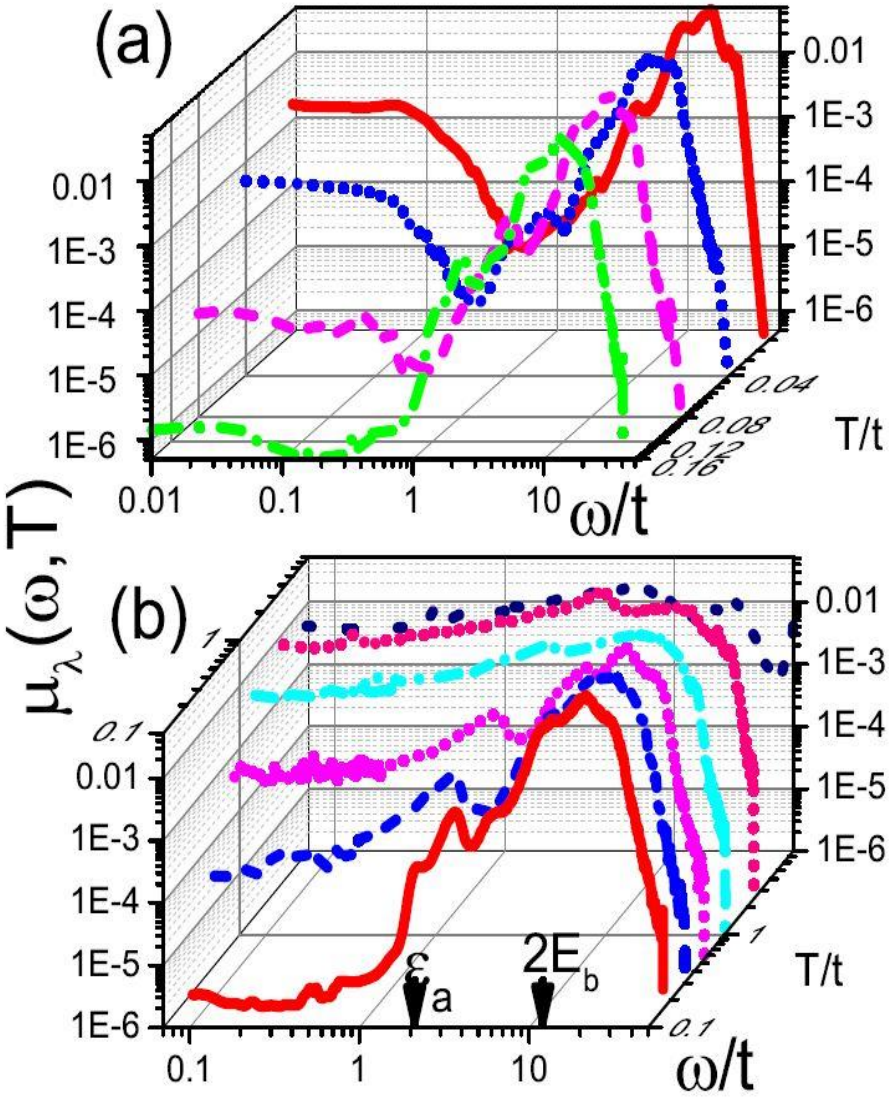

# Mobility of 1D Holstein polaron

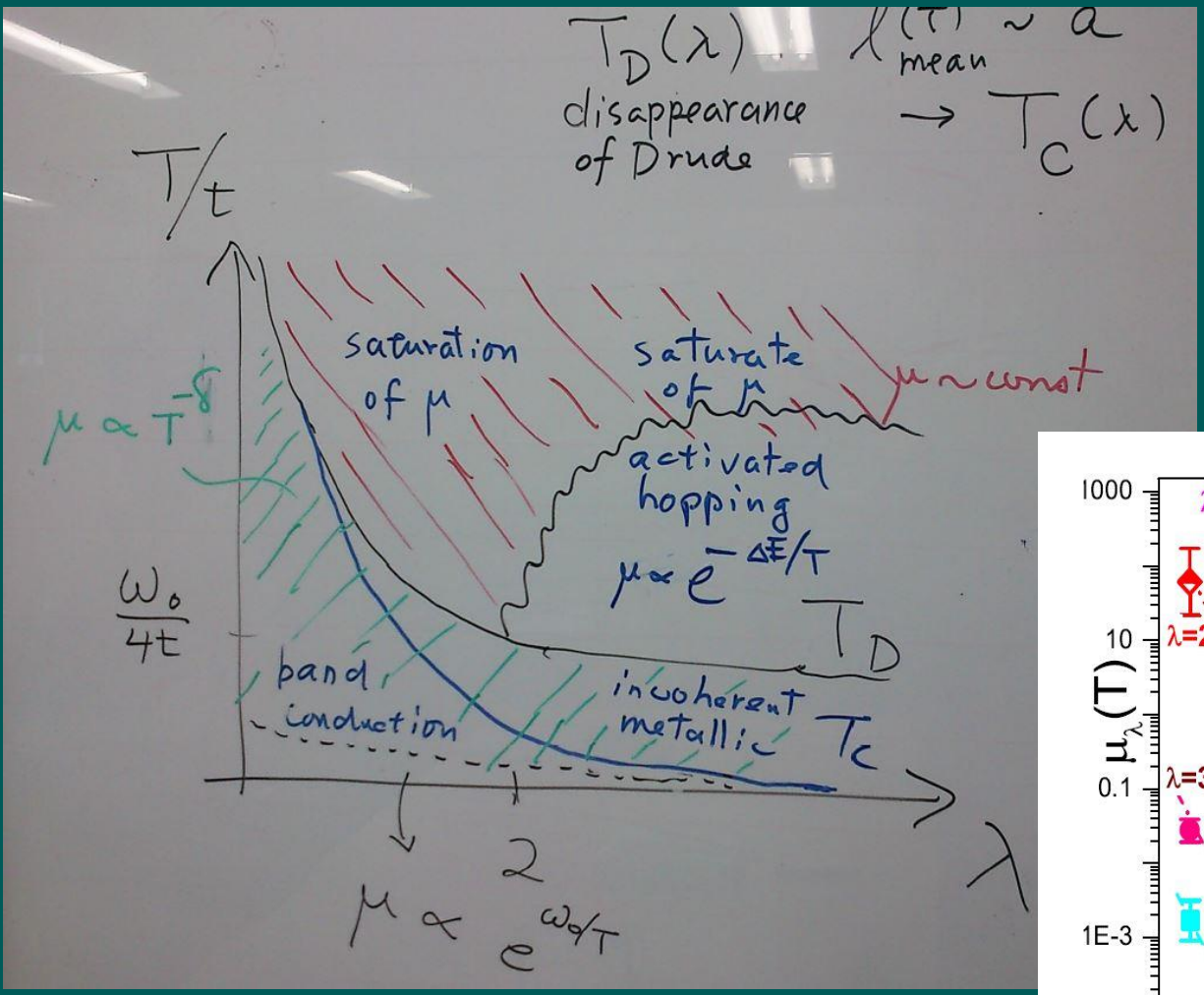


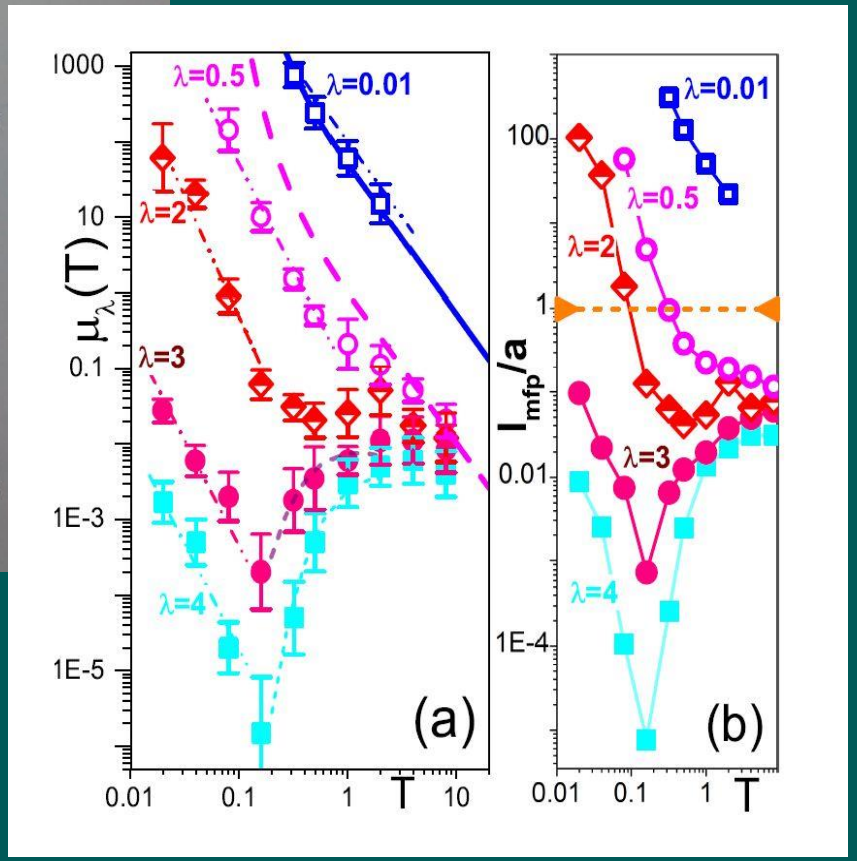

# Mobility of 1D Holstein polaron

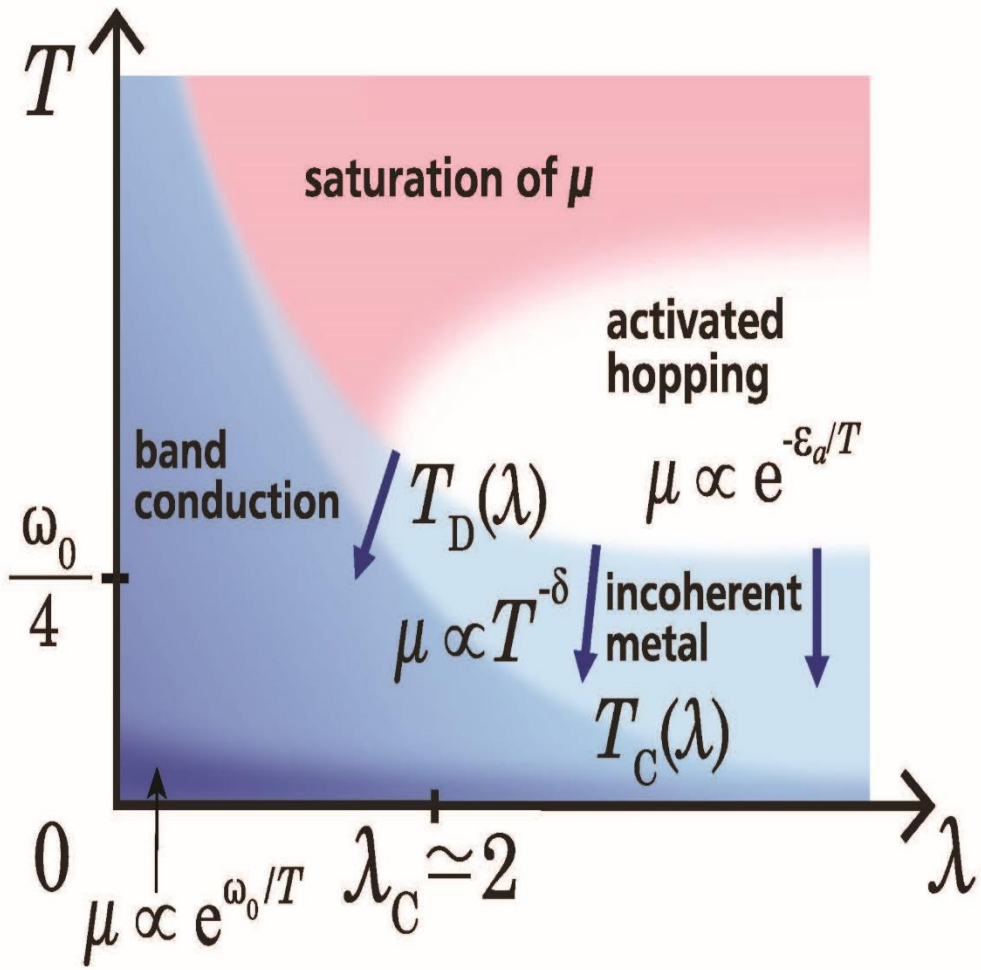


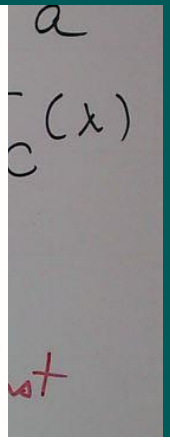

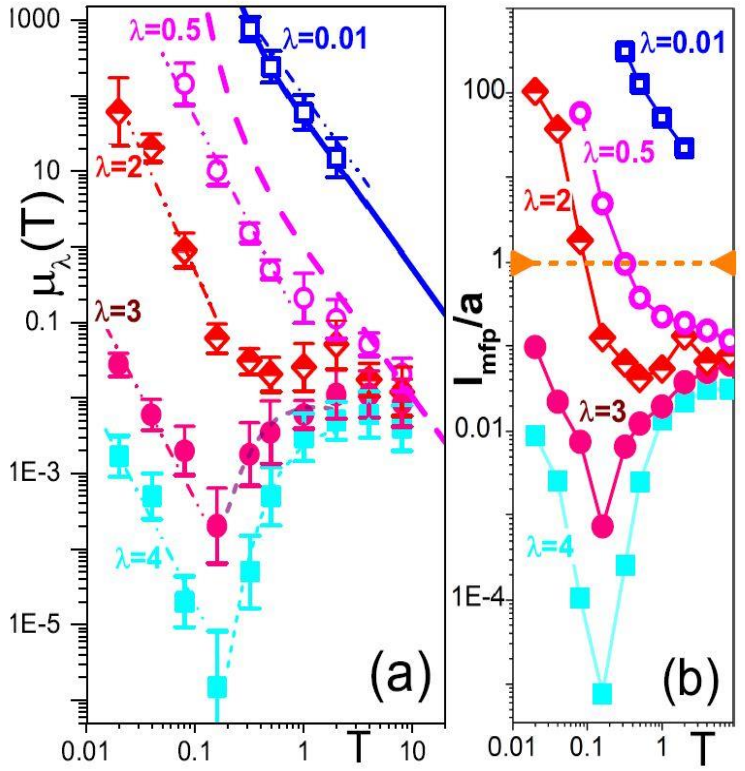


Phys. Rev. Lett., vol. 114, 146401 (2015)

# Part II. Further reading for details:

Phys. Rev. Lett., vol. 86, 4624 (2001) : Pseudo-Jahn-Teller polaron
Phys. Rev. Lett., vol. 87, 186402 (2001) : Exciton in semiconductors
Phys. Rev. Lett., vol. 91, 236401 (2003) : Optical conductivity of Frohlich polaron
Phys. Rev. Lett., vol. 93, 036402 (2004) : ARPES in high $T_c$ cuprates
Phys. Rev. Lett., vol. 96, 136405 (2006) : Franck-Condon principle
Phys. Rev. Lett., vol. 99, 146405 (2007) : Nonlocal el-ph in high $T_c$ cuprates
Phys. Rev. Lett., vol. 99, 226402 (2007) : ARPES in high $T_c$ cuprates
Phys. Rev. Lett., vol. 100, 166401 (2008) : Optical conductivity in high $T_c$ cuprates
Phys. Rev. Lett., vol. 101, 116403 (2008) : Exciton-polaron in semiconductors
Phys. Rev. Lett., vol. 104, 056602 (2010) : ESR in organic transistors
Phys. Rev. Lett., vol. 105, 266605 (2010) : SSH polaron in organic compounds
Phys. Rev. Lett., vol. 107, 076403 (2011) : Optical conductivity of Holstein polaron
Phys. Rev. Lett., vol. 109, 176402 (2012) : Time dependent Holstein-Hubbard
Phys. Rev. Lett., vol. 113, 166402 (2014) : Finite density polaron gas
Phys. Rev. Lett., vol. 114, 086601 (2015) : Conductivity in organic materials
Phys. Rev. Lett., vol. 114, 146401 (2015) : Unbiased mobility of Holstein polaron
……